

2019 • 2020

Faculteit Industriële ingenieurswetenschappen
master in de industriële wetenschappen: chemie

Masterthesis

Leaching technology to recover metals from mineral waste,
recovery technology to capture metals from leachates (sorption,
precipitation)

PROMOTOR :

Prof. dr. ir. Leen BRAEKEN

PROMOTOR :

dr. ir. Maarten EVERAERT

Sam Haenen

Scriptie ingediend tot het behalen van de graad van master in de industriële wetenschappen: chemie

Gezamenlijke opleiding UHasselt en KU Leuven



KU LEUVEN



KU LEUVEN

2019 • 2020

Faculteit Industriële ingenieurswetenschappen
master in de industriële wetenschappen: chemie

Masterthesis

Leaching technology to recover metals from mineral waste,
recovery technology to capture metals from leachates (sorption,
precipitation)

PROMOTOR :

Prof. dr. ir. Leen BRAEKEN

PROMOTOR :

dr. ir. Maarten EVERAERT

Sam Haenen

Scriptie ingediend tot het behalen van de graad van master in de industriële wetenschappen: chemie



DEZE MASTERPROEF WERD GESCHREVEN TIJDENS DE COVID-19 CRISIS IN 2020. DEZE WERELDWIJDE GEZONDHEIDSCRISIS HEEFT MOGELIJK EEN IMPACT GEHAD OP DE OPDRACHT, DE ONDERZOEKSHANDELINGEN EN DE ONDERZOEKSRESULTATEN.

LITERATURE STUDY

Acknowledgements

For my master's thesis appropriate with the education Master of Chemical Engineering Technology, I worked in the Sustainable Materials Management unit of VITO (Mol), which focusses on the development of waste and recycling technologies. This unit is a sophisticated player in the research and development of closing material cycles for companies in Flanders and all over the world. It reduces the risk of innovation for companies and strengthens the economic and social fabric of Flanders with interdisciplinary research and large-scale demonstrators.

My study was about a leaching technology to recover metals (Zn, Cu, Ni, Pb) from a mineral waste stream and in the end to employ these valuable metals for the aqueous synthesis of metal organic frameworks (MOFs). This study required a step-by-step approach to reach these goals.

During my period in VITO, I had the opportunity to work in a high-tech, professional surroundings with dedicated employees. They were always into a new adventure and they supported me by learning new laboratory techniques, methods, analyzing techniques,... Especially I want to thank my external promotor Dr. Ir. Everaert Maarten who assisted me from day one until the end. He guided me in the lab and improved the whole study by teaching me a part of his knowledge. Furthermore he helped me with writing tips and corrected my thesis.

From our university, I want to put Prof. Dr. Ir. Braeken in the spotlight because she always supported me and reassured me in hard times as soon as possible.

I also want to thank Warre Van Dun for giving me training about new devices like the ICP-OES and his technical support. Beside Warre, I want to thank Wendy Wouters. She was responsible for the lab where I worked in and coordinated me to keep my working environment safe and clean. Thanks to her, I could work in optimal circumstances. Furthermore she gave me technical advice and training for the XRF apparatus.

This internship gave me the ability to earn a lot of new experience/knowledge and thereby it was ideal to end my education. I am thankful for the VITO society.

Sam Haenen
Student Master of Chemical Engineering Technology
UHasselt- KU Leuven
June 2020

Table of Contents

Acknowledgements	3
List of tables	8
List of figures	10
Glossary	12
Abstract	13
Abstract (Dutch version)	14
1. Introduction	15
1.1 Context	15
1.2 Problem definition/Research question	15
1.3 Research objectives	16
2. Literature	17
2.1 Situation	17
2.2 Primary resources	17
2.3 Metal recycling	19
2.3.1 Advantages of metal recycling	19
2.3.2 Role of the government	20
2.4 Current state of metal industry	20
2.4.1 Metal containing waste streams	21
2.4.2 Waste water	22
2.4.3 Tailings	23
2.5 Metal leaching/extraction	26
2.5.1 Ammoniacal leaching	26
2.5.2 Cyanide leaching	28
2.5.3 High pressure sulphuric leaching	29
2.5.4 Bio-extraction	30
2.6 Metal recovery from leachates	31
2.6.1 Electrowinning	31
2.6.2 Chemical precipitation	32
2.6.3 Metal adsorption	33
Adsorption by magnetic nanoparticles	34
Bio-sorption	34
Molecular recognition	35
Zeolites	36
Situation Part Metallic organic frameworks	36
2.7 Metal-organic frameworks (MOFs) for metal recovery	36

2.7.1 MOFs as a subclass of coordination polymers	36
2.7.2 Applications	37
Gas storage	37
Separation	37
Catalysator	37
Drug delivery	37
Corrosion inhibition	38
Other applications	38
2.7.3 Available MOF-based metal recovery technology	38
2.8 Imidazole-based MOFs chemistry	39
2.8.1 ZIF-8 structure	39
2.8.2 ZIF-8 chemical characteristics	40
2.9 Formation of ZIF-8.....	42
2.10 Synthesis methods	43
3. Materials and methods	47
3.2 Future experiments	49
4. Results and discussion.....	49
4.1 Metal leaching results	49
4.2 Conclusions of the experimental work	53
5. Conclusion	53
Bibliography	54
Appendix 1	61
MOF synthesis	61
Deel 2 Artikel	65
Een nieuwe methode voor de uitloging van metalen door het gebruik van basische, organische uitloogmiddelen Master's thesis	66
Abstract	66
Introductie.....	66
Methodologie	68
Resultaten en Discussie.....	68
Conclusie	75
Aanbeveling voor verder werk	76
References.....	76
Annexes	79

List of tables

Table 1 Metal concentration in common wastewater streams (mg/L) [18]	23
Table 2 Metal amounts in tailings [20]	24
Table 3 Overview of the synthesis parameters of the 2-methylimidazole based MOF	44
Table 4 Concentration distribution of the lixiviants	47
Table 5 Maximum reachable metal concentrations and initial content from the roasted tailing	49
Table 6 Leaching efficiencies of a roasted tailing with TEA as lixiviant	49
Table 7 Metal concentrations of the leachates from the roasted tailing with TEA as lixiviant	50
Table 8 Leaching efficiencies of a roasted tailing with NH ₄ OH as lixiviant	51
Table 9 Metal concentrations of the leachates from the roasted tailing with NH ₄ OH as lixiviant	51
Table 10 Maximum reachable metal concentrations in the leachates and initial content in Cr/Ni sludge	52
Table 11 Leaching efficiencies of the Cr/Ni sludge with TEA as lixiviant	52
Table 12 Metal concentrations of the leachates from the Cr/Ni sludge with TEA as lixiviant	52

List of figures

Figure 1 Ternary system of slags [2].....	18
Figure 2 Revolution of steel capacity [4].....	18
Figure 3 global estimation of waste production of metals [16].....	21
Figure 4 EOL-RR values of metals [17].....	22
Figure 5 Formation of secondary minerals examples [22].....	25
Figure 6 Pourbaix diagram of Cu-ammonia system at 298.15 K and 10^5 Pa, [Cu]=1 M and [NH ₃]=1 M	27
Figure 7 Kinetics of cyanide leaching of CuO[28].....	28
Figure 8 Leaching recovery sulphuric acid [29].....	29
Figure 9 Electrowinning procedure [35].....	31
Figure 10 pH dependency of Cobalt precipitation.....	32
Figure 11 Pourbaix diagram of Cu-H ₂ O system, [Cu]=0,259 M.....	33
Figure 12 Molecular recognition of Cu ²⁺ by a crown ether.....	35
Figure 13 Adsorption pattern of Cu by a crown ether [44].....	35
Figure 14 Cation exchange zeolites [45].....	36
Figure 15 Corrosion inhibition mechanism of ZIF-8 in HCl [53].....	38
Figure 16 ZIF-8 [62].....	39
Figure 17 Bridging angles in metal imidazolates and zeolites [63].....	39
Figure 18 Crystal structure evolutions ZIF-8 [65].....	40
Figure 19 TGA curves of ZIF-8 nanocrystals synthesized from different Zn sources [68].....	41
Figure 20 Hydrolysis of ZIF-8 [74].....	42
Figure 21 Formation of ZIF-8 [75].....	42
Figure 22 Hydrolysis of 2-methylimidazole [75].....	42
Figure 23 Hydrolysis of TEA [75].....	42
Figure 24 Deprotonation of Hmim by the use of TEA [75].....	43
Figure 25 Comparison of Zn sources in the formation of ZIF-8 [68].....	47
Figure 26 Centrifuge Eppendorf 5810 apparatus.....	48
Figure 27 XRF Niton apparatus.....	48
Figure 28 The pH values of the TEA leachates after reaction, relative to the initial concentration of TEA.....	50
Figure 29 Autoclave reactors.....	62

Glossary

Abbreviation/Chemical formula	Description
DL	Detection limit
Hmim	2-methylimidazole
ICP-OES	Inductively Coupled Plasma-Optical Emission Spectroscopy
MOF	Metallic Organic framework
XRF	X-Ray Fluorescence
XRD	X-Ray diffraction
ZIF-8	Zeolitic imidazole framework 8

Abstract

METAL RECOVERY FROM A MINERAL WASTE STREAM- SYNTHESIS OF METAL ORGANIC FRAMEWORKS

By: Sam Haenen

Promotors: Dr. Ir. Maarten Everaert
Prof. Dr. Ir. Leen Braeken

Metal recycling technologies have gained a lot of interest due to concerns of material availability and the environment. In this master's thesis, an advanced metal recovery pathway is investigated to selectively recover metals (Zn, Cu, Pb and Ni) from a mineral waste stream. In the end, these valuable metals were employed in an aqueous synthesis of imidazolate metal organic frameworks (MOFs).

In the first step, optimal leaching conditions for metal dissolution from mineral waste were examined by varying the concentration of the lixiviant triethylamine. Leaching results obtained with triethylamine were compared with those of ammoniacal leaching. The leaching solutions were analyzed by ICP-OES, XRF and pH measurements to define the leaching efficiencies as well as the selectivity.

Secondly, the optimal synthesis conditions of imidazolate MOFs were determined. The concentration of 2-methylimidazolate and triethylamine were varied. These samples were characterized by ICP-OES analyses, pH measurements and XRD analyses.

In the end, the leaching method and MOF synthesis were executed consecutively to optimize the whole procedure. Analysis with XRD and ICP-OES were included to assess the leaching efficiency, material yield and selectivity of metal precipitation.

Further progress in the development of this new metal recovery technology can be achieved by examining the MOF crystal structure and crystal size related to the procedure. Furthermore, up-scale possibilities of this recycling method must be investigated.

Abstract (Dutch version)

Metaal winning uit een minerale afvalstroom om uiteindelijk Metallic Organic frameworks mee te synthetiseren

Door: Sam Haenen

Promotors: Prof. Dr. Ir. Leen Braeken

Dr. Ir. Maarten Everaert

De metaal recyclage industrie heeft vandaag de dag zeer veel interesse vergaard doordat het milieu meer en meer centraal komt te staan. Het doel van deze masterproef is het bepalen van een geavanceerde uitloog methode om de metalen Zn, Cu, Pb en Ni selectief te herwinnen uit een minerale afvalstroom. Uiteindelijk zullen deze metalen gebruikt worden om *imidazole Metallic Organic Frameworks* (MOFs) te synthetiseren in waterig milieu.

Allereerst zijn de optimale loog condities bepaald waarbij de concentratie TEA, de actieve stof in het loogmiddel, is gevarieerd. Daarnaast is de methode vergeleken met de klassieke ammonium logging. De stalen zijn geanalyseerd door middel van ICP-OES, XRF en pH metingen om de looгеfficiëntie en de selectiviteit te bepalen.

Ten tweede zijn de optimale synthesecondities van de imidazole MOFs bestudeerd waarbij de concentratie 2-methylimidazole en triethylamine zijn gevarieerd. De stalen zijn onderzocht door ICP-OES analyses, pH metingen en XRD analyses.

Uiteindelijk zijn de loog methode en MOF synthese achtereenvolgens uitgevoerd om de hele methode te optimaliseren. XRD en ICP-OES analyses zijn uitgevoerd om het resultaat te evalueren.

Verdere verbeteringen kunnen in de toekomst behaald worden door de kristalstructuur van de MOFs gerelateerd aan de hele procedure te onderzoeken. Daarnaast kunnen ook opschaalmogelijkheden bekeken worden.

1. Introduction

1.1 Context

The project is executed in VITO, situated in Mol, in the department of Sustainable Materials Management. The project can be divided into two different parts. The first part focusses on an innovative method to recycle valuable metals such as Zn, Cu, Pb and Ni from mineral waste streams. In theory, metals can be reused endlessly. The main advantage of metal recycling is the fact that nature/bio-system can be maintained as well as the natural resources in the contrary with the classic mining industry. Therefore, the transition of a waste stream into a valuable product is required to close the circle of material.

In this case, the recovery of metals is performed on a mineral waste stream (e.g. sulfidic tailing or Cr/Ni-sludge). These residues often still contain low, yet interesting amounts of valuable metals. This remaining fraction of metals can be recovered via leaching, for the objectives of i) efficient raw material use and ii) avoiding environmental issues related to metal toxicity (e.g. soil and water contamination). Leaching of metals from mineral residues is, however, often not selective, yielding leaching solutions containing a range of metals. In order to recover metals selectively from leachates and to valorize those metals, a novel approach is considered to use the leachate as a mixed-metal solution for the selective in-situ synthesis of metal-organic frameworks (MOFs). MOF materials, known for their high surface area and thermal stability, can be used in gas adsorption, catalysis and separation technology, and can thus be valuable end-products of a selective metal recovery process.

The second part consists of an article where an advanced leaching method is investigated to selectively recover metals from mineral waste streams by the use of organic, alkaline lixiviants. The implementation of organic, alkaline lixiviants could enhance the leaching selectivity.

1.2 Problem definition/Research question

The motivation of this study was to use leachates obtained from mineral residues, containing, Zn, Cu, Pb and Ni, to create a valuable end-product, a MOF material, and thereby suggest a new environmentally-friendly metal recovery process.

The main research question is: "Is it possible to synthesize MOFs from the remaining metals (Zn, Cu, Pb, Ni) originating from a tailing?" This question can be further divided in four parts.

1. What is the optimal leaching method to obtain most of the leachable target metals (Zn, Cu, Ni and Pb) without addition of many interfering metals as Fe, Si, Al,...?
2. What are the optimal synthesis conditions to prepare MOFs in a leachate stream, considering the reaction time/temperature, concentration 2-methylimidazole and concentration triethylamine?

To answer this question, it is important to study the concentrations of the target metals reached by leaching to adapt the reaction variables.

3. Is it possible to capture the different metals selectively and consecutively by changing the leaching conditions and the MOF synthesis conditions ?
4. What are the optimal MOF synthesis conditions for the selective recovery in terms of reaction temperature, reaction time, reagents concentrations/ratios, pH, presence triethylamine, ...?

1.3 Research objectives

The main objective is the development of a selective recovery pathway for valuable metals from leachates (Zn, Cu, Pb, Ni) via the synthesis of MOFs, this by the addition of an organic linker 2-methylimidazole and organic base triethylamine. This new recovery method is intended to be possible on an industrial scale regarding economic factors and recovery efficiency. Furthermore, this technology must be environmentally friendly.

The first challenge is to find the optimum leaching conditions depending on the effect of the concentration of triethylamine for Zn, Cu, Pb and Ni from mineral residues. Therefore, the leaching concentrations of these metals, as well as those of other interfering elements, must be determined by ICP-OES. Additionally, the reaction kinetics of metal leaching will be investigated to determine the most optimal reaction time for maximal metal leaching.

Secondly, the optimal MOFs synthesis conditions will be determined by synthesis of pure metal reagents (metal nitrate salts). This will help in the design of the conditions needed for MOF formation from actual leachate solutions containing metals derived from mineral residues. The optimal reaction conditions will be defined by considering the TEA concentration, reaction temperature, reaction time, 2-methylimidazole/metal ratio, pH,...

Thirdly, the MOFs reaction kinetics must be understood to be able to form selectively MOFs with one metal, starting from a mixed-metal solution. E.g. first form MOFs with Zn, afterwards with Cu and in the end selectively with Pb.

Finally, MOFs will be made starting from an actual leachate derived from the extraction of metals from a mineral residue. By following this approach, the aim is to obtain maximal and selective recovery of the metal as a phase-pure MOF material. Eventually, the final method can be overviewed to look for further possibilities on a larger scale, or to expand this technology towards other leachate streams.

2. Literature

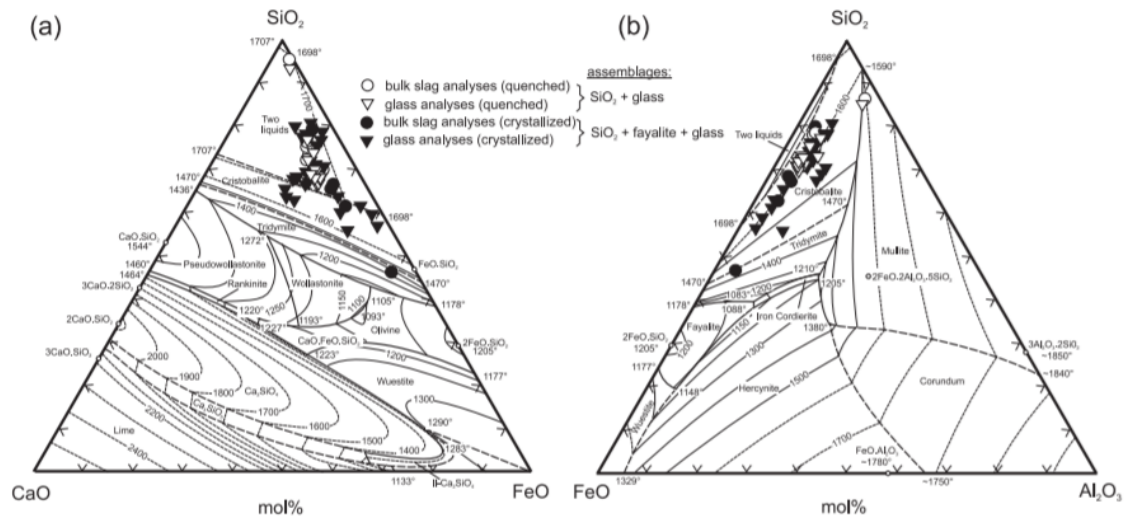
2.3 Situation

First there is given a broad introduction of the metal recycling industry, starting from the traditional processes of the primary resources. It is important to understand these principles to introduce a sustainable recycling method. Afterwards a broad overview of metal containing waste streams is presented. Furthermore certain leaching methods are listed to examine an appropriate method for the target metals (Zn, Cu, Ni and Pb) which will form the base of the metallic organic framework (MOF) synthesis. Finally certain metal recovery techniques are discussed. Afterwards the MOF synthesis is examined. Section ... contains more information of the discussed literature about MOFs.

2.2 Primary resources

The primary source of metals are mineral resources, i.e. ores present in the earth crust. Extracting metals involves a complex and numerous series of steps, each of which requires expertise and investments. The exploration and development phase from initial discovery to actually mining may last 10 years and longer. The mining itself is based on two main principles: surface mining and sub-surface mining. Surface mining indicates the removal of surface vegetation, dirt and layers of bedrock to reach buried ore deposits in the contrary with sub-surface mining where tunnels or shafts were dig into the ground to reach deeply buried ore deposits. Another possibility is in-situ leaching but this technology is still in the experimental phase.

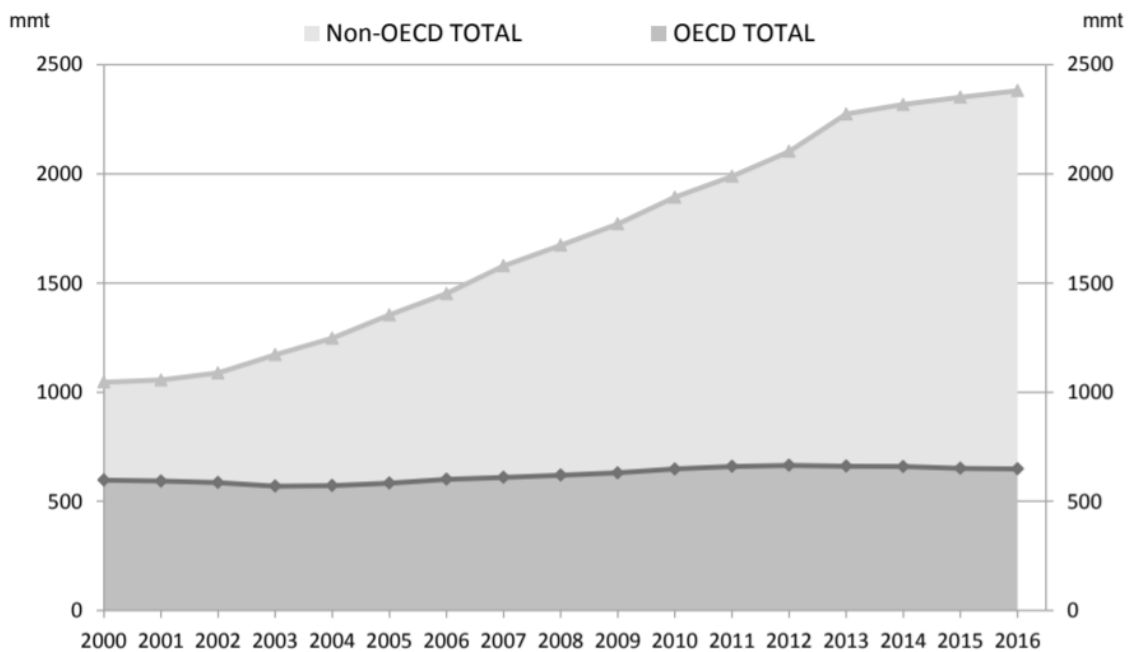
After the ore is gained, the metal bearing minerals are separated from waste material to form a concentrate. This separation is performed by crushing and sieving the ores. Afterwards a chemical agent can be added to gain a higher metal fraction. The received waste from these processes is called tailings. The tailing can contain certain ppm's to several wt% of valuable metals, depending on the source and the treatment. Afterwards, the concentrates are treated to gain pure metals. For this, a variety of methods are available. The most common technique is smelting. Due to the heating and melting the minerals undergo a chemical breakdown resulting in impure metal shapes which are purified in refineries. The metals are combined with oxygen and due to the high temperatures the oxygen will bond to the carbon to form carbon monoxide or carbon dioxide. Furthermore, a flux is added which is substance introduced to remove other impurities in the form of slag and to increase the fluidity. Examples of a flux are limestone, borax, silica and dolomite. [1] Recent slag studies developed $\text{SiO}_2\text{-FeO-CaO}$ or $\text{SiO}_2\text{-Al}_2\text{O}_3\text{-FeO}$ ternary diagrams for the reconstruction of crystallization sequences, estimation of the formation temperature and cooling rate. Figure 1 shows the according ternary systems. These diagrams are valuable for CaO- and Al_2O_3 - enriched slag smelts. [2]



- Figure 1 Ternary system of slags [2]

Another possible method for gaining pure metals is hydrometallurgy. The metals are separated from the minerals by dissolving them. This process often requires acids or cyanide followed by a method to remove the metals from the leachate, for example electrowinning or solvent extraction [3]. Hydrometallurgy is based on thermodynamic principles, electro-chemical reductive processes and crystallization of salts.

To give an idea of the production capacity of metals, the production of steel is examined. This production capacity is increased drastically from 1,05 billion metric tons in 2000 to 2,39 billion tons in 2016 resulting in an overcapacity of 540 million tons. Figure 2 shows this evolution.



- Figure 2 Revolution of steel capacity [4]

The data originates from the Organization for Economic Co-operation and Development (OECD). Figure 2 shows the incline in production, although the increase since 2015 has a slower rate than in the past. [4]

2.3 Metal recycling

Recently, research towards technology to recycle metals from waste streams has gain a lot of interest. From the viewpoint of the society as a whole, metal recycling technology puts forward a range of advantages compared to traditional practices. The main advantage is the opportunity to reduce the extraction of natural ores resulting in a longer lifetime of those resources. The following paragraphs discuss other positive effects of metal recycling. There is started with the environmental aspect followed by an energy efficiency analysis. In the end the role of the government is slightly touched.

2.3.1 Advantages of metal recycling

Metal recycling will lead to more environmentally friendly industries. Limited metal recycling can cause a possible threat for the public health. For example small metal fractions can indirectly end in the food chain after passing several steps examined in this section. Heavy metals are not biodegradable and can accumulate in organisms leading to unwanted side effects, e.g. interference with essential metals, interactions with cellular macromolecules, such as phospholipids, nitrogen or sulphur within RNA or even DNA and exerting oxidative stress [5]. Metals such as Cd, Cr, Hg and Pb are examples of potentially harmful contaminants which can negatively affect plant development and may influence the elemental composition of harvested crops, leading to the contamination of the food chain. Also via aquatic ecosystems, heavy metals can be distributed in the food chain. In this case, planktons play an important role, because they serve as food source for many aquatic organisms. Zooplankton accumulate metals at a faster rate because they are more active in utilizing the detrital and suspended organic particles, which are effective in complexing heavy metals. Therefore, plankton can also be used as biomonitor to study metal pollution. Soil and water contaminations are the most common threats. Mining, metallurgy, pesticides and fertilizers act as the main sources of contamination [6]. Now the effects of Zn, Cu, Ni and Pb on the human body are declared. Zinc is an important element for the human body, e.g Zn is required for the optimal function of more than 300 enzymes by serving as catalyst. Generally it is responsible for a large amount of interactions with proteins which are crucial for the human body. A RDA value (recommended daily allowance) of 15 mg for men and 12 mg for women is allowed. An excess of Zn, however, can result in many diseases. It create problems in the pancreas and liver by disturbing the enzymatic working [7]. The human body also requires small amounts of Cu. Furthermore Cu forms a low risk for the human health due to the defence system of the human body. Therefore the liver and kidneys produce metallothionein which can bond with Cu to form a complex. The advantage of this complex formation is the increased water solubility of Cu, which facilitates excretion. Cu appears in the blood between 120-140 µg/l [8]. Besides Zn and Cu, an excess of Pb causes a reduced cognitive development and intellectual performance in children. In adults it leads to cardiovascular diseases together with an increased blood pressure [9]. Also Ni has many health risks. An excess can cause several cancers, heart disorders and lung disorders [10]. Specifically for mining activities, acid mine drainage (AMD) and the greenhouse gas emissions form a risk for respectively the water ecosystems and the climate. However, the impact on the environment depends on the mining and processing methods, the ore type, the quality of environmental management and risk control and the ability of the local ecosystem to buffer the impacts. [11]

Metal recycling has potential to be much more energy-efficient than traditional metal production. It is known that a factor of 10 or 20 can be saved in the energy consumption by recycling, depending on the metal and the waste stream [12]. Note that this energy reduction is not valuable for every metal

waste stream. Recycled aluminium requires 95% less energy, while copper needs 90 percent less and steel 56 percent less by scrap metal recycling. Additionally the recycling of one ton of steel avoids the use of 1134 kg of iron ore, 1400 kg of coal and 54 kg of limestone [13]. Thus metal waste will always be a potential source of metals as pointed by Jacobsen (1960): "the cities of today are the mines of tomorrow. [12]" It is clear that the recycling of metal scrap leads to energy savings in the contrary with the metal recovery of waste streams containing small amounts of metals where often the energy efficiency is disputed. Therefore, recycling is become an integral part of industrial activity and has become a major challenge. Mining and metallurgy are slow and energy intensive processes in comparison with recycling [14]. Moreover they cause an extensive environmental degradation while recycling conserves the natural resources while decreasing the amount of waste. Examples of important facilities with high production capacities for recycling include Umicore, (-Belgium), Boliden, (-Sweden), Xstrata, (-Australia), Xstrata, (-Canada). On the other hand, in some developing countries, e.g. India, recycling activities are carried out by an unorganized sector using highly polluting technologies leading to extensive damage to the environment and causing severe health hazards due to the handling of hazardous substances and poor work place environment [14].

2.3.2 Role of the government

The government can play an important role in the metal industry, by installing subsidy and tax systems to influence the use of primary or secondary metal (recycling) sources. In literature, there is proven that secondary metal sources have the potential to reach more profit [15]. However, the established market conditions are adapted to the primary production by low taxes on favour of energy-intensive primary production, while the labour intensive secondary sector is disadvantaged by high taxes on labour. Furthermore, the primary sector receives much higher support of governments by higher research funds and extra support to locate metals. These factors contribute to a less profitable recycling industry. It is clear that the political fight between the energy reduction as a consequence of recycling versus rural development as a result of opening new mines will go on tomorrow [15].

2.4 Current state of metal industry

In modern times rapid industrialization and increased human activities generate large amounts of waste, which is often enriched in metals. In this section, a broad overview of the metal waste production is given. Afterwards certain metal containing waste streams are discussed, zooming in on waste water and tailings because these are two common metal-rich waste streams originating from mining activities.

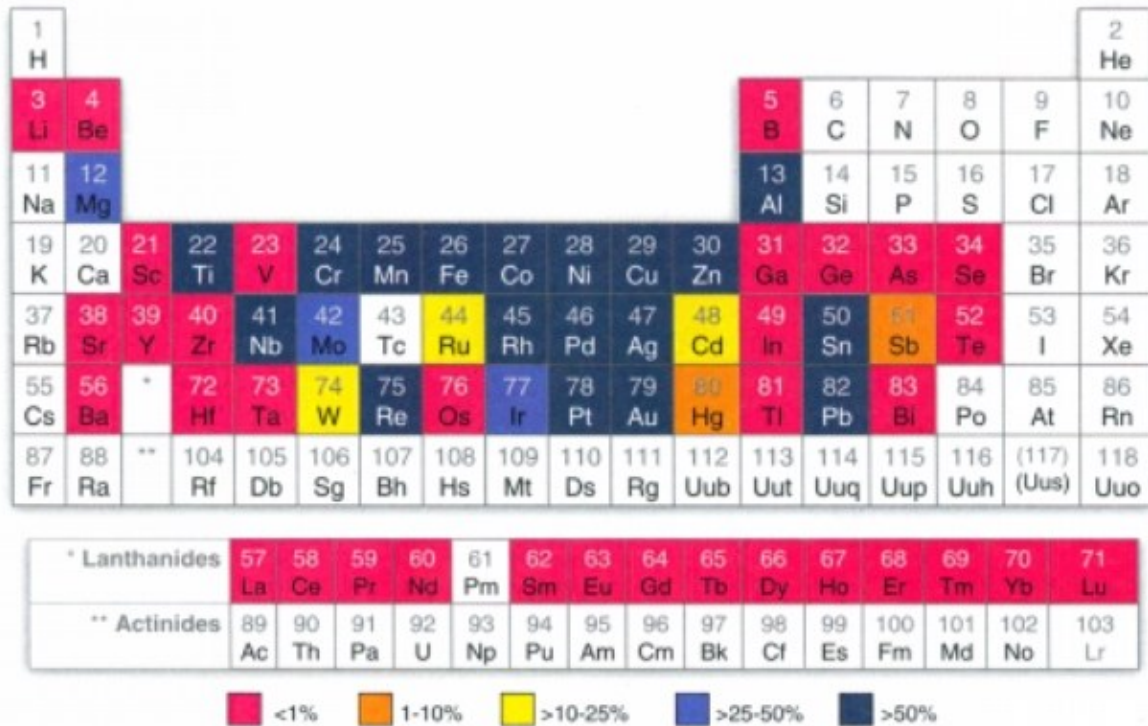
2.4.1 Metal containing waste streams

Numerous industries, such as electroplating, metal-finishing, electronic, steel and nonferrous, petrochemical and pharmaceutical industries, produce a variety of waste containing (toxic) metals. An estimation of the global waste production of metals in different industries is presented in Figure 3.

Industries	Metals	Quantities (t/year)
Electronic	As, Cr, Hg, Se, Ni, Cu	1,200,000
Oil and Coal	As, Pb, V, Cd, Ni, Zn	1,200,000
Mining and Metallurgy	Hg, Cr, Cu, As, Zn, Pb	390,000
Agriculture	Mg, As, Cu	1,400,000
Manufacturing	Cr, Co, Ni, Fe	240,000
Others		720,000

- *Figure 3 global estimation of waste production of metals [16]*

In theory, metals are infinitely recyclable. Yet, in practise recycling processes are often inefficient or even non-existent due to limits imposed by social behaviour, product design, recycling technologies or thermodynamics of separation. The current industrial reality is still far away from closed-loop material systems. However, industry and research take important steps to close the material cycle [17]. The economic value of the metals and the volumes of the waste stream are the two most important factors to influence the recycling efficiency. The largest fraction of currently recycled metals is represented by metals that are typically used in large quantities. These metals occur in a relatively pure form, making it relatively straightforward to remelt and reuse. Examples of this are steel, aluminium, copper, zinc, lead and nickel. In order to quantify the amount of metal recycling, the End-of-Life Recycling Rate indicator (EOL-RR) can be used. Figure 4 shows the EOL-RR indicator for each element. This indicator is defined as the fraction of metal in discarded products that is reused in such a way that it retains its functional properties. This general indicator factor thus depends of the collection rate of end-of-life products and the efficiency of the subsequent separation and processing steps, all involving complex interactions of a wide variety of players.



- Figure 4 EOL-RR values of metals [17]

A clear distinction in the EOL-RR value for metals can be observed (Figure 4). On the one hand, commonly used base metals (Fe, Cu, Zn, etc.) typically have EOL-RR values above 50%. On the other hand, less common elements (Li, V, Ba, etc.) are seldom recycled. These metals are used as small amounts for very precise technology demands, such as red phosphors, high-strength magnets, thin film solar cells and computer chips. Especially for this last group, recovery is technologically and economically challenging and, therefore, the consideration of recycling is barely made.

2.4.2 Waste water

Waste water streams from all over the world contain certain amounts of metals. Nowadays there are still a lot of factories who discharge their metal contaminated waste stream on the municipal water net due to the high costs and maintenance of a proper water purification. Table 1 shows typical metal concentrations that can be found in common wastewater streams (mg/L).

- *Table 1 Metal concentration in common wastewater streams (mg/L) [18]*

Name	Symbol	Price (USD/kg)	Municipal treatment plant	Road wash water	Tannery	Mining	Battery factory
Aluminum	Al	1.85 ^a		0.467–26.1		0.161	0.2–7.3
Antimony	Sb	9.75 ^b					
Arsenic	As	1.43 ^c	0–0.0019				
Barium	Ba	100 ^c					
Bismuth	Bi	23.4 ^d					
Cadmium	Cd	1.87 ^e	0–0.0033		0.056	0.004	0.02–0.12
Calcium	Ca	110 ^f			255	548	83–255
Chromium	Cr	8.8 ^c	0.04–0.56	0.004–0.107	391		<0.0044–0.08
Cobalt	Co	30.2 ^a			1.55	0.0126	
Copper	Cu	6.72 ^a	0.079–0.58	0.0111–0.177		0.244	<0.0033–0.38
Gold	Au	46378.6 ^a					
Iron	Fe	0.2 ^g	0.48–3.9	2.59–26.8	4.4	0.033	0.02–20
Lead	Pb	2.09 ^a	0–0.039	<0.018–0.053	0.872		4.0–13
Magnesium	Mg	5.84 ^a			268	29.52	15–26
Manganese	Mn	2.2 ^a	0.067–1.16		0.396		0.04–0.6
Mercury	Hg	2.9 ^h	0–0.0002				
Molybdenum	Mo	33.0 ^a		0.0154–0.021			
Nickel	Ni	18.45 ^a	0.0067–0.77	<0.006–0.0525	0.179	0.142	0.07–0.38
Potassium	K	22 ⁱ			183	34.9	
Silver	Ag	735.8 ^a	0–0.0014				
Sodium	Na	3.3 ^j			25519	100.05	
Strontium	Sr	1000 ^c					
Tin	Sn	22.6 ^a	0–0.028				
Vanadium	V	26.5 ^a					
Zinc	Zn	2.14 ^a	0.26–0.75	0.105–1.56	0.684	0.023	0.6–17
Estimated monetary value (USD) ^k			0.02	0.06	121.35	61.56	28.29

It can be concluded that, generally, industrial wastewaters contain much higher amounts of metals than municipal wastewater, including metals with a higher market value (ex. Ag, Cu, Au, etc.) following table 1. In general, the concentrations of metals in wastewaters are relatively low, ranging from µg/L to mg/L level. Large volumes of wastewater and efficient separation procedures are needed to make a recovery process meaningful. Nowadays, several physical, chemical and biological technologies are developed to this goal, such as electrodialysis, membrane-based processes and chemical precipitations.

2.4.3 Tailings

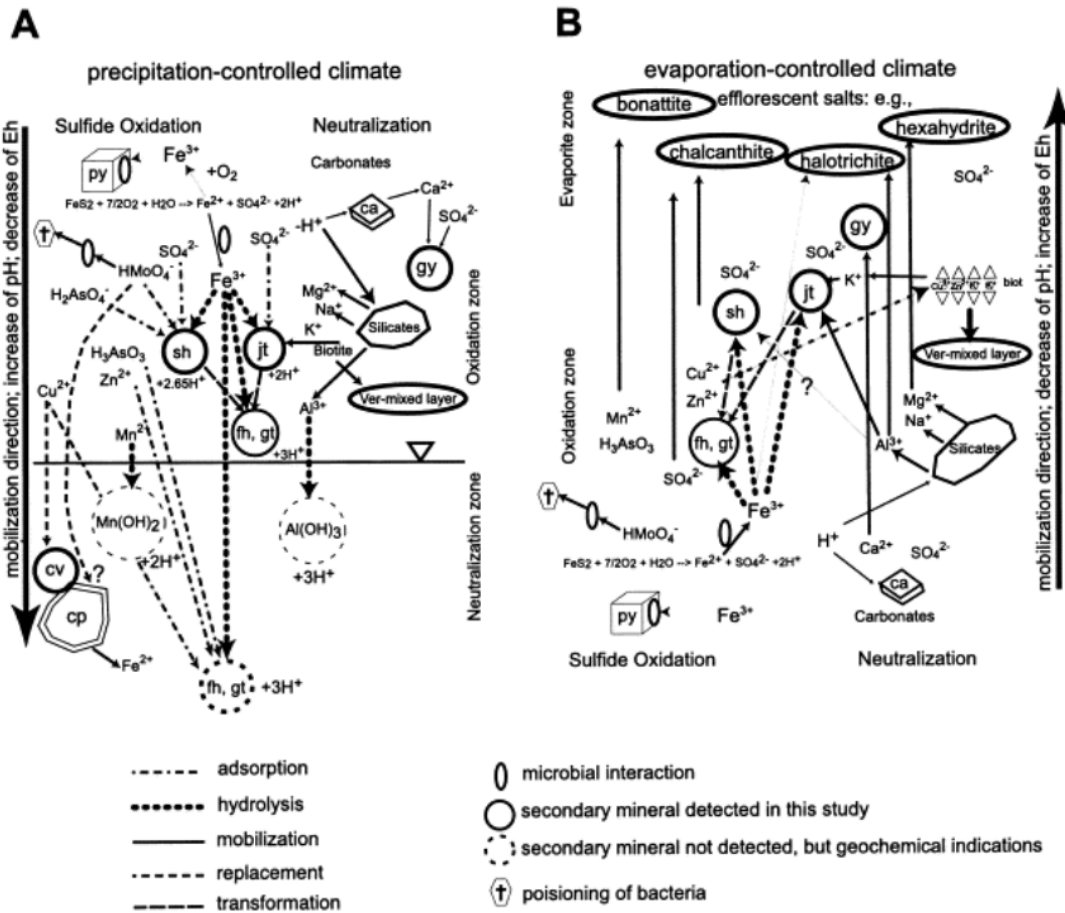
In section 2.2 the emergence of tailings is explained. Furthermore it is made clear that this waste stream still consist certain amounts of metals. Due to improvements in technology, lower grade ores can now be exploited resulting in much higher amounts of tailings consisting much lower metal percentages in comparison with the past [18]. Thousands tonnes of tailings are produced yearly and this amount still rises due to the declining grade of metals in available ores, e.g. in Canada the Ni grade was 5% in 1885 and declined to 1,5% in 2005, moreover in Australia the Cu grade was 10% in 1885 and lowered to 1% [19]. Table 2 shows the amounts of Zn, Pb, Ni and Cu present in tailings from all over the world to give an idea of recent amounts.

- *Table 2 Metal amounts in tailings [20]*

Location	Aznalcollar, Spain	Piscinas, Sardinia	San Luis, Potosi, Mexico	Leechang, China	Lavrion, Greece	Algares, Portugal	Virginia, USA	Boliden, Sweden	Milluni, Bolivia	Potosi, Bolivia
Reference	Hudson-Edwards et al (2003)	Concas et al (2006)	Castro-Larragoitia et al (1997)	Ye et al (2002)	Kontopoulos et al (1995)	Bobos et al (2006)	Seal et al (2008)	Gleisner and Herbert et al (2002)	Salvarredy-Aranguren et al (2008)	Kossoff et al (2011)
Zn (mg/kg)	7400	7300	2000	5021	5000-50000	3723	2178	5290	26700	26600
Pb(mg/kg)	8500	4100	3000	1642	10000-30000	6805	3528	1850	846	2180
Ni(mg/kg)	20	25				5	10	11,3		
Cu(mg/kg)	1600	84	400	192		727	453	640	3350	502

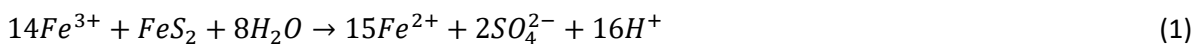
This table proves the opportunities of metal recovery from tailings due to production amounts of these tailings together with the remaining metal fraction. This remaining fraction is still small in comparison with Fe and Si which are present in abundance. The chemical composition of tailings depends on the type of ores, the treatment to gain the target metals, the efficiency and the storage of the tailings. In general, there are three categories of tailings: the gangue fraction, the sulphide-oxide fraction and the secondary mineral fraction [19]. The gangue fraction contains particularly quartz (SiO_2). Also, feldspar structures characterize this fraction which are $\text{KAlSi}_3\text{O}_8 - \text{NaAlSi}_3\text{O}_8 - \text{CaAl}_2\text{Si}_2\text{O}_8$. The earth's crust consist about 42% of these Si-riche structures and arise by sedimentation through air or wind followed by compacting pressure of overlying deposits and precipitation of minerals, Kumar et al (2017) [20]. This waste fraction is often utilized in the concrete production, whereby it enhances the thermal resistance resulting in better insulation properties [20]. In the sulphide-oxide fraction especially metal-sulphides are present, most of all FeS_2 . Although, sphalerite (ZnS), chalcopyrite (CuFeS_2) and galena (PbS) will be found in this matrix. Secondary minerals form the third category. The characteristics depends on the mineral source and local conditions such as micro-organisms, pH, presence of oxygen, climate,... Micro-organisms will serve as a source of protons due to the release of acids. Moreover they can decompose into carbonic acid. Thus microorganisms can decrease the pH [21]. The climate will determine the evaporation and precipitation cycle of water which influence the mobility of the metals. Furthermore, the presence of oxygen will cause oxidation of sulphide compounds together with the formation of iron oxide/hydroxide phases.

To conclude, the formation of secondary minerals in tailings is presented in Figure 5. This figure does not present all secondary minerals but gives the main examples from a porphyry Cu tailings. The left part of the figure deals with precipitation-controlled tailings and the right part with evaporation-controlled tailings.

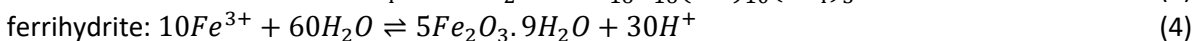
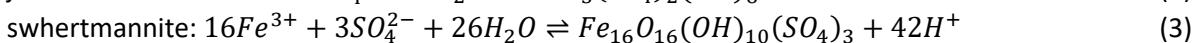
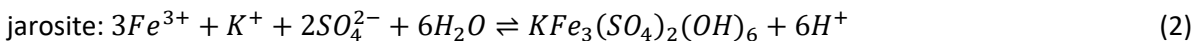


- Figure 5 Formation of secondary minerals examples [22]

In Figure 5 the abbreviations mean the following: jarosite(=jt), schwertmannite(sh), ferrihydrite(fh), goethite(gt), covellite(cv), gypson(gy), pyrite(py). Figure 5A shows that sulfide oxidation results in the release of Zn^{2+} , Cu^{2+} , Fe^{2+} , Mn^{2+} , $HMoO_4^-$, $H_2AsO_4^{2-}$, SO_4^{2-} and protons. The following equation shows that Fe^{3+} can serve as sulfide oxidant:



Furthermore, Fe^{3+} can contribute to the formation of secondary minerals as sh, jt, fh, gt. The following equations declare these formations:



The protons can react with the neutralizing minerals, silicates and carbonates. Moreover, the release of protons does not only control the pH, but can also result in the release of certain cations (e.g. Ca^{2+} , Mg^{2+} , Al^{3+} , K^+ , Na^+) and thereby the formation of secondary minerals. For example, K^+ is the limiting reagent during the formation of jarosite. Furthermore Figure 5A is divided into two vertical parts: an oxidation and neutralization zone. In the oxidation zone, the divalent cations have a large mobility due to the acidic conditions. Therefore, they are leached out of this zone and end up in the neutralization zone where the pH is higher. This fact results in a change of the solubility whereby reduction processes can take place. However, anions are particularly absorbed to secondary ferric minerals in the oxidation zone due to the acidic character. Although the different oxidation states and local pH

differences can cause an increase of mobility of the anions resulting in an enrichment of the neutralization zone. These facts explain the arsenic problem which is often present in neutral effluents. Arsenic achieves a higher mobility even under neutral circumstances.

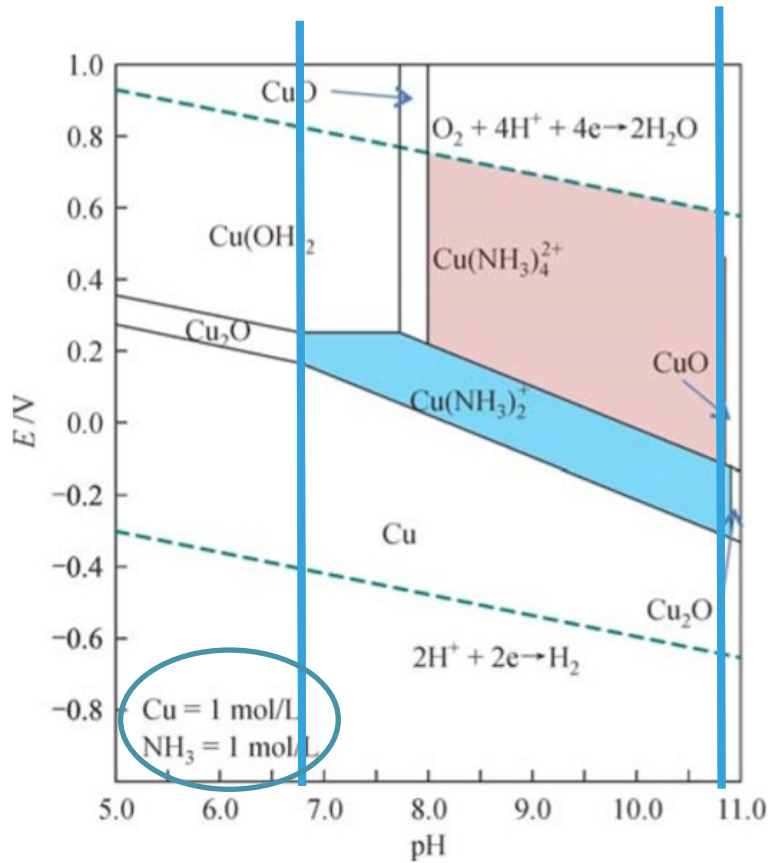
In figure 5B, the in-situ climate conditions are evaporation controlled leading to an upwards mobilization direction of the elements. The precipitation of secondary salts is controlled by supersaturation. Some examples of these secondary salts are chalcantite ($\text{CuSO}_4 \cdot 5\text{H}_2\text{O}$), bonattite ($\text{CuSO}_4 \cdot 3\text{H}_2\text{O}$), halotrichite ($\text{FeAl}_2(\text{SO}_4)_4 \cdot 22\text{H}_2\text{O}$) and hexahydrite ($\text{MgSO}_4 \cdot 6\text{H}_2\text{O}$). In this system, sulfide has not an important role in the formation of secondary minerals because it has high activity in the low pH oxidation zone. Furthermore metals in water-soluble form are present in the top of the tailings resulting in efficient and economic opportunities for metal recovery. Although this presence can pose a danger for the environment due to flush-outs during rainfalls [22].

2.5 Metal leaching/extraction

Metal leaching is the process of extracting a metal from a solid material, after it has been in contact with a liquid to form a solution. It is a selective way to gain metals, present in small amounts, with a high efficiency. Depending on the desired metal, and the original solid matrix, different solvents, named lixiviants, can be used. Here, the leaching technology for Zn, Cu, Ni and Pb recovery is examined.

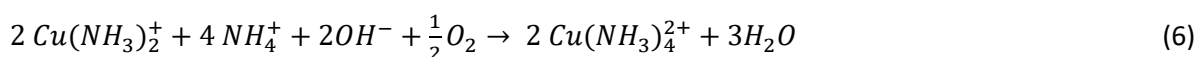
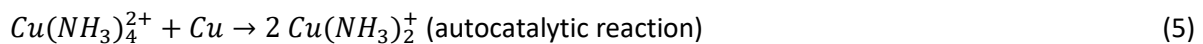
2.5.1 Ammoniacal leaching

Ammonia-based leaching process is a widely used leaching method to recover metals because of its low toxicity, low cost, easy recovery and high selectivity. Moreover, this method alleviates several corrosion problems. This approach is frequently practised to extract Cu from ore and for electronic waste enriched with Cu. The selectivity for Cu recovery by ammonia salts can reach 95%. Another approach to recover metals is the use of acidic reagents, e.g. HNO_3 , H_2SO_4 and HCl . However, this has as a consequence that a large amount of impure metals are leached, especially Fe and Pb. The removal of these impurities decreases the effectiveness of the approach together with the possibility of Cu loss. Therefore ammonia-based leaching can be seen as a promising approach together with the pH buffer capacity. Figure 6 shows the Pourbaix diagram of a copper ammonia phase.



- Figure 6 Pourbaix diagram of Cu-ammonia system at 298.15 K and 10^5 Pa, $[Cu]=1$ M and $[NH_3]=1$ M

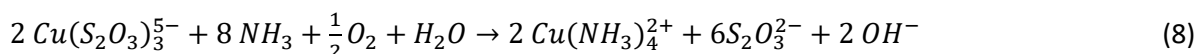
The $Cu(NH_3)_4^{2+}$ and $Cu(NH_3)_2^+$ are the stable amine complexes in the solutions according to the E-pH diagram. Furthermore, it can be found that ammonia complexes are stable in the pH range of 6.5 to 10.8. [23] The following reactions occur:



Due to the character of the autocatalytic dissolution of Cu from the alloy, cupric ions can be introduced to the leaching solution to force this autocatalytic reaction. This approach is only useful for copper-rich alloys, since various phase composition can inhibit spontaneous copper dissolution from the metallic phase. Moreover, Cu^+ ions are inert for the spontaneous dissolution of copper. Thereby ammonium thiosulfate is less effective because the homogeneous reaction between Cu^{2+} and $S_2O_3^{2-}$ ions can take place:

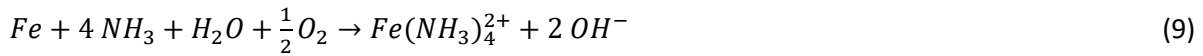


Due to this reaction the leaching solution will change from intensely blue to colourless. This problem can be prohibited by agitation and aeration:



Dissolved air enhances the homogeneous reaction and generates Cu^{2+} cations. Agitation of the bath, helps to get more dissolved oxygen in solution.

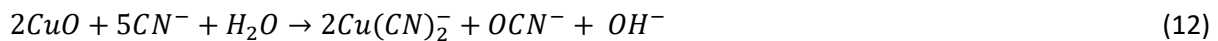
Other metals (e.g. Ni, Ag, Zn) present in the metallic phase could also be transferred into electrolyte as soluble amine complexes. Their rate of dissolution is determined by oxygen transport to the surface. Additionally, ammonium salts could remove iron by precipitation of Fe^{3+} hydrated oxides [24]. Following reactions occur:



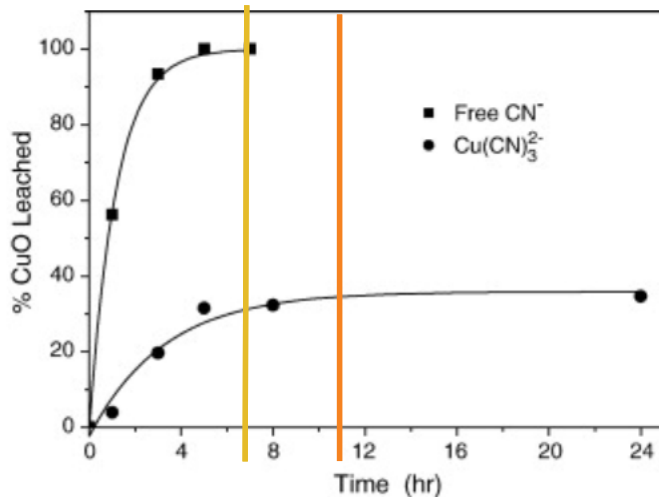
The ammonium chloride salts deliver the highest amounts of recovered iron due to their aggressive action towards corrosion of metals. A micro-environment is formed wherein chloride ions react with protons resulting in hydrochloric acid which is responsible for the accelerated iron dissolution [25]. Thus other ammonium salts, e.g. ammonium carbonate, will recover less iron due to the absence of chloride.

2.5.2 Cyanide leaching

E-waste contains a lot of small amounts of high valuable metals, e.g. Au and Cu. Cyanide leaching is often utilized for the recovery of these metals. This technique offers a high selectivity but is restricted due to the high toxicity of cyanide [26]. In this case the copper is dissolved by the formation of copper cyanide complexes: $CuCN$, $Cu(CN)_2^-$, $Cu(CN)_3^{2-}$. Here, the leaching kinetics of certain tenorite (CuO) are explained. Following reactions occur in the presence of cyanide:



The second reaction equation can occur due to the presence of CN^- ions in the $Cu(CN)_3^{2-}$ solution:

$$Cu(CN)_3^{2-} \rightleftharpoons CN^- + Cu(CN)_2^- \quad (14)$$


- Figure 7 Kinetics of cyanide leaching of CuO [28]

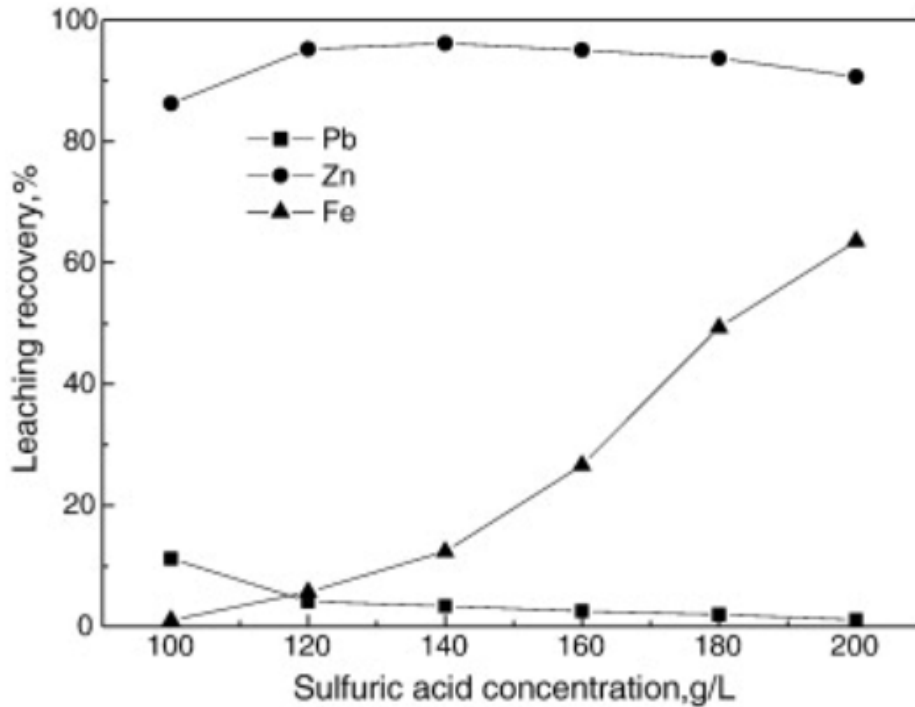
Figure 7 shows that the leaching of tenorite has a recovery rate of Cu for ca. 100% in 7 hours in a free CN^- solution. In a $Cu(CN)_3^{2-}$ solution the maximum Cu recovery amounts 30%, reached after 11 hours due to the restricted amount of CN^- ions [27].

2.5.3 High pressure sulphuric leaching

In this procedure, H_2SO_4 serves as lixiviant and is appropriate for the target metals discussed in this thesis (Zn, Cu, Ni and Pb). The main reaction is given for the dissolution of zincite:



For zinc a recovery of 98% can be reached as presented in Figure 8.



- Figure 8 Leaching recovery sulphuric acid [29]

In this case there is worked under pressure with the aim to reduce the dissolution of iron. A higher pressure brings more oxygen in solution which oxidizes the iron resulting in a decrease of 10% iron recovery. The following reaction represent this influence:



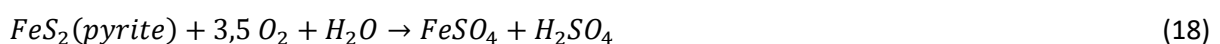
Pressures between 0.4 and 0.6 MPa are typically used. A further increase of pressure does not result in more effects, according to the literature. Many parameters influence the recovery results. A smaller particle size of the ores will lead to higher recovery rates. Besides the particle size, the stirring speed influences the procedure. In literature, many lab tests are described to reach the optimal stirring speed. A higher stirring speed leads to a higher Reynold number ending in a smaller mass transfer resistance. After a certain speed a plateau value is reached which indicates the minimum layer thickness is achieved [28].

Another challenge is formed by sewage sludge compost and soil for metal leaching procedures especially in China. In China, the concentrations of heavy metals in sewage sludge are markedly higher than sewage sludge in the USA and in Europe because municipal sewage treatment plants in China are likely to accept industrial wastewater. Pb, Cd, Ni, Cr, Hg, etc. are examples of the toxic metals. There is a very high environmental risk due to the lifecycle of sewage sludge. The heavy metals will be absorbed by plants and finally transferred to the food chain causing several threats to human health [29] [30]. It is

observed that the leaching results are highly dependent of the pH, therefore the EPA tests (Environmental Protection agency of the United states) are implemented. This test is widely adopt to investigate the leaching behaviour of various materials, such as contaminated soil, concrete and coal combustion fly ash. Europe produces yearly over 40 million tonnes of fly ash. Today there is a lot of effort to develop new technologies that allow the recycle of coal fly ash into added-value products. Therefore, geopolymeric matrices are synthesised for the retention of potentially harmful elements, such as Be, Bi, Cd, Co, Cr, Cu,... Geopolymers describe inorganic materials obtained from the chemical reaction of aluminosilicate oxides with alkali silicates, yielding polymeric Si-O-Al bonds. The network consists of SiO_4 and AlO_4^- tetrahedra linked alternately by sharing all the oxygen. The Al is represented in the Al^{3+} cationic form which demands the presence of cations in the framework to balance the negative charge. Possible cations are K^+ , Na^+ or Ca^{2+} . Due to these matrices, a leaching scenario under highly alkaline environment is required to encapsulate the pollutants [31].

2.5.4 Bio-extraction

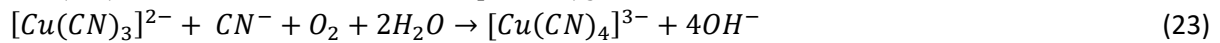
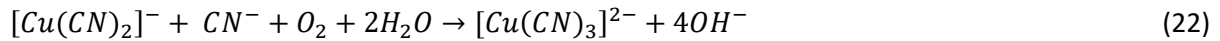
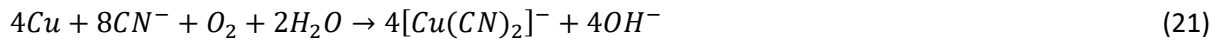
Furthermore, bio-extraction of metal contaminated waste of various industries with bacteria, archaea and fungi is explored. In nature, the role of microorganisms is investigated for the weathering of metal-containing minerals, rocks, metals and coals using oxidation and reduction processes where the metals are transformed to a different state as oxide, hydroxide, sulphate, etc. These principles have induced the development of commercially viable metal extraction technologies through microbial action. The first bio-leaching was implemented from a mine dump for the recovery of Cu. Today, even minerals/ores containing Cu, Au and Co are processed on industrial scale using microbes. Furthermore, microbial leaching has major opportunities for the processing of sulphides of Ni, Zn, Mo, Co, Ga, and Pb and the platinum group metals (Pt, Rh, Ru, Pd, Os, Ir) associated with sulphide minerals. Advantages of this leaching technique are low cost, low hazardous emissions and low-tech systems with the use of naturally occurring biocatalysts [32]. The bacteria *Thiobacillus ferrooxidans* is utilized for the Cu and Zn extraction and is studied intensively due to its commercial applications. This organism uses carbon dioxide as carbon source in an acid environment and acquired energy from the oxidation of iron or sulfur. The following reactions are believed to take place during the leaching by this bacteria starting with pyrite:



The end product of these reactions is ferric sulphate ($\text{Fe}_2(\text{SO}_4)_3$). This molecule will serve as oxidizing agent which can react with metal sulphides, represented as MS in the following equations:



Thereby the leaching procedure is declared. An advantage of this bacteria is the capability to oxidize sulphur to sulphuric acid and ferrous ions to ferric ions. This advantage makes the previous reactions cyclic. Zn from pulverized rock is recovered for 38% by the *Thiobacillus ferrooxidans* at 26°C in 15 days. Cu from a native sediment shows recovery rates of 100% in 24h by this bacteria. The literature explains this promising result of Cu by the smaller particle size of the native sediment (5 µm) [33]. Furthermore the *Aspergillus niger* reached recoveries for Cu and Ni from a slag of respectively 78,5% and 45,5%. A last example is given by cyanogenic microbes. These organisms can solubilize metals in solid wastes due to the release of CN^- and HCN as secondary metabolite. Cyanide can form complexes with solid Cu and dissolve them in water under alkaline circumstances. The *Bacillus megatorium* reached recovery rates of 96.73% for Cu from E-waste [34]. The following reactions declare the complex formation:

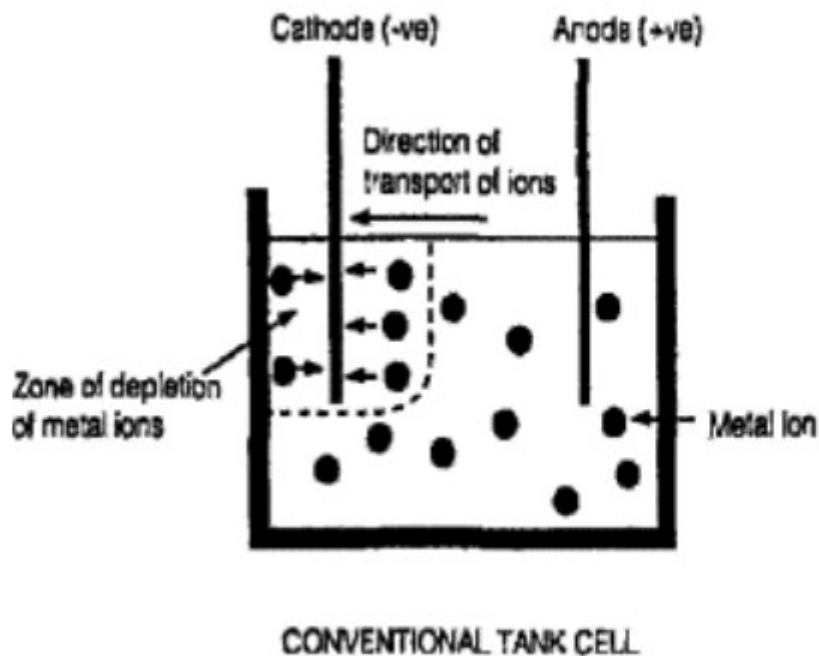


2.6 Metal recovery from leachates

Leaching technologies lead to a highly concentrated metal leachates production. The metals must be recovered from the leachates with the aim to recycle them. Possible technologies include electro-winning, chemical precipitation, sorption and adsorption.

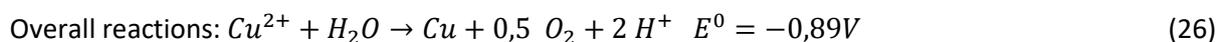
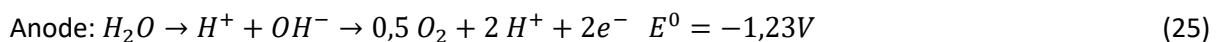
2.6.1 Electrowinning

Electrowinning is a commonly-used technology for wastewater treatment and widely diffused in the mining industry, especially for Cu. For this a bath with two electrodes is used: one inert Pb-alloy anode and a stainless steel or Cu cathode. The bath consist of a purified electrolyte. Furthermore a direct electrical current from an external source is required to cause a current to flow through the electrolyte between the cathode and anode. Figure 9 below shows the working principle.



- Figure 9 Electrowinning procedure [35]

The negative potential of the cathode attracts the metal ions. After a certain period (6-7 days) the metals are stripped from the cathode. At the anode oxygen gas is released. The chemistry behind this process can be explained by following reactions for Cu [35]:



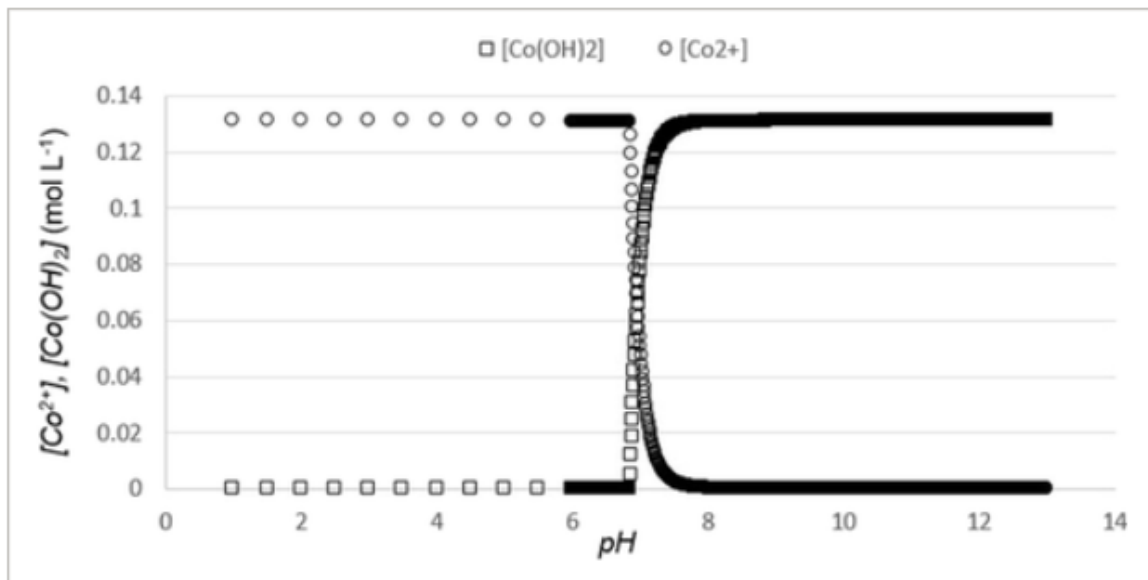
2.6.2 Chemical precipitation

Chemical precipitation is one of the most applied techniques for heavy metal removal from effluents. It is based on the follow concept: $M^{2+}(aq) + 2(OH)^-(aq) \leftrightarrow M(OH)_2(s)$ where M^{2+} and OH^- represent respectively the dissolved metal ions and the precipitant, while $M(OH)_2$ is the insoluble metal hydroxide. In this case it is clear that the pH will influence the metal removal. The most commonly utilised precipitants are lime and limestone due to their availability and low-cost in most countries. Here the available carbonates will react with the available protons:



Thus this reaction will raise the pH which results in an increase of metal hydroxide precipitation.

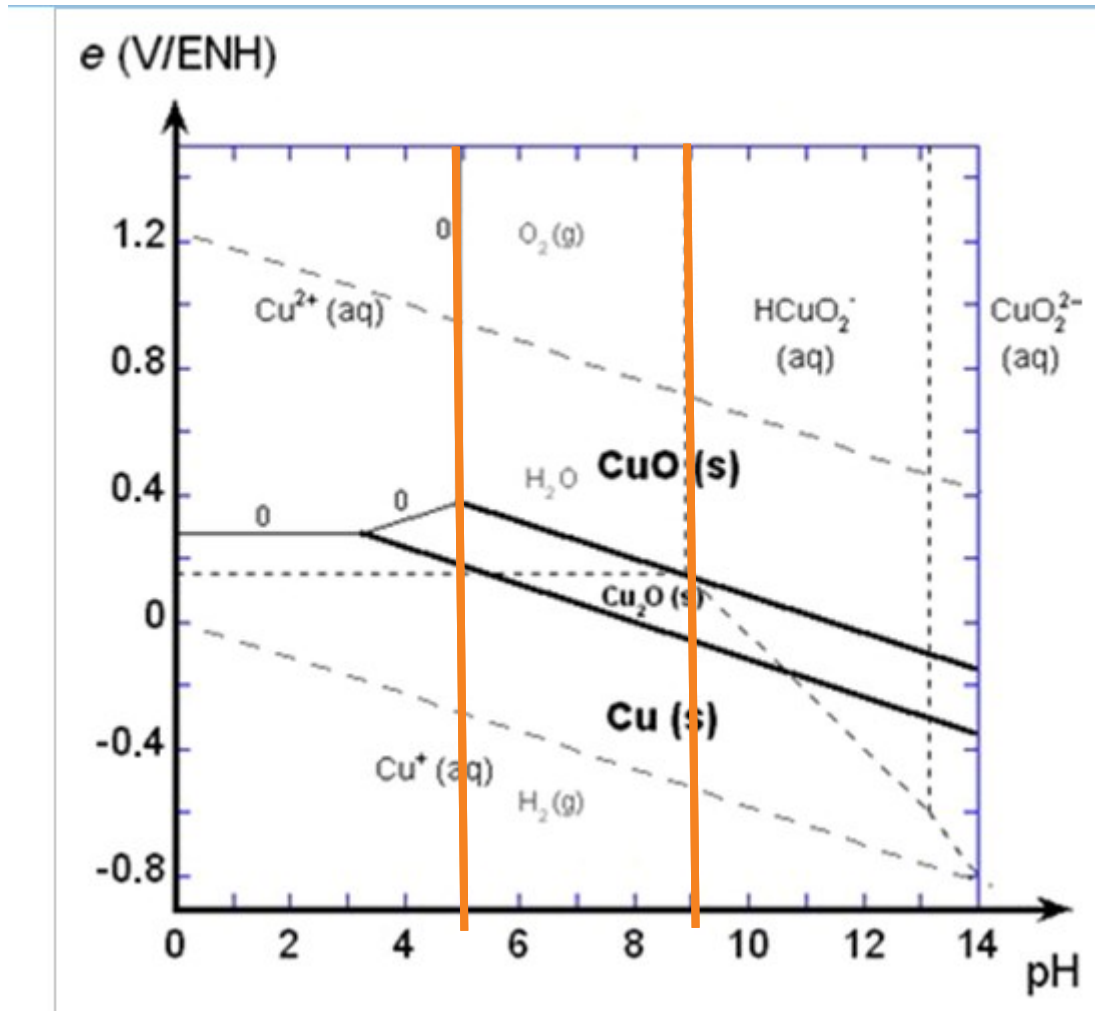
Other advantages are the safe operation conditions and an inexpensive equipment. However, a large amount of chemicals is required to reach an acceptable level for discharge in combination with its excessive sludge production that must be treated [36]. As an example, Figure 10 indicates the pH dependency of cobalt hydroxide precipitation.



- Figure 10 pH dependency of Cobalt precipitation

This experiment of Co precipitation was performed with a solution containing only Co(III), while NaOH was used as a precipitation agent. It was shown that the precipitation begins at pH 6.9, the Co-concentration drops while the cobalt hydroxide concentration starts to increase. Furthermore, it is important to study the influence of other metals on a precipitation process. For example, in the case of

Li-ion batteries leachates, which contain next to Co also large amounts of Cu. First Cu must be precipitated since it is present in the highest concentration. To predict the behaviour of the metal a Pourbaix diagram is utilised. As an example, the Pourbaix diagram of Cu is shown (Figure 11).



- Figure 11 Pourbaix diagram of Cu-H₂O system, [Cu]=0,259 M

It is reported that copper hydroxide tends to transform into a more stable form, copper oxide, due to thermodynamically reasons. The CuO will precipitate in a pH range of 5-9 [37].

It can be noted that the Cu concentration in the Pourbaix diagram is higher than the Cu concentration of the studied material. Maximum Cu concentration of the studied material is ±6 mM.

Another possibility to precipitate metals is achieved by the use of H₂S gas. Cu, Zn and Ni will form in presence of this gas a sulphide precipitate. The following the reaction occurs:

$$M^{2+} + H_2S \rightarrow MS + 2H^+ \quad (28)$$

With M representing a metal. In a Cu-Zn-Ni system the precipitation selectivity was 96.6% for Cu at pH =1.5, 96.0% for Zn at pH 4.5 and 99.4% for Ni at pH 6.5 ± 0.4, according to Tokuda et al.(2008) [38].

2.6.3 Metal adsorption

Adsorption is the process whereby molecular species called the adsorbate will accumulate at the surface of the adsorbent. The surface can refer to the external surface as well as the internal surface,

e.g. crevices, capillaries. The adsorption process can be divided into 2 groups based on the interactions. First group based on physical interactions characterized by weak van der Waals forces and the second group were chemical interactions between adsorbent and adsorbate take place. This process can be described by isotherms because adsorption is a temperature dependent process [39].

Adsorption by magnetic nanoparticles

An effective removal of metal ions from an aqueous solution is performed by magnetic nanoparticles. For example, the magnetic nano-adsorbent MNP-NH₂ developed by the covalent binding of 1,6-hexadamine on the surface of Fe₃O₄ nanoparticles. This is developed especially for removal of Cu²⁺ ions from aqueous solution. Various factors influence the metal removal, e.g. contact time, temperature, pH, amount of MNP-NH₂ and initial concentration of Cu²⁺. The influence of the pH is shown by following equations:



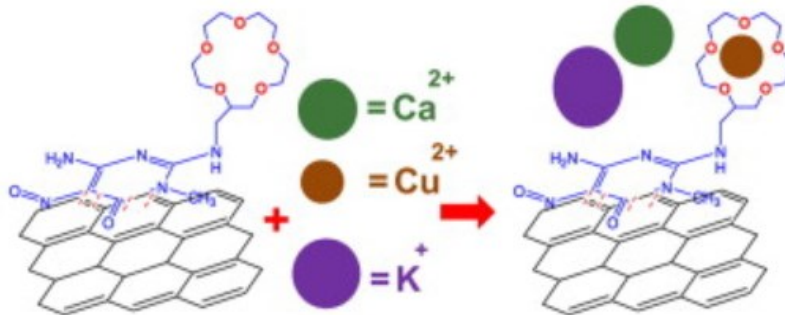
It is clear that, in low pH systems, protons will compete for binding sites with Cu²⁺ ions. Furthermore, the electrostatic repulsion between Cu²⁺ and MNP-NH₂ is enhanced with more NH₃⁺ present on the surface of the nanoparticles. These effects contribute to less adsorption of Cu²⁺ ions with lower pH. The isoelectric point of MNP-NH₂ is 5.8, revealing that the amino functionalised nanoparticles are positively charged at pH<5.8. In the pH area from 3 till 6 the Cu is present in the following species: Cu²⁺, Cu(OH)₂ and Cu(OH)⁺. The Cu²⁺ species is predominant while the Cu(OH)₂ concentration is negligible since the logarithm of the solubility constant of Cu(OH)₂ is 19.66. In general magnetic nanoparticles attract much attention due to their large adsorptive surface area, low diffusion resistance, high adsorption capacity and fast separation for large volumes of solution. Via this technique, the best of nanoparticles are combined with the ideal performance of magnetic separation leading to a cost-effective, simple to use and environmental friendly method [40].

Bio-sorption

Recently, there is a lot of interest in research for the removal of heavy metals by the use of activated carbon. Zn, Cu, Ni and Pb can be removed by activated carbon, up to 75 mg metal/g activated carbon. This adsorbent can be produced from agricultural by-products, e.g. hazelnut shell, rice husk, pecan shells and jackfruit. This process is known as bio-sorption utilizing inactive (non-living) biomass to bind and concentrate heavy metals from waste streams by mainly chelation and adsorption [36]. High temperatures and activating agents are required to achieve activated carbon. The activating agent will create the unique macro-, meso- and micro-porous structure by penetrating into the core of the carbon particle [41]. The advantages of activated carbon are a high active surface area, a well-developed pore structure and a low density. Furthermore, a variety of functional groups can be implemented, which make this adsorbent adaptable to its environment/target metals. The pH plays also an important role. The presence of certain functional groups on the activated carbon, e.g. COOH-group and OH-groups, will lose its proton in high pH areas. This results in a negatively charged activated carbon structure which will attract more the positively charged metal ions. Thus, an increase of pH results in an improvement of the adsorption. In low pH areas, these functional groups will bind protons, resulting in protonated functional groups, which are unable to coordinate metal ions [42].

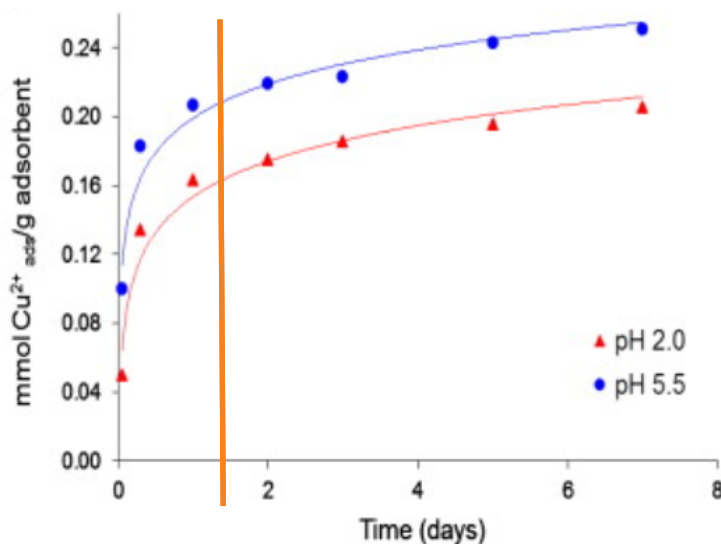
Molecular recognition

Another technique to separate metals from leachates is achieved by molecular recognition technology. The approach is developed in the late of 1960s with the synthesis of crown ethers. A selective complexation reaction with cations will occur due to the design of these macrocycle molecules with determined cavity sizes and shapes. With these cavities matching the selected cation diameters, that specific cation can be removed from the solution. [43] Figure 12 shows an example of an activated carbon gel containing a crown ether, designed to capture Cu^{2+} ions.



- *Figure 12 Molecular recognition of Cu^{2+} by a crown ether*

Figure 12 shows the relationship between the selectivity and the size of the crown ether, which is the main advantage of this technique. For example, adsorption by activated carbon has made a poor selectivity towards Ca^{2+} , Cu^{2+} and K^+ resulting in a non-selective approach [44]. Figure 13 visualizes the amount of Cu^{2+} adsorption that can be achieved by this crown ether.



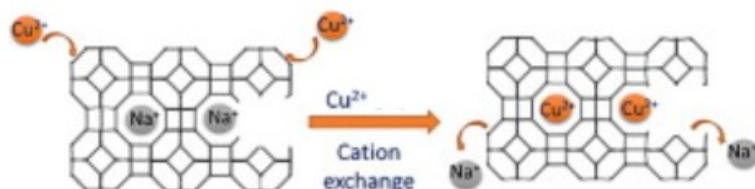
- *Figure 13 Adsorption pattern of Cu by a crown ether [44]*

The curve shows initially a fast incline. After circa 1.5 day a much smaller adsorption incline is visible. Perhaps the pores reach after 1.5 day their maximum capacity, after which the Cu^{2+} ions can be captured by bonds between Lewis base functions placed into narrow pores (e.g. $-\text{NH}$ groups). Furthermore it is shown that a higher pH achieves better adsorption due to the presence of less protons which decrease the surface active sites of the activated carbon. In this situation, the activated represents a

secondary role in the Cu^{2+} removal. The crown ether itself does not have a Brönsted acid-base character [44].

Zeolites

Zeolites are promising adsorbents for metals, ideal for Cu, Ni, Pb and Zn uptake. This results from their chemical and mechanical stability, ion exchange capacity and high affinity for heavy metal cations. Zeolite structures consist of Al, Si and O from which they form three dimensional networks resulting in microporous aluminosilicate frameworks of corner-sharing $[\text{XO}_4]$ tetrahedra in which X represents Al or Si. Nowadays, more than 220 zeolite types are known. They appear in nature, but are already made synthetically, allowing the Si/Al ratio to be varied from one to infinity. This ratio determines the charge of the structure, as a pure SiO_4 is neutral in the contrary with zeolites consisting Al with a charge of 3+ as substitute for Si with a charge of 4+ resulting in a negatively charged structure. This negative structural charge is compensated by extra framework cations (e.g. Na, Ca). These cations are solvated with a specific number of water molecules and located on specific sites in the framework. Besides the charge, this ratio determines also the hydrophilicity. Sorption on zeolites is a complex process due to the mineralogical heterogeneity, crystal edges, broken bonds,... As a result, many studies have expressed different opinions on the exact sorption mechanism. Figure 14 illustrates the cation exchange between Cu and Na [45] [46].



- *Figure 14 Cation exchange zeolites [45]*

Situation Part Metallic organic frameworks

In this part first MOFs are defined. Afterwards, common applications are examined based on their structure characteristics. After this section, there is focused on the imidazolate based MOFs. Thereby zeolitic imidazole framework 8 (ZIF-8) plays a central role because this is the targeted end-valuable product synthesized with the metals collected in the leaching step. Remember the 4 targeted metals Zn, Cu, Ni and Pb. The chemical properties of ZIF-8 will be discussed together with possible syntheses ways.

2.7 Metal-organic frameworks (MOFs) for metal recovery

In this section, the properties of MOFs are defined. Afterwards their applications are examined ending with the metal recovery application of MOFs, which is particularly relevant for this study.

2.7.1 MOFs as a subclass of coordination polymers

Metal-organic framework (MOFs) materials are a subclass of coordination polymers (CPs). CPs consist of one-, two- or three dimensional polymeric compounds formed by repeating coordination substances. The substances can be inorganic, organic or hybrid inorganic-organic, which will lead to several subclasses. For example metal-organic frameworks (MOFs), amorphous CP's, porous coordination polymers (PCPs), coordination networks (CNs) and so forth. There is a lot of diversity in CPs in terms of crystal size, porosity, geometry and functionality due to the various possible combinations of metallic centres and organic ligands. This thesis will mostly focus on MOFs. A possible definition of this term is:

“A class of CPs promising organic linkers wherein metal-ligand interaction/bonding leads to 2D or 3D crystalline network structures, according to Navarro Poupard et al. [47]”. These structures know various applications thanks to their high specific surface area and good thermal stability.

2.7.2 Applications

As a result of their porous, crystalline nature, MOFs can be of interest in several applications. This section includes gas storage, separation of different molecules, catalyst function, drug delivery and corrosion inhibition which are the most common applications. Furthermore, a short introduction is given of the applications of non-porous MOFs.

Gas storage

MOFs are ideal for the storage of different molecules and macromolecules. In this case, gas storage by porous MOF's forms a potential technology to reduce greenhouse gases, SO_x and NO_x emissions, produced by energy production processes, by the use of alternative fuels such as methane, a primary component of natural gas and biogas. The main drawback of CH_4 is its low volumetric energy density. Therefore highly porous materials, especially MOFs, represent an interesting category of adsorbents for CH_4 due to their combination of a high surface area with a suitable pore shape and functionality [48].

Separation

Another application of MOFs is the separation of different molecules, e.g. CO_2 separation. CO_2 is believed to be responsible for the world climate change. Certain MOFs have been identified to have excellent CO_2 separation performance, such as the MOF-74 series, which are efficiently produced in ton-scale. Nowadays the water stability and recyclability of these MOFs under real working conditions remain a challenge, according to Hu et al. (2015) [49].

Catalysator

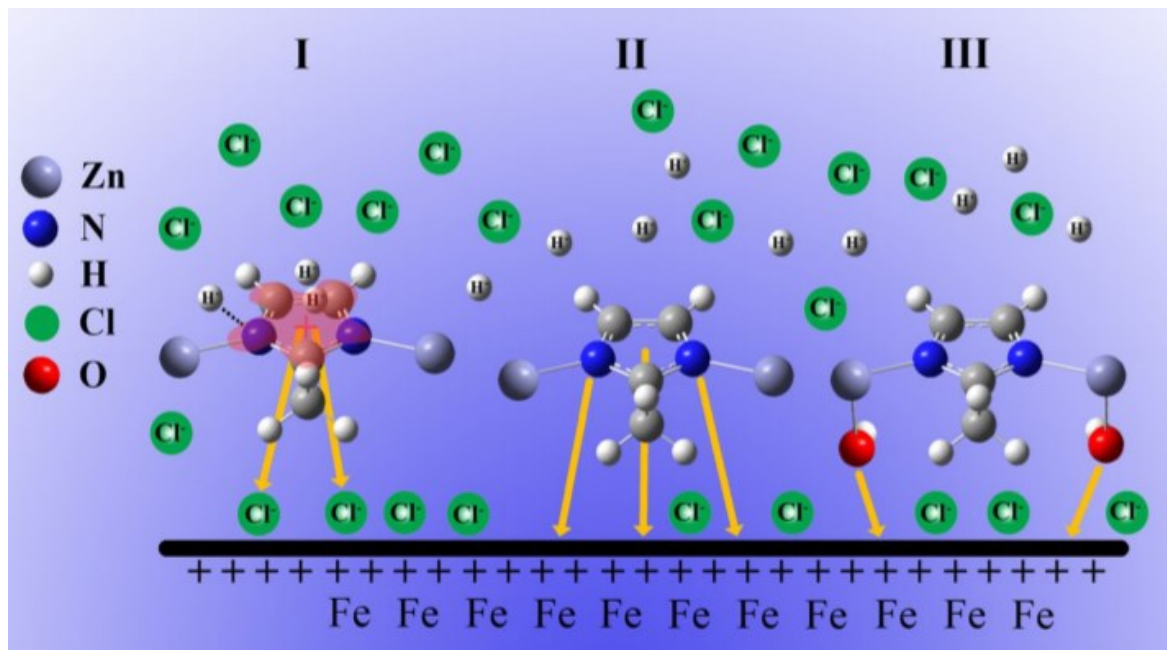
Furthermore, MOFs can be used as catalysts due to their porous structure which enhance the formation of active sites.

Drug delivery

Also the delivery of drugs via MOFs has received increasing attention in recent years. Scientists have made progression in the field of nanomedical applications of MOFs due to their facile synthesis on the nanoscale and alternative functionalization via inclusion and surface chemistry. MOFs can be seen as innovative drug vehicles for controllable drug release together with decreased side effects and enhanced therapeutic efficacy. Moreover, the weak coordination bonds ensure their biodegradability and the large surface areas and high porosities facilitate MOFs with high loading capacity. Furthermore, their versatile structures contribute to their multi-functionality and stimuli-responsive drug controlled release. Zeolitic imidazole framework 8 material (ZIF-8), the MOF examined in this study, is appropriate for nanomedical applications since the low toxicity of Zn^{2+} . Thereby Zn shows an anti-inflammatory and anti-bacterial effects since Zn^{2+} can transport across bacterial membranes [50]. ZIF-8 can encapsulate small, negatively charged molecules and organic molecules (e.g. anticancer drug DOX). The drug release is based on the instability of this framework under acidic conditions which benefits for targeting tumour tissues whose extracellular pH is lower compared to normal tissues. [51] [52]

Corrosion inhibition

MOFs and specific in this example ZIF-8 are employed as corrosion inhibitors for carbon steel in acidic media like HCl. The corrosion inhibition mechanism of ZIF-8 in HCl can be declared by Figure 15.



- *Figure 15 Corrosion inhibition mechanism of ZIF-8 in HCl [53]*

Figure 15 shows that the π -electrons of imidazole rings and the nitrogen atoms present the organic linker will attract the acidic hydrogen atoms resulting in positive sites which bond with the negative charge of the steel surface due to the presence of chloride anions. Another possibility is the adsorption of the positive nitrogen present the linker and oxygen bound to Zn^{2+} ions on the surface. Both phenomenon's result in a passive film of attached inhibitor molecules on the metal surface. Via this way, ZIF-8 can act as a cathodic type inhibitor. [53]

Other applications

Nowadays, also nonporous high-density MOFs are being developed and they could be the next generation functional materials in various fields. These nonporous MOFs could be converted to an amorphous semiconductor [54]. Another surprising application is the use as energetic material (explosives, propellants and pyrotechnics) by combining these high energy density materials with the combination of fuel and oxidizer covalently bonded with the inclusion of atoms such as nitrogen. This can provide additional heat upon decomposition [55].

2.7.3 Available MOF-based metal recovery technology

A selection of MOF materials have proven characteristics for metal recovery. Examples are porous MOF-based membranes, films or other shape-bodies with ultra-efficient metal ion permeation, strong chemical and thermal stability and high selectivity. Electrospinning makes it possible to generate continuous and flexible fibers with diameters over a scale from nano- to micrometers. Furthermore, specific functional groups can be implemented into the MOF matrix during synthesis to alter their sorption properties, as functional groups strongly determine the selectivity [56]. The disadvantages of metal recovery by MOFs are problems with the uniform dispersion of MOFs in the operating environment, the permeability or diffusion of the flowing phase, the output efficacy compared to pristine MOFs,... [57].

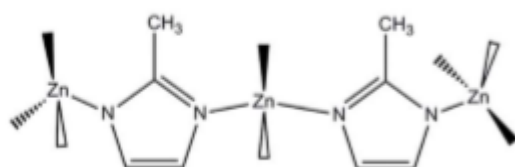
For the removal of Pb^{2+} , Co/Zn-ZIF crystals were synthesized onto carboxymethylcellulose sodium coated cloth resulting in the formation of a compact MOF membrane at room temperature. Yang et al. (2018) show an adsorption efficiency of 862.44 mg/g toward Pb^{2+} . The adsorption experiments were performed between 1-6 pH to avoid metal hydroxide precipitation. Pb was adsorbed by the MOFs via a complexation reaction with a free N-atom [58]. Another example is the Cu removal by amino group(-NH₂) functionalized Zr-MOFs. In this case, adsorption capacities of 988 mg/g were achieved at pH=6 and a temperature of 40°C. Cu will accept electrons from the amino group resulting in adsorption [59]. Besides these examples, a broad-spectrum heavy metal ion trap (BS-HMT) is illustrated, i.e. the EDTA functionalized MOF-808. The MOF serves as a host material for EDTA, which must chelate the metal ions. MOF-808 is a Zr-based $Zr_6O_4(OH)_4(BTC)_2(HCOO)_6$ structure and EDTA is a strong chelating group due to the six binding sites it counts. Four of them are hard carboxylic and two relatively softer tertiary amine groups. Therefore, this species can remove simultaneously Zn, Cu, Ni and Pb with a removal efficiency exceeding 99%, even for metal concentrations of 5 ppm. After 5 minutes a remove of 90% is achieved. The metals will form a complex with EDTA, resulting in adsorption. This metal-ligand complex is water-soluble, therefore the use of a MOF was required. MOF-808 will immobilize this complex resulting in an improvement of separation and recovery for reuse [60] [61].

2.8 Imidazole-based MOFs chemistry

In this section first the structure of ZIF-8 is discussed. Good knowledge of the structure characteristics is required because this affects the functional properties and performance of these valuable products. Afterwards the chemical characteristics of ZIF-8 are studied. The characteristics will give further insights to the various applications discussed in the previous sections.

2.8.1 ZIF-8 structure

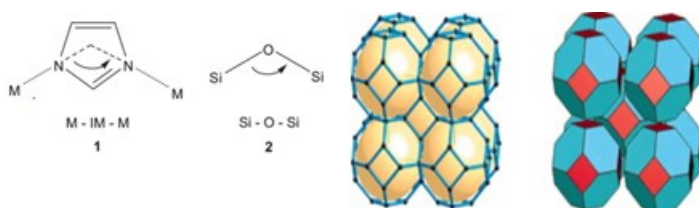
This study focusses on the MOFs prepared with a 2-methylimidazole linker (Hmim, C₄H₆N₂). The zeolitic imidazolate framework 8 material (ZIF-8) is a well-known example of this (Figure 16).



-

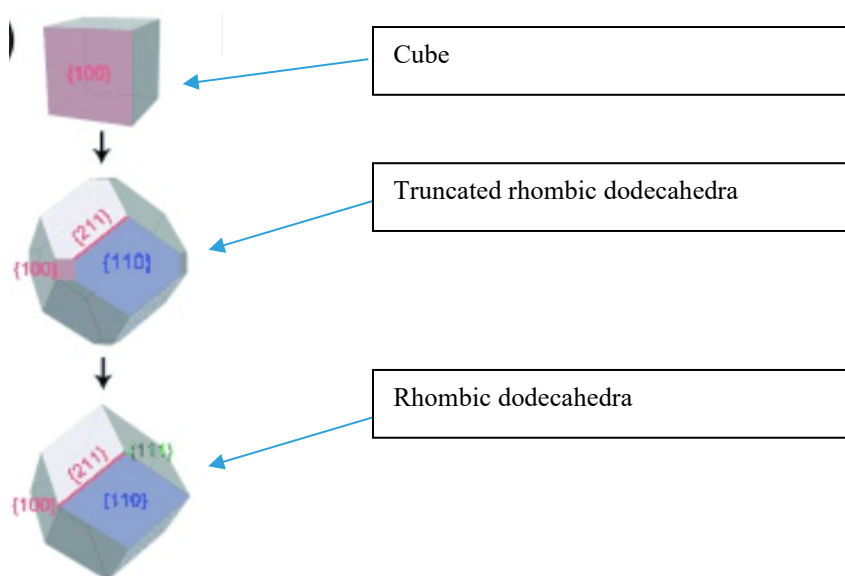
- *Figure 16 ZIF-8 [62]*

In Figure 16 a divalent metal cation Zn^{2+} is tetrahedrally surrounded by nitrogen atoms from the five-membered imidazole rings, serving as a bridging linker [75]. The result is a three-dimensional framework. The $\{M^{2+}(Im^-)_2\}$ units in ZIFs are equally to the $\{SiO_2\}$ tetrahedra in zeolites and the bond angle in the M-Im-M bond is similar to the Si-O-Si bond angle (close to 145°), which form zeolite-like networks (Figure 17).



- *Figure 17 Bridging angles in metal imidazolates and zeolites [63]*

Besides the comparison of bonding angles between ZIF-8 and zeolites, also the density can be considered. To compare the densities of ZIFs with zeolites the traditional number of tetrahedral vertices per unit volume (T/V) is utilized. In ZIF-8, the Zn-Zn distance is 6 Å compared, while the corresponding Si-Si distance in zeolites is 3 Å. Therefore the density in T/V is eight times less for ZIF-8 compared with zeolites. Literature describes a T/V value for ZIF-8 in the range of 2.0-3.7 nm⁻³ [63]. Figure 16 also shows the sodalite crystal structure of ZIF-8 has large cavities (11.8 Å) and small apertures (3.4 Å). Generally, the structural evolution of these nanoparticles can be divided into three stages. First nucleation will start followed by the growth stage. In the end the stationary phase takes place where Oswald ripening occurs [64]. In literature, it is described that the crystal growth of ZIF-8 starts with the formation of cubes exposing six {100} facets. This cube will evolve into a truncated rhombic dodecahedra with six {100} and twelve {110} facets. This evolution will further develop to a rhombic dodecahedra which contains only twelve {110} facets. These structural developments results in a thermodynamically favorable structure [65]. Figure 18 gives the structural evolutions of ZIF-8 crystals.



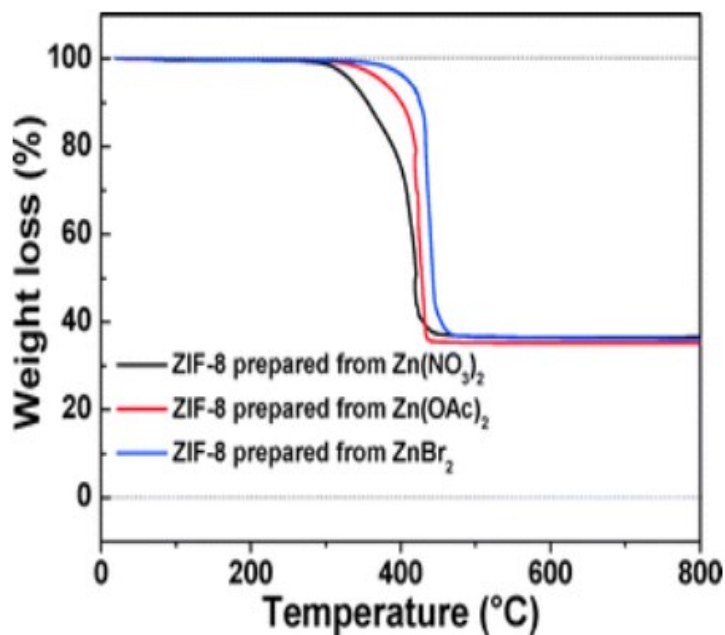
- Figure 18 Crystal structure evolutions ZIF-8 [65]

2.8.2 ZIF-8 chemical characteristics

2-methylimidazole (Hmim, C₄H₆N₂) is implemented as linker resulting in a MOF with general formula [Zn(Hmim)₂·2H₂O]_∞. This molecular formula is important to know the molar Zn/Hmim ratio in the MOFs. In the case of ZIF-8, this ratio is 0.5. To reach optimum synthesis conditions, this ratio must be concerned. Due to the magnitude of this imidazolate linker a large cage structure can be formed. It is clear that this linker has 2 available N-donors: one imine N group and one amine NH group [66].

Huang et al. found that the addition of a methyl or ethyl substituent at the 2-position of the imidazolate ligand serves as structure directing agent and leads to formation of zeolite-type MOF's possessing exceptional thermal stability (up to 550°C in N₂) [67]. TGA curves show a small mass loss of less than 0.5% originating from the removal of the excess of Hmim or the presence of CO₂ in the MOF cavities [68]. From 500 till 1000°C, there are three stages of mass loss. At 600°C, the liberation of -CH₃ takes place. Between 600 and 900°C the liberation of -C-N-H- mixtures and ligand decomposition occurs. Above 900°C, Zn will evaporate [69]. In general, the thermal stability of MOFs depends on the strength of the bond between the metal centres and the ligand. The bonding between Zn²⁺ and the imidazolate linker is among the most stable for N-donor ligands on the scale of metal complex formation constants due

to the high bond energy [70]. A complex formation is similar to a Lewis acid-base interaction. The positively charged metal ion act as the Lewis acid and the organic linker as electron donor. Small, highly charged metal ions serve as ideal Lewis acids. Therefore, different divalent metal cations are possible to implement. This study specifically focusses on Zn^{2+} cations, but the possibility to implement Cu, Pb or Ni is also considered. Also, the particle size can have an influence on the thermal stability. Figure 19 declares this correlation.



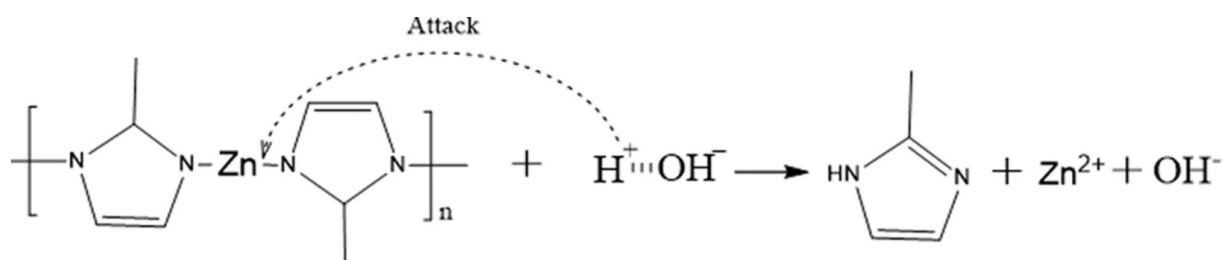
-

- *Figure 19 TGA curves of ZIF-8 nanocrystals synthesized from different Zn sources [68]*

Note that the circumstances in figure 19 are not under inert atmosphere, which leads to a lower heat resistance as discussed before. It is clear that $Zn(NO_3)_2$ shows the lowest thermal resistance ($\pm 300^\circ C$) due to the smaller particle size of 141 nm in comparison with the MOFs prepared from $ZnBr_2$ ($\pm 390^\circ C$) with a particle size of 1050 nm [68].

Furthermore, imidazole based MOFs, especially ZIF-8, show a high chemical resistance to various solvents, allowing their use in several applications. In comparison with other MOFs, they exhibit an exceptional stability in water, but it is unknown whether the high stability of ZIF-8 can be challenged by ions in the solvent and which changes they cause in the crystal structure. The stability in water is the result of the hydrophobic character of ZIF-8 besides the strong bonding between N and Zn [71]. In general, the stability of MOFs is severe when water, alcohol or amines are the reaction medium. These polar solvents can cause deterioration of the crystal structure. MOF structures are determined by the interactions between the molecules: coordination bonds and Coulomb attractions between metal and organic linker. Thereby these polar solvents can solvate the metal ions and can separate the ion-pairs due to their high dielectric constant (e.g. water, $\epsilon = 78,5$ at 298K). In general the crystalline stability depends on the thermodynamic balance of free energy before and after solvation. Thus, it is possible that the crystalline structure is maintained due to the strength of the framework [72].

Generally, acid conditions are challenging for MOFs. Also ZIF-8 will decompose in low pH areas. This instability results in collapsing of the pore structure and the formation of ZnO due to for example hydrolysis showed in Figure 20 [73].

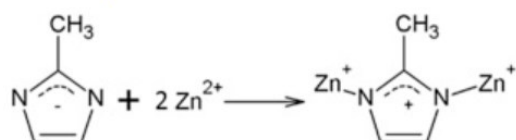


- *Figure 20 Hydrolysis of ZIF-8 [74]*

The hydrolysis process can be divided into two steps. First the pH will increase since the ligands get protons from the decomposition of water molecules. Secondly, the Zn ions can react with water and come off from the ZIF-8 structure. Remark that the increase in pH associated with the release of OH⁻ ions in step one is not drastic. Furthermore a large excess of Hmim can protect ZIF-8 crystals against hydrolysis but an excess indicates several disadvantages including the presence of unreacted ballast linker in the end-product resulting in an additional washing step [74].

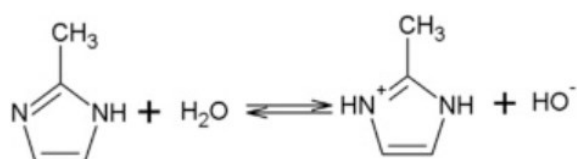
2.9 Formation of ZIF-8

To form MOFs a complexation reaction between the metal cation and the free electrons of the nitrogen atom (after it has loses a proton) is required, given in figure 21.



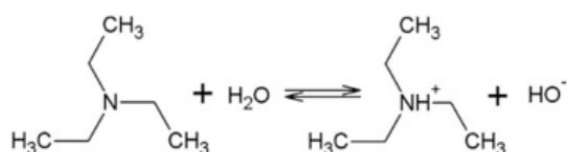
- *Figure 21 Formation of ZIF-8 [75]*

Hmim has an alkaline character, with its pK_a is 7.86 [76]. This means the molecule will bind protons via the free electrons of the nitrogen atom which can be seen as a concurrent reaction for the MOF formation. The following reaction takes place:

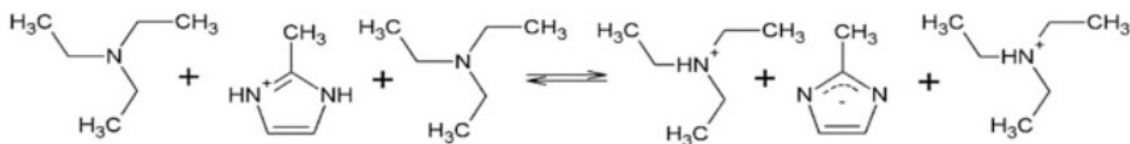


- *Figure 22 Hydrolysis of 2-methylimidazole [75]*

To avert protonation of Hmim, the base triethylamine (TEA, C₆H₁₅N) is often added to the synthesis solution. Triethylamine has a pK_a of 10.75 and therefore has a stronger alkaline character than Hmim [77]. This result in a facilitated deprotonation of the linker and nucleation of the framework without unwanted formation of metal hydroxides. The following reactions occur:



- *Figure 23 Hydrolysis of TEA [75]*



- *Figure 24 Deprotonation of Hmim by the use of TEA [75]*

2.10 Synthesis methods

In general, most of the synthesis efforts of MOF remain limited to the laboratory scale. Further progress toward industrial applications is restricted by factors such as high production costs, issues concerning chemical and mechanical stability under real conditions and problems of synthesis reproducibility for scaling-up methods [75]. Yet, some types of MOFs are already available from commercial suppliers in quantities up to kilos.

It is clear that there is still a need for the development of a straightforward, economically and green way of synthesis of massive amounts of MOFs. MOFs are generally prepared by solution-based methods. Taking these factors into account, there is a need of a simple aqueous synthesis at room temperature, or in hydrothermal or microwave conditions to make the production possible on an industrial scale. The most valuable, up-scalable method will be the aqueous synthesis at room temperature due to its short reaction time and reduced energy and solvent consumption. Moreover, some organic solvents (e.g. DMF) are complicated to be removed from the porous crystal structure of ZIF-8 [62]. Another problem is the production of dangerous hydrogen gas with the use an organic solvent [67]. Furthermore, it is hard to produce pure ZIF-8 crystals with a highly regular particle morphology in water at room temperature without using any additives. Besides the crystal morphology, most of the organic ligands show low solubility in water, which can be improved by hydrothermal synthesis since it enhances the diffusion degree of reactive components [78]. The solubility in water of Hmim values 8.09×10 g/l at 25°C [79]. Table 3 gives an overview of synthesis parameters of the 2-methylimidazole based MOF described in literature.

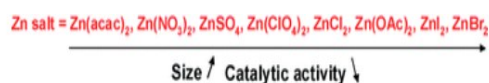
- *Table 3 Overview of the synthesis parameters of the 2-methylimidazole based MOF*

	Metal cation	Metal source	Synthesis conditions	Solvent	Synthesis temperature	Metal concentration in synthesis solution	Hmim concentration in synthesis solution	Molar ratio metal/Hmim	Additives	Reaction time	Post-treatment	Drying
Unit					°C	mM	mM			h/min		
Zn												
(Yao et al., 2013) [74]	Zn ²⁺	Zn(NO ₃) ₂ ·6H ₂ O	Room temperature	Deionized water	Room temperature	0.03933	2.7649	0.014225	/	5 min	Washing with deionized water and centrifuging (6000 rpm, 1 h) for three times	80°C overnight
(Butova et al., 2017) [75]	Zn ²⁺	Zn(NO ₃) ₂ ·6H ₂ O	Hydrothermal	Ultra-pure water	120°C in autoclave	0.0448	0.178	0.251685	Triethylamine	24 h	Collected by centrifugation (7000 rpm, 15 min) and washed with 50 ml of water	80°C for 12 h
Jian et al.; 2015 [80]	Zn ²⁺	Zn(OAc) ₂	Room temperature	Ultra-pure water	Room temperature (25°C)	0.78	2.2285714	0.0285714285	/	24 h	Collected by centrifugation (7000 rpm, 5 min) and washed with deionized water three times.	60°C for 24 h
Tanaka et al., 2012 [81]	Zn ²⁺	Zn(NO ₃) ₂ ·6H ₂ O	Room temperature	Deionized water	Room temperature	25.00773	100.0309-2500,773	0.01-0.25 (Amount of Zn is constant)	/	24 h	Collected by centrifugation (6000 rpm, 10 min) and washed 5 times with methanol and centrifuged again.	40°C for 48 h under reduced pressure
Nordin et al., 2014 [82]	Zn ²⁺	Zn(NO ₃) ₂ ·6H ₂ O	Room temperature	Total deionized water	Room temperature	102.501		0.16667	Triethylamine	30 minutes	Collected by centrifugation (3000 rpm, 30 min) and then washed several times with deionized water	60°C for at least 12 h
Cravillon et al., 2011 [83]	Zn ²⁺	Zn(NO ₃) ₂ ·6H ₂ O	Room temperature	Methanol	Room temperature	24.69	98.74	0.250051	/	24 h (stirring)	Collected by centrifugation and washed with methanol	Drying overnight at room-

												temperature under reduced pressure
Zhou et al, 2019 [84]	Zn ²⁺	Zn(NO ₃) ₂ ·6H ₂ O	Room temperature	Methanol	Room temperature		140.68		/	24 h (stirring)	Collected by centrifugation at 4000 rpm for 5 min and washed three times with methanol	Drying overnight at 80°C in vacuum.
Beh et al, 2018 [85]	Zn ²⁺	Zn(NO ₃) ₂ ·6H ₂ O	Room temperature Ice bath	Methanol	Room temperature Ice bath	0.025-0.05-0.10-0.15-0.20	0.20-0.40-0.80-1.20-1.60	0.37 0.25 0.125 0.0625	/	stirring, no time mentioned	Collected by centrifugation at 8000 rpm for 20 min and washed two times with methanol and a centrifugation step again	Drying in vacuum condition at 65°C for 24 h.
Cu												
Navarro et al, 2018 [86]	Cu ²⁺	CuCl ₂ ·2H ₂ O	Room temperature	Ultra-pure water	Room temperature	25-200	1000 (invariable)	0.025- 0.2	Hexadecyltrimethylammonium bromide (CTAB)	1 min stirring + 45 min undisturbed	Collected by centrifugation (7000 rpm, 15 min). The precipitate was redispersed and stored in 3 mL acetone.	/
Jin et al, 2020 [87]	Cu ²⁺	Cu(NO ₃) ₂ ·6H ₂ O Mol (Zn:CU) = 1:1	hydrotherma	DMF solution	140°C in autoclave				Triethylamine (TEA)	1 h	Collected by centrifugation (8000 rpm, 8min) and washed three times with methanol	Dried at 85°C overnight.

Ni												
Li et al, 2014. [88]	Ni ²⁺	Ni(NO ₃) ₂ Zn(NO ₃) ₂	Room temperature	Methanol	Room temperature	Not mentioned			/	24 h	The solid is precipitated and washed with methanol.	/

The most common Zn source is $\text{Zn}(\text{NO}_3)_2 \cdot 6\text{H}_2\text{O}$ combined with synthesis conditions at room temperature and a reaction time of 24 hours. Schejn et al. compared different Zn sources [68]. Figure 25 resumes their investigations.



- *Figure 25 Comparison of Zn sources in the formation of ZIF-8 [68]*

Figure 25 suggest that the Zn source will influence the size of the MOFs together with the catalytic activity. Thereby $\text{Zn}(\text{NO}_3)_2$ shows a small particle size together with high catalytic activity since the surface area values $1700 \text{ m}^2/\text{g}$ which is the highest one obtained [68].

It is hard to discuss the optimal molar ratios for the Zn based MOFs since the differences between the sources is high. But it is clear that the organic linker must be present in excess or minimum in equivalent molar amounts relative to the Zn^{2+} source. This high amount of linker increases the rate of nucleation. A higher rate of nucleation means more nuclei are formed resulting in a smaller crystal size since the high amounts of small nuclei can only reach small crystal sizes together with the fast decrease in supersaturation [68]. For Cu and Ni based MOFs, no clear information is available to make a proper decision on this matter. Although, they can easily bind with nitrogen atoms and they have comparable characteristics as Zn.

3. Materials and methods

3.1 Experiments

3.1.1 Metal leaching experiments

The selected tailing, originating from the Neves-Corvo mine in Portugal, was divided in two series: non-roasted and roasted. The roasting was performed at 600°C for 1 hour in a Milestone PYRO Microwave Muffle Furnace, using a ramp time of 30 minutes. The other sample derived from the metal industry and is called Cr/Ni sludge. Both samples were stored in a desiccator to avoid the absorption of water from air. In total, 56 samples were prepared in separated vials of 25 ml. Each vial contained 3 g (tolerance of 0.01g) of the sample weighted on an analytical balance. Afterwards the samples were divided into two different series to compare two different leaching pathways. One traditional leaching aqueous pathway using NH_4OH and the other with triethylamine. The table below shows the concentration distribution of the lixivants.

- *Table 4 Concentration distribution of the lixivants*

Solutions ammonia (mM)	Solutions triethylamine (mM)
0	0
10	10
30	30
100	100
300	300
600	600

To obtain representative results, duplicate samples were used. To each sample, 30 ml of the required lixiviant is added by using a pipette. Afterwards the vials were closed and mixed by an end-over-end mixer for 24 hours. During this step, the reaction took place. After the reaction, the tubes were placed in the centrifuge Eppendorf 5810 apparatus for 10 minutes at 3000 rpm showed in figure 26.



- *Figure 26 Centrifuge Eppendorf 5810 apparatus*

Subsequently, the supernatant was collected by a syringe and filtered by a spray filter Chromafil® OA 45/25. The remaining solids were dried in an oven at 40°C for ± 48 hours. Subsequently, the supernatant was analysed by the *Mettler Toledo SevenExcellence Labvantage 160229-00001* to measure the pH, conductivity and redox potential of solutions. Also an ICP-OES analysis was performed on the supernatant. The dried powder was analysed by the *XRF Niton apparatus (X-ray fluorescence)* visible Figure 27.



- *Figure 27 XRF Niton apparatus*

3.2 Future experiments

In the future, the MOF syntheses must be started. The MOF synthesis requires metal nitrates, TEA and 2-methylimidazole as organic linker molecule. A more detailed procedure of this experiments can be found in appendix 1. Afterwards pH measurements must be done together with ICP-OES analyses of all the previous MOF samples. This data must be processed, therefore I must following an ICP-OES software training educated by a specialist.

When this data is analysed, it must clarify which synthesis conditions are optimal to generate MOFs. Afterwards an up-scale experiment of these optimized MOF syntheses are possible since a sufficient amount of MOF solids can be analysed by the XRD-apparatus. The XRD-patterns will determine the structure of the end-products, possibly there are metal oxides present. To discuss the XRD-patterns my external promotor will give me an education. Depending on the XRD-results modifications must be taken. A final experiment with the four metals together is also a possibility.

Now the reaction time of the MOF synthesis must be studied. During the syntheses, samples must be taken periodic. For example: after 10, 20, 30, 45, 60, 120,... minutes. The samples must also be analysed by ICP-OES. Furthermore, the pH can also be monitored to estimate the result. This experiment can be executed for each metal separately but also for a mixture of the 4 metals. Thus, this experiment must give insights of the reaction kinetics and the selectivity of the MOF formation.

In the end, the optimal leaching procedure is repeated and consecutively the MOF synthesis is performed with now the leachates as reagents. ICP-OES, XRD analyses are required to evaluate the whole procedure. After promising XRD results, a SEM analysis is also possible to examine the MOF structure.

4. Results and discussion

4.1 Metal leaching results

Table 5 gives the metal content in the roasted tailing and maximum reachable molar concentrations of the targeted metals in the supernatant. Cr is also considered to compare later on with the Cr/Ni sludge.

- *Table 5 Maximum reachable metal concentrations and initial content from the roasted tailing*

	Zn	Cu	Ni	Pb	Cr
Content in roasted tailing (mg/g)	8.405	3.723	<DL	4.175	0.400
Expected concentration in leachate at complete extraction (mM)	12.8	5.9	<DL	2.01	0.77

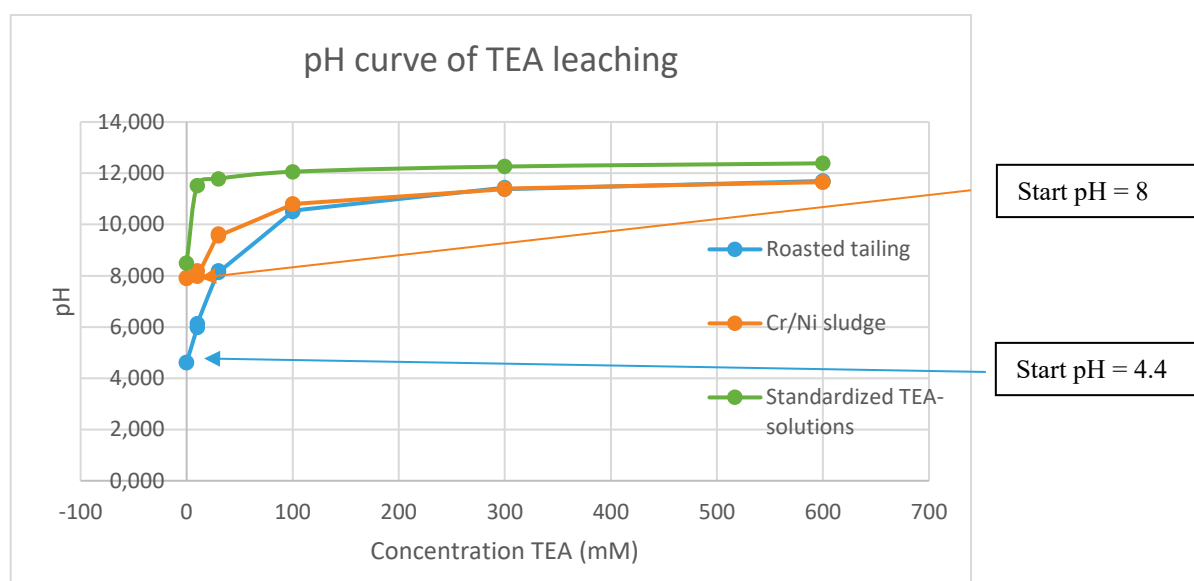
*DL = Detection limit

- *Table 6 Leaching efficiencies of a roasted tailing with TEA as lixiviant*

Concentration TEA (mM)	Leaching efficiency (%)			
	Zn	Cu	Ni	Pb
0	58%	26%	0%	1%
10	45%	1%	0%	0%

30	0%	0%	0%	0%
100	0%	0%	0%	0%
300	0%	0%	0%	0%
600	0%	0%	0%	1%

Table 6 shows the ICP-OES results of the leaching experiments of a roasted tailing with TEA as lixiviant. From these results it is made that the use of TEA as lixiviant was not promising for Ni and Pb, given the low leaching efficiencies obtained for these metals. For both Zn and Cu the highest leaching efficiencies were achieved in pure water, i.e. in absence of TEA. For Zn, a promising efficiency of 58% was reached together with a Cu leaching efficiency of 26%. To explain the relatively negative effect of TEA on the metal leaching, the corresponding pH values need to be considered. Figure 28 shows the pH values of the leachates after the experiments.



- *Figure 28 The pH values of the TEA leachates after reaction, relative to the initial concentration of TEA.*

Figure 28 shows a fast increase of the pH with an increasing concentration of TEA. After a certain concentration, the buffering effect occurred, resulting in a stabilized pH value. The high pH values indicated that metal hydroxides could have been formed. These hydroxides are insoluble, and therefore, could have caused a low metal leaching efficiency. A higher concentration of TEA thus decreased the leaching efficiency. Besides the influence of the pH, it was possible that TEA could have formed complexes with the targeted metals. These complexes would have been water soluble, and would have contributed to the leaching efficiency. Probably, the formation of complexes remained, however, limited. Table 7 gives the molar concentrations in the leachates from the roasted tailing with TEA as lixiviant.

- *Table 7 Metal concentrations of the leachates from the roasted tailing with TEA as lixiviant*

TEA concentration (mM)	Zn (mM)	Cu (mM)	Ni (mM)	Pb (mM)	Fe (mM)	Cr(mM)
0	7.436763	1.546589	0.003298	0.012992	0.228849	0.000962
10	5.755909	0.074564	0.003795	0.008061	0.000448	0.000962
30	0.004834	0.000787	0.001704	0.001448	0.000448	0.000962
100	0.000229	0.000787	0.001704	0.001211	0.000448	0.000962

300	0.001451	0.000787	0.001704	0.005431	0.000448	0.000962
600	0.005078	0.000787	0.001704	0.011525	0.000655	0.000962

It is clear that the concentrations of Zn and Cu in the leachates were relatively high for the leaching method in pure water in comparison with Ni and Pb. Furthermore the concentration of Fe in the leachates was also very low starting from 10 mM TEA which will form a benefit in further experiments on the leachates. Fe can react with the Hmim since a cooperative bond can erase [89]. Remark that the concentration of Fe shows a strongly decline between 0 and 10 mM TEA. The same pattern was shown for Cu. The optimal TEA concentration for metal leaching is thus a consideration between a higher amount of the target metal Cu and the unwanted Fe at 0 mM TEA and a smaller amount of the target metal Cu and unwanted Fe at 10 mM. Table 8 shows the ICP-OES results of the roasted leaching with NH₄OH as lixiviant, with which the leaching results with TEA can be compared.

- *Table 8 Leaching efficiencies of a roasted tailing with NH₄OH as lixiviant*

Concentratie (mM) NH ₄ OH	Leaching efficiency (%)			
	Zn	Cu	Ni	Pb
0	61%	26%	0%	1%
10	59%	12%	0%	1%
30	45%	1%	0%	0%
100	2%	8%	0%	0%
300	11%	26%	0%	0%

Table 9 shows for Ni and Pb a similar pattern in comparison with table 6, also showing very low leaching efficiencies. Note that the concentration of NH₄OH was maximum 300 mM instead of 600 mM, due to a lack of time. For Zn the highest leaching efficiency was reached in pure water, which was similar to the previous results in table 7. In the contrary with table 7, Zn showed a leaching efficiency of 45% for 30 mM. This result can be declared by the formation of coordination bonds between Zn and NH₃. Thus, Zn likely formed coordination bonds more easily with NH₃ (derived from NH₄OH) instead of with TEA. An explanation can be found in the structure of the lixiviant: the tertiary amine caused more steric hinderance in comparison with the primary amine NH₄OH. For Cu, the highest efficiency (26%) was reached in pure water and with a NH₄OH concentration of 300 mM. This positive influence of 300 mM NH₄OH can be declared by the formation of complexes between lixiviant and Cu as described in literature ($Cu(NH_3)_2^+$ and $Cu(NH_3)_4^{2+}$), even in higher pH regions. Table 9 shows the molar concentrations of the leachates corresponding with table 8.

- *Table 9 Metal concentrations of the leachates from the roasted tailing with NH₄OH as lixiviant*

NH ₄ OH concentration (mM)	Zn (mM)	Cu (mM)	Ni (mM)	Pb (mM)	Fe (mM)
0	7.833727	1.532599	0.005112	0.011976	0.205592
10	7.613991	0.702427	0.005112	0.010057	0.000559
30	5.831266	0.078097	0.005112	0.007669	0.000708
100	0.272223	0.479158	0.001704	0.001448	0.000448
300	1.396514	1.505061	0.001704	0.001931	0.000448

The concentration values in table 9 are in general equal to the concentration values of table 7 except from a few differences corresponding with the differences in leaching efficiencies (declared below table 8). The concentration of Fe in the leachates was also low in this case and shows a strong decline between 0 and 10 mM NH₄OH.

For the Cr/Ni sludge, the metal Cr was also considered since this was assumed to be present in high amounts. Table 10 shows the concentrations maximum reachable concentrations of the metals in the leachates.

- *Table 10 Maximum reachable metal concentrations in the leachates and initial content in Cr/Ni sludge*

	Zn	Cu	Ni	Pb	Cr
Content in Cr/Ni sludge(mg/g)	0.035	0.420	12.735	<DL	25.385
Expected concentration in leachate at complete extraction (mM)	0.05	0.66	21.69	<DL	48.81

In comparison with the maximum reachable metal concentrations in the leachates from the roasted tailing (table 5), the concentrations of Zn, Cu and Pb were low and the concentration of Ni was very high. The concentration of Cr compared with the other metals was relatively high. Table 11 and 12 present, respectively, the leaching efficiencies with TEA as lixiviant and the corresponding metal concentrations of the leachates.

- *Table 11 Leaching efficiencies of the Cr/Ni sludge with TEA as lixiviant*

Cr/Ni sludge	Leaching efficiency (%)			
	Zn	Cu	Ni	Cr
Concentration TEA (mM)				
0	0%	0%	0%	0%
10	0%	0%	0%	0%
30	0%	0%	0%	0%
100	0%	0%	0%	0%
300	0%	0%	0%	0%
600	0%	0%	0%	0%

- *Table 12 Metal concentrations of the leachates from the Cr/Ni sludge with TEA as lixiviant*

TEA concentration (mM)	Zn (mM)	Cu (mM)	Ni (mM)	Pb (mM)	Fe (mM)	Cr (mM)
0	0.000229	0.000787	0.001704	0.001448	0.000483	0.003236
10	0.000229	0.000787	0.001704	0.001448	0.000538	0.005804
30	0.000229	0.000787	0.001704	0.001448	0.000448	0.013607
100	0.000229	0.000787	0.001704	0.001448	0.000448	0.022931
300	0.000229	0.000787	0.001704	0.001448	0.000448	0.028765
600	0.000229	0.000787	0.001704	0.001448	0.000448	0.034465

Table 12 shows that all the leaching efficiencies are rounded 0% and the corresponding metal concentrations were low. Furthermore the ICP-OES results showed for Zn, Cu, Ni and Pb exact the same concentrations in function of the TEA concentration. Thus the presence of TEA did not show any influence for the leaching of these elements. Note that the maximum reachable concentrations of Zn, Cu and Pb were low, which automatically resulted in low leachates concentrations. Although Ni and Cr had high maximum reachable concentrations in comparison with the roasted tailing, these elements have even lower concentrations in the leachates. Ni has even a lower concentration in the leachates in comparison with the roasted tailing (0.0017 mM < 0.0033 mM). An explanation can be found in the relatively high initial pH of the Cr/Ni sludge in comparison with the roasted tailing (see Fig. 28). This relatively high pH will cause insoluble metal hydroxides resulting in low leaching efficiencies. Table 7 shows the leaching efficiencies of the roasted tailing were it is visible that starting from 30 mM TEA gives also 0% leaching efficiencies for the metals. Remark that the pH corresponding with this 30 mM is the same as the start pH for the Cr/Ni sludge. Thus from a pH of 8 with TEA as lixiviant the leaching efficiencies are reduced to rounded 0%.

4.2 Conclusions of the experimental work

The metal leaching from roasted sulphide tailings and Cr/Ni sludge was evaluated using TEA and NH₄OH as lixiviants. For the roasted tailing, 0 and 10 mM TEA delivered promising leaching efficiencies of Zn (58%) and Cu (26%), comparable with the efficiencies reached in the experiments with NH₄OH as lixiviant. Higher concentrations of TEA strongly reduced the leaching efficiencies. The formation of insoluble metal hydroxides in these higher alkaline conditions took the upper hand as the formation of coordination bonds between TEA and the metals likely was minimal. To identify an optimal TEA concentration for leaching of interesting metals, the consideration between a higher Cu amount with 0 mM TEA or a smaller Fe amount with 10 mM must be considered. The Fe concentration in the leachates showed a strong decline from 0 till 10 mM TEA. For the Cr/Ni sludge the leaching efficiencies were all close to 0% for each metal with TEA as lixiviant. Note that the Cu and Zn contents were much smaller in this waste stream compared with the roasted tailing, in the contrary with the Ni content which was much higher present in the Cr/Ni sludge. Although, the leaching efficiencies for Ni were close to 0% for the Cr/Ni sludge. An explanation for this was the the higher pH of the Cr/Ni sludge which also leads to insoluble metal hydroxide precipitates.

5. Conclusion

This master's thesis focused on an advanced leaching pathway to recover the target metals Zn, Cu, Ni and Pb from a mineral waste stream. In the end, these metals will be separated from the leachates to create MOFs. This is a whole new approach of recycling a mineral waste stream ending with a valuable end-product. It is clear that the development of this technique remains a major challenge, and a proper literature study could help guiding this development in the most promising direction. In the included literature study, first an overview of the current state of the metal industry is summarized. This part specifically focused on the importance of recycling within the metal industry. Several metal containing waste streams were examined, including waste water and tailings, which are two main waste products of the mining industry. To better understand the emergence of these waste streams, the mining procedure from ores to pure metals was examined. Also modern leaching methods were studied to gain knowledge on these techniques. Beside leaching, different techniques to recover metals were considered to understand the main principles. Afterwards, MOF materials were introduced, starting with a definition and their various applications. Later on, the chemistry behind MOFs and their

chemical composition/structure were considered. For this, the study focused specifically on ZIF-8, because this MOF material was of interest for the experimental section of the thesis. Furthermore, in the form of a summary table, an overview was given of the synthesis parameters of the 2-methylimidazole based MOFs, which will help to set the boundary conditions of MOF synthesis from leachates on laboratory scale. Literature only described combinations between Zn, Cu or Ni and the organic linker. For Zn, it could be concluded that the organic linker must be present in excess or minimum in equivalent molar ratios relative to the Zn^{2+} source. For Cu and Ni, no general conclusions could be made due to the absence of patterns. Although, they can easily bind with nitrogen atoms and they have comparable characteristics as Zn.

Due to the exceptional circumstances, only one main experiment could be performed. The leaching experiments described relatively high leaching efficiencies for Zn and Cu originating from the roasted tailing for 0 and 10 mM TEA. Higher concentrations of TEA resulted in substantially no metal exchange. Remark that Ni and Pb were present in much smaller amounts in the roasted tailing, which will automatically result in a lower leachate concentration. When an optimal TEA concentration must be pointed out, the consideration between a higher leaching efficiency of Cu with 0 mM TEA or a smaller leaching efficiency of Fe with 10 mM TEA must be made. Fe is unwanted in the leachates because it can negatively influence the MOF precipitation, since Fe can form unwanted precipitates in the alkaline MOF synthesis solution with the organic linker, and it is less valuable in comparison with the target metals. For the Cr/Ni sludge, the leaching efficiencies were all close to 0% for each target metal. The Cr/Ni sludge itself contains very low Zn and Cu concentrations in comparison with the roasted tailing. On the contrary, the Ni content was much higher in the Cr/Ni sludge. These results showed that pH has a large influence on the leaching efficiencies. In the future, the MOF syntheses starting from pure metal salts must determine the optimal synthesis conditions by considering the metal concentrations, temperature, reaction time, Hmim/metal ratio and TEA concentration. Afterwards, the selectivity of the MOF precipitation must be examined, for example the Zn based MOF will precipitate first followed by the Cu based MOF. Finally, the MOF synthesis procedure will be adapted for metal leachates instead of synthetic metal solutions. Once the method delivers pure MOFs, this could result in new opportunities for the separation of valuable metals from waste streams. For example, the crystal formation can be further investigated to gain a more valuable material for a given MOF application. Further up-scale experiments can also be investigated due to the large production volumes of mineral waste streams

Bibliography

- [1] The Editors of Encyclopaedia Britannica, „www.britannica.com,“ Encyclopaedia Britannica , 2020. [Online]. Available: <https://www.britannica.com/technology/smelting>. [Geopend 19 March 2020].
- [2] V. Ettler, R. Cervinka en Z. Johan, „Mineralogy of medieval slags from lead and silver smelting (G (BOHUTÍN, PR ĚBRAM DISTRICT): towards estimation of historical smelting conditions,“ *Archaeometry*, vol. 51, nr. 6, pp. 987-1007, 2009.

- [3] International council on mining & metals, „www.icmm.com,” ICMM, 2020. [Online]. Available: <https://www.icmm.com/en-gb/metals-and-minerals/producing-metals/where-and-how-does-mining-take-place>. [Geopend 18 March 2020].
- [4] O. Hokuto, „Capacity developments in the world steel industry,” Organisation for Economic Co-operation and Development, 2017.
- [5] M. Pizzol, P. Christensen, J. Schmidt en M. Thomsen, „Impacts of "metals" on human health: a comparison between nine different methodologies for life cycle impact assessment(LCIA),” *Journal of cleaner production*, nr. 19, pp. 646-656, 2011.
- [6] M. S. Achary, K. Satpathy, S. Panigrahi, A. K. Mohanty, R. K. Padhi, S. Biswas, R. K. Prabhu, S. Vijayalakshmi en R. C. Panigrahy, „Concentration of heavy metals in the food chain components of the nearshore coastal waters of Kalpakkam, southeast coast of India,” *Food Control*, nr. 72, pp. 232-243, 2017.
- [7] C. T. Walsh, H. H. Sandstead, A. S. Prasad, P. M. Newberne en P. J. Fraker, „Zinc: Health effects and research priorities for the 1990s,” *Environmental health perspectives*, vol. 120, nr. 12, 2012.
- [8] F. Solomon, „Impacts of Copper on Aquatic ecosystems and human health,” *Environment and communities*, pp. 25-29, 2009.
- [9] C. Zaccone, R. Di Caterina, T. Rotunno en M. Quinto, „Soil – farming system – food – health: Effect of conventional and organic fertilizers on heavy metal (Cd, Cr, Cu, Ni, Pb, Zn) content in semolina samples,” *Soil and tillage research*, vol. 107, nr. 2, pp. 97-105, 2010.
- [10] Water treatment solutions, „www.lentech.com,” Water treatment solutions, 2020. [Online]. Available: <https://www.lenntech.com/periodic/elements/ni.htm>. [Geopend 1 April 2020].
- [11] M. Tuusjärvi, I. Mäenpää, S. Vuori, P. Eilu, S. Kihlman en S. Koskela, „Metal mining industry in Finland e development scenarios to 2030,” *Journal of cleaner production*, nr. 84, pp. 271-280, 2014.
- [12] M. Yellishetty, G. M. Mudd, P. Ranjith en Tharumarajah, „Environmental life-cycle comparisons of steel production and recycling: sustainability issues, problems and prospects,” *Environmental science and policy*, vol. 14, nr. 6, pp. 650-665, 2021.
- [13] R. Leblanc, „About metal recycling,” Small business, 7 August 2019. [Online]. Available: <https://www.thebalancesmb.com/about-metal-recycling-2877921>. [Geopend 6 Februari 2020].
- [14] L. Rahupathy en A. Chaturvedi, „Secondary resources” and recycling in developing economies,” *Sciences of the total environment*, nr. 461-462, pp. 830-834, 2013.
- [15] N. Johansson, J. Krook en M. Eklund, „Institutional conditions for Swedish metal production: A comparison of subsidies to metal mining and metal recycling,” *Resources policy*, nr. 41, pp. 72-82, 2014.

- [16] F. Veglio, R. Quaresima, P. Fornari en S. Ubaldini, „Recovery of valuable metals from electronic and galvanic industrial wastes by leaching and electrowinning,” *Waste management*, nr. 3, pp. 245-252, 2003.
- [17] K. Barbara en T. E. Graedel, „Challenges in Metal Recycling,” *Science*, nr. 337, pp. 690-695, 2012.
- [18] Engels, J,, „tailings.info,” tailings.info, 2020. [Online]. Available: <http://www.tailings.info/basics/tailings.htm>. [Geopend 2 April 2020].
- [19] D. Kossoff, W. E. Dubbin, M. Alfredsson, S. J. Edwards, M. G. Macklin en K. A. Hudson-Edwards, „Mine tailings dams: Characteristics, failure, environmental impacts, and remediation,” *Applied geochemistry*, vol. 51, pp. 229-245, 2014.
- [20] S. G. S. C. Kumar en S. Shrivastava, „Effective utilisation of quartz sandstone mining wastes: A technical note on its thermal resistance,” *Journal of cleaner production*, vol. 140, nr. 3, pp. 1129-1135, 2017.
- [21] E. Brucker en M. Spohn, „Formation of soil phosphorus fractions along a climate and vegetation gradient in the Coastal Cordillera of Chile,” *Catena*, vol. 180, pp. 203-211, 2019.
- [22] B. Dold en L. Fontbote, „Element cycling and secondary mineralogy in porphyry copper tailings as a function of climate, primary mineralogy, and mineral processing,” *Journal of Geochemical Exploration*, vol. 74, nr. 1-3, pp. 3-55, 2001.
- [23] Z. Sun, H. Cao, P. Venkatesan, W. Jin, Y. Xiao, J. Sietsma en Y. Yang, „Electrochemistry during efficient copper recovery from complex electronic waste using ammonia based solutions,” pp. 308-316, 2017.
- [24] E. Rudnik, M. Pierzynka, Handzlik en P, „Ammoniacal leaching and recovery of copper from alloyed low-grade e-waste,” nr. 18, pp. 318-328, 2016.
- [25] F. Ma, „Corrosive effects of chlorides on metals, Pitting corrosion,” InTech, Rijeka, 2012.
- [26] C. Bong-Gyoo, L. Jae-Chung en K. Yoo, „Valuable metal recycling,” *Metals*, nr. 5, pp. 345-349, 2018.
- [27] P. Breuer, X. Dai en M. I. Jeffrey, „Leaching of gold and copper minerals in cyanide deficient copper solutions,” *Hydrometallurgy*, vol. 78, nr. 3-4, pp. 156-165, 2005.
- [28] F. E. B. Coelho, J. C. Balarini, E. M. R. Araujo, T. L. S. Miranda, A. E. C. Peres, A. H. Martins en A. Salum, „Roasted zinc concentrate leaching: Population balance modeling and validation,” *Hydrometallurgy*, vol. 175, pp. 208-217, 2018.
- [29] R. Singh en M. Agrawal, „Variations in heavy metal accumulation, growth and yield of rice plants,” *Ecotoxicology and Environmental Safety*, vol. 73, pp. 632-641, 2010.
- [30] F. Wen, W. Yonghong en L. Jianguo, „Comparative characterization of sewage sludge compost and soil: Heavy metal leaching characteristics,” *Journal of Hazardous Materials*, nr. 310, pp. 1-10, 2016.

- [31] M. Izquierdo, X. Querol, J. Davidovits, D. Antenucci, H. Nugteren en C. Fernandez-Pereira, „Coal fly ash-slag-based geopolymers: Microstructure and metal leaching,” *Journal of Hazardous Materials*, pp. 561-566, 2009.
- [32] J. Lee, B. Pandey en D., „Bio-processing of solid wastes and secondary resources for metal extraction – A review,” *Waste management*, nr. 1, pp. 3-18, 2012.
- [33] C. Hsu en R. G. Harrison, „Bacterial leaching of zinc and copper from mining,” *Hydrometallurgy*, vol. 37, nr. 2, p. 169_179, 1995.
- [34] B. Arab, F. Hassanpour, M. Arshadi, S. Yaghmaei en J. Hamedi, „Optimized bioleaching of copper by indigenous cyanogenic bacteria isolated from the landfill of e-waste,” *Journal of environmental management*, vol. 261, 2020.
- [35] M. Schlesinger, M. J. King, K. C. Sole en W. G. I. Davenport, „Electrowinning,” in *Extractive Metallurgy of copper*, Elsevier, 2011, pp. 349-366.
- [36] M. Barakat, „New trends in removing heavy metals from industrial wastewater,” *Arabian Journal of Chemistry*, nr. 4, pp. 361-377, 2011.
- [37] N. Djoudi, M. Le Page Mostefa en H. Muhr, „Precipitation of Cobalt salts for recovery in leachates,” *Chemical engineering& technology*, nr. 7, 2019.
- [38] H. Tokuda, D. Tuchar, N. Mihara, M. Kubota, H. Matsuda en T. Fukuta, „Study on reaction kinetics and selective precipitation of Cu, Zn, Ni and Sn with H₂S in single-metal and multi-metal systems,” *Chemosphere*, vol. 73, nr. 9, pp. 1448-1452, 2008.
- [39] G. Okolo, R. Everson, H. Neomagus, M. Roberts en R. Sakurovs, „Comparing the porosity and surface areas of coal as measured by gas adsorption, mercury intrusion and SAXS techniques,” *Fuel*, vol. 141, pp. 293-304, 2015.
- [40] Y. Hao, M. Chen en Z. Hu, „Effective removal of Cu (II) ions from aqueous solution by amino-functionalized magnetic nanoparticles,” *Journal of hazardous materials*, pp. 392-399, 2018.
- [41] J. Moon en J. Lee, „Use of curdlan and activated carbon composed adsorbents for heavy metal removal,” *Process biochemistry*, vol. 40, nr. 3-4, pp. 1279-1283, 2005.
- [42] J. Kong, R. Gu, J. Yuan, W. Liu, J. Wu, Z. Fei en Q. Yue, „Adsorption behavior of Ni(II) onto activated carbons from hide waste and high-pressure steaming hide waste,” *Ecotoxicology and Environmental Safety*, vol. 156, pp. 294-300, 2018.
- [43] I. S. S. Pinto, M. Sadeghi, N. E. Izatt en H. Soares, „Recovery of metals from an acid leachate of spent hydrodesulphurization catalyst using molecular recognition technology,” *Chemical engineering science*, pp. 353-362, 2015.
- [44] M. Godino-Salido, A. Santiago-Medina, P. Arranz-Mascaros, R. Lopez-Garzon, M. D. Gutierrez-Valero, M. Melguizo en F. J. Lopez-Garzon, „Novel active carbon/crown ether derivative hybrid material for the selective removal of Cu(II) ions: The crucial role of the surface chemical functions,” *Chemical engineering science*, vol. 116, pp. 94-104, 2014.

- [45] M. Hong, L. Yu, Y. Wang, J. Zhang, Z. Chen, L. Dong, Q. Zan en R. Li, „Heavy metal adsorption with zeolites: The role of hierarchical pore architecture,” *Chemical engineering journal*, vol. 359, pp. 363-372, 2019.
- [46] C. Peric, M. Trgo en V. Medvidovic, „Removal of zinc, copper and lead by natural zeolite—a comparison of adsorption isotherms,” *Water research*, vol. 38, nr. 7, pp. 1893-1899, 2004.
- [47] M. F. Navarro Pouard, E. Polo, P. Taboada, A. Arenas-Vivo, P. Horcajada, B. Pelaz en P. Del Pino, „Aqueous Synthesis of Copper(II)-Imidazolate Nanoparticles,” *Inorganic Chemistry*, vol. 57, nr. 19, pp. 12056-12065, 2018.
- [48] D. Alezi, Y. Belmabkhout, M. Suyetin, P. M. Bhatt, L. J. Weselinski, V. Solovyeva, K. Adil, I. Spanopoulos, P. N. Trikalitis, A. Emwas en M. Eddaoudi, „MOF crystal chemistry paving the way of gas storage needs: ALuminum-based soc-MOF for CH₄, O₂ and CO₂ storage,” *Journal of the American chemical society*, nr. 137, pp. 13308-13318, 2015.
- [49] Z. Hu, S. Faucher, Y. Zhuo, Y. Sun, S. Wang en D. Zhao, „Combination of optimization and metalated-Ligand exchange: an effective approach of functionalize UiO-66(Zr) MOFs for CO₂ separation,” *A European Journal*, nr. 48, pp. 17246-17255, 2015.
- [50] M. D. Telgerd, M. Sadeghinia, G. Birhanu, M. Daryasari, A. Zandi-Karimi, A. Sadeghinia, H. Akbarijavar, M. H. Karami en E. Seyedjafari, „Enhanced osteogenic differentiation of mesenchymal stem cells on metal–organic framework based on copper, zinc, and imidazole coated poly-l-lactic acid nanofiber scaffolds,” *Journal of biomedical materials research*, vol. 107, nr. 8, pp. 1841-1848, 2019.
- [51] R. Bian, T. Wang, L. Zhang, L. Li en C. Wang, „A combination of tri-modal cancer imaging and in vivo drug delivery by metal-organic framework based composite nanoparticles,” *Biomaterials Science*, nr. 9, pp. 1270-1278, 2015.
- [52] M. Wu en Y. Yang, „Metal-organic framework(MOF) based drug/cargo delivery and cancer therapy,” *Advanced materials*, nr. 29, p. 1606134, 2017.
- [53] S. Zafari, M. N. Shahrak en M. Ghahramaninezhad, „New MOF-Based Corrosion Inhibitor for Carbon Steel in Acidic Media,” *Metals and Materials International*, nr. 26, pp. 25-38, 2019.
- [54] S. Tominaka, H. Hamoudi, T. Suga, T. D. Bennett, A. B. Cairns en A. K. Cheetham, „Topochemical conversion of a dense metal-organic framework from a crystalline insulator to an amorphous semiconductor.,” *Chemical Science*, vol. 6, nr. 2, pp. 1465-1473, 2015.
- [55] K. A. McDonald, S. Seth en A. J. Matzger, „Coordination polymers with high energy density: an emerging class of explosives,” *Crystal Growth and Design*, vol. 15, nr. 12, pp. 5963-5972, 2015.
- [56] Q. Zhang, M. Chen, L. Zhong, Q. Ye, S. Jiang en Z. Huang, „Highly effective removal of metal cyanide complexes and recovery of Palladium using quaternary-ammonium-functionalized MOFs,” *Molecules*, vol. 23, p. 19, 2018.
- [57] Y. Liu, S. Lin, Y. Liu, A. K. Sarkar, J. K. Bediako, H. Y. Kim en Y. Yun, „Super-stable, highly efficient, and recyclable fibrous metal-organic framework membranes for precious metal recovery from strong acidic solutions,” *Metal organic fibrous membranes*, vol. 15, p. 19, 2019.

- [58] W. Yang, J. Wang, Q. Yang, H. Pei, N. Hu, Y. Suo, Z. Li, Zhang, D en J. Wang, „Facile fabrication of robust MOF membranes on cloth via a CMC macromolecule bridge for highly efficient Pb(II) removal,” *Chemical engineering journal*, vol. 339, pp. 230-239, 2018.
- [59] K. Wang, Z. Tian en N. Yin, „Significantly Enhancing Cu(II) Adsorption onto Zr-MOFs through Novel Cross-Flow Disturbance of Ceramic Membrane,” *Industrial and Engineering chemistry research*, vol. 57, nr. 1à, pp. 3773-3780, 2018.
- [60] Y. Peng, H. Huang, Y. Zhang, C. Kang, S. Chen, L. Song, D. Liu en C. Zongh, „A versatile MOF-based trap for heavy metal ion capture and dispersion,” *Nature communications*, vol. 187, nr. 9, 2018.
- [61] Z. Li, J. Yang, K. Sui en N. Yin, „Facile synthesis of metal-organic framework MOF-808 for arsenic removal,” *Materials letter*, vol. 160, pp. 412-414, 2015.
- [62] M. Jian, B. Liu, R. Liu, J. Qu, H. Wang en X. Zhang, „Water-based synthesis of zeolitic imidazolate framework-8 with high morphology level at room temperature,” *RSC Advances*, nr. 5, pp. 48433-48441, 2015.
- [63] K. S. Park, Z. Ni, A. P. Coté, J. Y. Choi, R. Huang, F. J. Uribe-Romo, H. K. Chae, M. O’Keeffe en O. M. Yaghi, „Exceptional chemical and thermal stability of zeolitic imidazolate frameworks,” *PNAS*, vol. 103, nr. 27, p. 10186 –10191, 2006.
- [64] X. Wang, Q. Cheng, Y. Yu en X. Zhang, „Controlled Nucleation and Controlled Growth for Size Predictable Synthesis of Nanoscale Metal–Organic Frameworks (MOFs): A General and Scalable Approach,” *Angewandte Chemie*, vol. 57, nr. 26, pp. 7836-7840, 2018.
- [65] C. Avci, J. Arinez-Soriano, A. Carné-Sanchez, V. Guillerm, C. Carbonell, I. Imaz en D. Maspoch, „Post-Synthetic Anisotropic Wet-Chemical Etching of Colloidal Sodalite ZIF Crystals,” *Angewandte Chemie*, vol. 54, nr. 48, pp. 14417-14421, 2015.
- [66] S. Chen, „The roles of imidazole ligands in coordination supramolecular systems,” *CrystEngComm*, vol. 18, nr. 35, pp. 6523-6760, 2016.
- [67] L. Jian Bin, L. Rui-Biao, C. Xiao-Ning, Z. Jie-Peng en Z. Xiao-Ming, „Solvent/additive-free synthesis of porous/zeolitic metal azolate frameworks from metal oxide/hydroxide,” *Chemical Communications*, vol. 47, nr. 32, pp. 9185-9187, 2011.
- [68] A. Schejn, L. Balan, V. Falk, L. Aranda, G. Medjadhi en R. Schneider, „Controlling ZIF-8 nano- and microcrystal formation and reactivity through zinc salt variations,” *CrystEngComm*, vol. 16, nr. 21, pp. 4493-4500, 2014.
- [69] Z. Wang, Z. Si, D. Cai, G. Li, G. Li, S. Li, P. Qin en T. Tan, „Improving ZIF-8 stability in the preparation process of polyimide-based organic solvent nanofiltration membrane,” *Separation and purification technology*, vol. 227, 2019.
- [70] Q. Luo, H. Lin, Y. Y. Zhang en H. Peng, „Reactions of metal salts with bronsted acidic ionic liquid: Formations of imidazole template metal sulfates or imidazole-metal complexes,” *Inorganica Chimica Acta*, vol. 447, pp. 32-37, 2016.

- [71] L. Zhang en Y. Hang Hu, „Strong Effects of Higher-Valent Cations on the Structure of the Zeolitic Zn(2-methylimidazole)₂ Framework (ZIF-8),” *The journal of physical chemistry*, pp. 7967-7971, 2011.
- [72] A. Dhakshinamoorthy, A. M. Asin en H. Garcia, „Catalysis by metal-organic frameworks in water,” *Chem. Commun*, nr. 50, pp. 12800-12814, 2014.
- [73] H. Zhang, M. Zhao en Y. S. Lin, „Stability of ZIF-8 in water under ambient conditions,” *Microporous and mesoporous materials*, vol. 279, pp. 201-210, 2019.
- [74] H. Zhang, D. Liu, Y. Yao, B. Zhang en Y. S. Lin, „Stability of ZIF-8 membranes and crystalline powders in water at room temperature,” *Journal of membrane science*, vol. 483, pp. 103-111, 2015.
- [75] V. V. Butova, A. P. Budnyk, E. A. Bulanova, C. Lamberti en A. V. Soldatov, „Hydrothermal synthesis of high surface area ZIF-8 with minimal use of TEA,” International research center "Smart Materials", Rostov-on-Don, 344090, Russia.
- [76] ChemicalBook, „www.chemicalbook.com,” ChemicalBook, 2017. [Online]. Available: https://www.chemicalbook.com/ProductMSDSDetailCB6146227_EN.htm. [Geopend 5 March 2020].
- [77] PubChem, „www.pubchem.com,” Pubchem, [Online]. Available: <https://pubchem.ncbi.nlm.nih.gov/compound/2-methylimidazole>. [Geopend 20 Maart 2020].
- [78] C. Li en M. Du, „Role of solvents in coordination supramolecular systems,” *Chemical communications*, vol. 47, nr. 21, pp. 5958-5972, 2011.
- [79] pubchem, „pubchem.ncbi.nlm.nih.gov,” pubchem, 2020. [Online]. Available: <https://pubchem.ncbi.nlm.nih.gov/compound/2-methylimidazole#section=Computed-Properties>. [Geopend 24 March 2020].
- [80] M. Jian, B. Liu, L. Ruiping, J. Qu, H. Wang en X. Zhang, „Water-based synthesis of zeolitic imidazolate framework-8 with high morphology level at room temperature,” *RSC Advances*, nr. 5, pp. 48433-48441, 2016.
- [81] S. Tanaka, K. Kida, M. Okita, Y. Ito en Y. Miyaka, „Controlled Synthesis of Zeolitic Imidazolate Framework-8 (ZIF-8) Crystals in an aqueous System at Room Temperature,” *Chem. Lett.*, vol. 41, pp. 1337-1339, 2012.
- [82] N. A. H. M. Nordin, A. F. Ismail, A. Mustafa, P. S. Goh, D. Rana en T. Matsuura, „Aqueous room temperature synthesis of zeolitic imidazole framework 8 (ZIF-8) with various concentrations of triethylamine,” *RSC Advances*, nr. 4, pp. 33292-33300, 2014.
- [83] J. Cravillon, R. Nayuk, S. Springer, A. Feldhoff, K. Huber en M. Wiebcke, „Controlling Zeolitic imidazolate framework nano- and microcrystal formation: Insight into crystal growth by time-resolved in situ static light scattering,” *Chemistry of materials*, nr. 23, pp. 2130-2141, 2011.

- [84] L. Zhou, N. Li, G. Owens en Z. Chen, „Simultaneous removal of mixed contaminants, copper and norfloxacin, from aqueous solution by ZIF-8,” *Chemical Engineering Journal*, nr. 362, pp. 628-637, 2019.
- [85] J. J. Beh, J. K. Lim, E. P. Ng en B. S. Ooi, „Synthesis and size control of zeolitic imidazolate framework-8 (ZIF-8): From the perspective of reaction kinetics and thermodynamics of nucleation,” *Materials Chemistry and Physics*, pp. 393-401, 2018.
- [86] M. F. Navarro Pouard, E. Polo, P. Taboada, A. Arenas-Vivo, P. Horcajada, B. Pelaz en P. Del Pino, „Aqueous Synthesis of Copper(III)-Imidazolate Nanoparticles,” *Inorganic Chemistry*, 2018.
- [87] Y. Jin, J. Wu, J. Wang, Y. Fan, S. Zhang, N. Ma en W. Dai, „Highly efficient capture of benzothiophene with a novel water-resistant-bimetallic Cu-ZIF-8 material,” *Inorganic Chimica Acta*, 2020.
- [88] R. Li, R. Ren, X. Feng, X. Li, C. Hu en B. Wang, „A highly stable metal-and nitrogen-doped nanocomposite derived from Zn/Ni-ZIF-8 capable of CO₂ capture and separation,” *Chem. Commun.*, vol. 50, pp. 6894-6897, 2014.
- [89] G. Bhargava, T. Ramanarayanan en S. L. Bernasek, „Imidazole–Fe Interaction in an Aqueous Chloride Medium: Effect of Cathodic Reduction of the Native Oxide,” *Langmuir*, vol. 26, nr. 1, pp. 215-219, 2010.
- [90] W. Heming en J. R. Zhiyong, „Bioelectrochemical metal recovery from wastewater: a review,” *Water research*, vol. 66, pp. 219-232, 2014.
- [91] S. He, J. Wang en J. Yan, „Pressure leaching of high silica Pb–Zn oxide ore in sulfuric acid medium,” *hydrometallurgy*, vol. 104, nr. 2, p. 235_240, 2010.

Appendix 1

MOF synthesis

The MOF synthesis requires metal nitrates, TEA and 2-methylimidazole as organic linker molecule. Table 13 shows the required chemical agents.

- Table 13 Chemical agents MOF synthesis

Chemical name	Chemical formula
Zincnitrate hexahydrate	$Zn(NO_3)_2 \cdot 6H_2O$
Cuppernitrate trihydrate	$Cu(NO_3)_2 \cdot 3H_2O$
Leadnitrate	$Pb(NO_3)_2$
Nickelnitrate hexahydrate	$Ni(NO_3)_2 \cdot 6H_2O$
2-methylimidazole	$C_4H_6N_2$

Triethylamine	$C_6H_{15}N$
---------------	--------------

First, metal stock solutions were prepared for each metal separately. Afterwards, 10 ml of the required stock solution was brought into a Falcon tube of 50 ml. In this experiment, none of the different metal solutions came in contact with each other. Totally, there were 48 samples, 12 samples for each metal. Furthermore, 3 stock solutions of TEA were prepared with different concentrations and 2 stock solutions of 2-methylimidazole. Each sample requires a second Falcon tube which will consist 20 ml of the TEA stock solution and 10 ml of 2-methylimidazole. In the end, the metal solution was added to the mixture of organic linker and TEA. The total amount of reaction mixture was 30 ml. The final concentrations of TEA were varied for each metal: respectively 0, 30 and 90 mM. The concentration of 2-methylimidazole were also varied. The concentrations were 30 or 90 mM.

The reaction itself was executed at three different temperatures depending of the sample: room temperature, 80°C and 120°C. This varying was introduced to study the temperature dependence. At room temperature, the samples were directly blend by an end-over-end shaker in the contrary with the reaction at 80 and 120°C were blending was impossible due to the need of a furnace. Especially for the samples at 120°C, autoclave reactors were used to avoid evaporation of the chemical agents. Figure 29 shows the autoclave reactors.



- Figure 29 Autoclave reactors

The reactors were provided with bursting discs to avoid high pressures and were manually sealed with a special key tool on a vice.

After a reaction time of 24 hours, the samples were first cooled down depending on the reaction temperature and afterwards placed in the centrifuge Eppendorf 5810 apparatus at 3400 rpm for 20 minutes. After centrifugation the supernatants is filtered by a sprayfilter Chromafil® OA 45/25. Subsequently milli-Q water is added to the precipitate and the centrifugation is executed again for 10 minutes. Thereafter, the supernatants is removed with a syringe and thrown away. The precipitate is dried in the oven at 40°C until it was dry.

For each sample the supernatant is analyzed by the ICP-OES apparatus and the pH was measured by the Mettler Toledo SevenExcellence Labvantage 160229-00001. These analyses must clarify of the metals were effectively removed and precipitated.

DEEL 2 ARTIKEL

EEN NIEUWE METHODE VOOR DE UITLOGING VAN METALEN DOOR HET GEBRUIK VAN BASISCHE, ORGANISCHE UITLOOGMIDDELEN

MASTER'S THESIS

Sam Haenen¹, Prof. dr. Ir. Leen Braeken¹ en Dr. Ir. Maarten Everaert²

¹ University Hasselt & University of Leuven, Faculty of Engineering Technology, Agoralaan Building B & H, B-3590 Diepenbeek, Belgium

² VITO, Boeretang 200, B-2400 Mol, Belgium

ABSTRACT

Omtrent het recycleren van metalen wordt er veel onderzoek verricht door de druk op het milieu en de alsmaar schaarsere grondstoffen. In deze studie wordt een innovatieve uitloogmethode onderzocht om selectief metalen te herwinnen uit vier minerale afvalstromen: goethiet slib, ferrochroom slakken, *shredder* filterkoek en FeCl₂ slib.

Voor de metaaluitloging werden drie organische, basische uitloogmiddelen onderzocht: cholinehydroxide, 2-methylimidazol (Hmim) en 1,1,3,3-tetramethylguanidine (GUA). Hmim en GUA kunnen metaalcomplexen vormen. De experimenten werden uitgevoerd waarbij de concentratie van uitloogmiddelen (0; 0,01; 0,1 of 1 M) bedroeg en zijn herhaald voor Hmim en GUA in aanwezigheid van 1 M NaOH om de vorming van coördinatiebindingen te stimuleren.

Uit de resultaten bleek dat deze uitloogmiddelen de uitlooefficiëntie van matrixelementen (Ca, Mg en Fe) sterk verlagen vanaf een pH van 8. Al daarentegen vertoonde wel uitloging vanaf een pH van 12. Hmim was in staat oplosbare complexen te vormen met Cu en vormde vermoedelijk met Zn het onoplosbare ZIF-8. Bij een pH hoger dan 13,3 vormde GUA met Cu en Zn oplosbare complexen.

Deze studie toonde aan dat vanaf een pH van 12 enkel de uitloging van het matrixelement Al bevorderd werd. Hmim verhoogde de uitlooefficiëntie van Cu door de vorming van coördinatiebindingen. Ook GUA verhoogde de uitlooefficiëntie van Cu, Zn bij pH waarden boven 13,3 door het vormen van oplosbare complexen met deze metalen. Verder onderzoek kan de exacte speciatie van de gevormde complexen uitwijzen.

Keywords: *Selectieve metaaluitloging; minerale afvalstromen; basische, organische uitloogmiddelen; metaalcomplexen.*

INTRODUCTIE

Inzichten in de herwinning van metalen zijn vandaag de dag van cruciaal belang. De toenemende druk op de natuur en de alsmaar schaarsere grondstoffen spelen hier een centrale rol. Ook vanuit het economisch standpunt kent de metaalrecyclage grote opportuniteiten. Daarnaast heeft het recycleren van metalen potentieel om energie efficiënter en veel sneller te zijn dan traditionele, trage mijnprocessen, afhankelijk van het soort afvalstroom. Er kan zo in sommige gevallen zelfs een factor 10 tot 20 energie bespaard worden^{[1][2]}. Deze energie reductie is niet alleen financieel interessant maar draagt ook bij tot een milieuvriendelijker aanpak, waarbij de uitstoot van broeikasgassen verlaagd kan worden^[3]. Verder vormt de aanwezigheid van metaalfracties in grondwater en de bodem een bedreiging voor de gezondheid van de mens doordat het slechts ettelijke stappen van de voedselketen verwijderd is. Talloze schadelijke effecten zijn gediagnostiseerd: bv. kanker, leverfalen, nierziekten^[4].

Bijgevolg is het dus, zowel vanuit economisch-, milieu- en gezondheidstandpunt, van belang om waardevolle en schadelijke metalen uit deze afvalstromen te verwijderen. In dit onderzoek worden vier verschillende minerale residuen bestudeerd, waarbij specifiek de herwinning van waardevolle metalen interessant is: goethiet slib, FeCl₂ slib, ferrochroom slakken en *shredder* filterkoek.

Het goethiet slib wordt gegenereerd in een gecombineerd roost-, uitloog- en elektrowinningsproces voor de productie van zink. De bekomen uitloogoplossing is een zure stroom na toevoegen H₂SO₄ en bevat grote hoeveelheden zink en ijzer. Ijzer dient verwijderd te worden omdat het de herwinning van Zn voorkomt op elektrodes in de elektrowinningsstap. Daarom wordt het ijzer neergeslagen onder de vorm van goethiet FeO(OH) nadat eerst zinksulfide is toegevoegd gevolgd door het aanpassen van de pH naar 3,5-4 door toevoegen van Ca(OH)₂ en lucht die zorgt voor de oxidatie van Fe²⁺ naar Fe³⁺. Goethiet slib is de voornaamste afvalstroom die vrijkomt tijdens het proces. Per ton gedolven erts ontstaat er 0,25 ton goethiet slib. Naast Fe bevat

deze afvalstroom ook 8-10% zink en enkele andere waardevolle metalen, *e.g.* Pb, In en As ^[5]. Zn komt hier vooral voor onder de vorm ZnO en ZnFe₂O₄ ^[6].

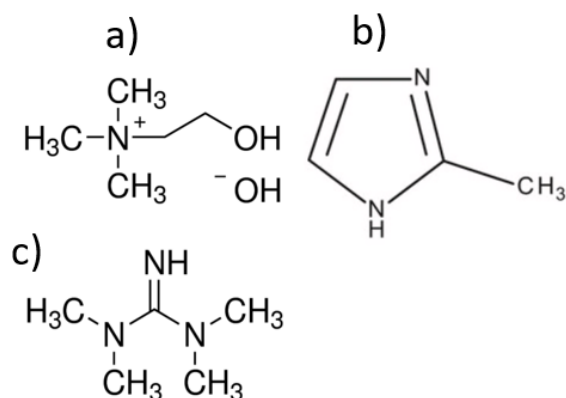
De ferrochroom slakken komen vrij bij de productie van ferrochroom: voor elke kg FeCr die geproduceerd wordt, wordt ook 1,1-1,5 kg slak gevormd ^[3]. FeCr wordt vooral gebruikt voor de productie van roestvast staal. Roestvast staal is een gegeerd materiaal en de productieaantallen kennen dan ook jaarlijks een grote groei met zodus bijhorende groei van het afval ^[3]. Het nuttig gebruik van deze afvalstroom blijft een grote uitdaging. Het storten van deze afvalstroom is meest voorkomend samen met het gebruik voor wegenwerken en bouwmaterialen ^[3]. De samenstelling van deze afvalstroom hangt af van de gedelfde ertsen. Verder bevat deze stroom voornamelijk Cr en Fe ^[7].

Het FeCl₂ slib is afkomstig van de TiO₂ productie volgens het chlorideproces. Hiervoor worden er ertsen gebruikt die een TiO₂-gehalte bevatten tussen 85 en 95%. Het belangrijkste nevenbestanddeel is Fe₂O₃. Tijdens het proces worden deze metaaloxides omgezet naar chlorides, waarna het kostbare TiCl₄ wordt afgescheiden. De reststroom wordt een vaste stof na afkoelen en wordt in water gesuspenderd waarin de metaalchloriden oplossen en er een zure afvalstroom overblijft. Hierna wordt deze gefiltreerd en geneutraliseerd door kalkmelk toe te voegen. De aanwezige chlorideconcentraties in de filterkoek limiteert op dit moment de mogelijkheden voor hergebruik van dit materiaal.

De *shredder* filterkoek is afkomstig van een *shredderbedrijf* gespecialiseerd in de verwerking van autowrakken en schroot. De filterkoek is rijk aan Fe₂O₃, zand en een heleboel restanten van verontreinigingen zoals plastic en hout.

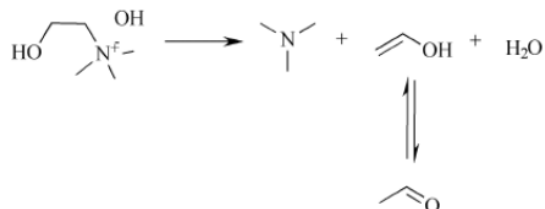
In dit artikel wordt de metaalherwinning via uitloogmethodes bestudeerd, gebruikmakend van organische, basische uitloogmiddelen. Het hoofddoel van deze innovatieve methode is selectiviteit bevorderen die in zuur midden niet haalbaar is om zo meer waardevolle metalen, *e.g.* Cu, Zn, Pb, Ni,... te herwinnen t.o.v. interfererende elementen, *e.g.* Fe, naast het exploreren van de uitloogmogelijkheden in basisch milieu ^[8]. De mogelijkheid van de organische basen om coördinatiebindingen te vormen via stikstof met de metalen draagt hieraan bij. De literatuur beschrijft vooral het gebruik van organische zuren, *e.g.* methaansulfonzuur, mierenzuur, asparaginezuur en citroenzuur, in tegenstelling tot organische basen besproken in deze studie ^{[9][10][11][12]}.

Er werd gebruik gemaakt van drie verschillende basen: cholinehydroxide (=2-hydroxy-N,N,N trimethylethanamium), 2-methylimidazol (Hmim) en 1,1,3,3-tetramethylguanidine (GUA), waarvan de structuren zijn weergegeven in Figuur 1.



Figuur 1. Structuurformules van de uitloogmiddelen: cholinehydroxide ^[13] (a), 2-methylimidazol ^[14](b) en 1,1,3,3-tetramethylguanidine ^[15](c).

Cholinehydroxide bevat een primaire alcohol groep en een quaternair ammoniumzout. Het heeft een pK_a waarde van 11,2 bij 25°C ^[16]. Het verhoogt de pH van de oplossing op een soortgelijke manier als de sterke base NaOH door zijn counter hydroxyl ion af te geven. Dit molecule kan niet rechtstreeks een complex vormen met een metaal, omdat het stikstofatoom niet over een vrij elektronenpaar beschikt. Echter, cholinehydroxide is een relatief onstabiel molecule en kan omgezet worden naar trimethylamine en acetaldehyde door een Hofmann-eliminatie ^[17]. Deze omzetting kan plaats vinden door het toevoegen van warmte ^{[18][19]}. Figuur 2 geeft het reactieschema weer van deze omzetting. De evenwichtsreactie tussen het gevormde alcohol en het acetaldehyde vormt een tautomeer evenwicht.



Figuur 2. Hofmann eliminatie cholinehydroxide ^[17].

Hmim heeft een pK_a van 7,89 bij 20°C en beschikt over twee vrije elektronenparen indien beide stikstofatomen gedeprotoneerd zijn ^[20]. In sterk alkalisch milieu heeft dit molecule zodus de mogelijkheid om op twee plaatsen coördinatie bindingen te vormen ^[21]. Daarnaast zal dan ook de sterkte van de coördinatiebinding toenemen door toenemende negatieve lading op het gecreëerde anion ^[21]. Zelf verhoogt deze organische base de pH van de oplossing door zelf protonen te binden waardoor er relatief meer OH⁻ ionen in oplossing blijven.

GUA heeft een pK_a van 13,0 en is zodus de sterkste organische base van de drie ^[22]. Het verhoogt de pH volgens hetzelfde principe als Hmim. Daarnaast kan GUA op drie verschillende plaatsen coördinatiebindingen aangaan doordat de drie N-atomen individueel over een vrij elektronenpaar beschikken. De literatuur beschrijft mogelijke coördinatiebindingen tussen guanidine verbindingen en de metaalkationen Pb²⁺, Co²⁺, Hg²⁺, Zn²⁺, As³⁺ en Cd²⁺ ^{[23][24]}.

Voorbehandeling

De vier materialen werden voorbehandeld om een fijnkorrelige structuur te garanderen (*i.e.* minstens <120 µm). Hiervoor werd een kogelmolen gebruikt om de vaste stalen eerst te malen. Verder werd er op deze afvalmaterialen een XRF-analyse uitgevoerd met een *XRF-Niton* toestel om de elementaire samenstelling te bepalen.

Uitloogexperimenten

Hoewel de algemene werkwijze voor de uitloogexperimenten gelijkaardig was, zijn de specifieke reactieomstandigheden voor elk uitloogmiddel weergegeven in Tabel 1. Er werden drie verschillende organische uitloogmiddelen getest: cholinehydroxide (46% w/w), 2-methylimidazol en 1,1,3,3-tetramethylguanidine. De uitloogreactie vond plaats in een over-de-kop schudder. De bekomen suspensies werden gefiltreerd met een spuitfilter Chromafil® OA met poriegrootte 45 µm. De vaste residu's werden nadien gedroogd op 105°C totdat een constante massa werd bereikt. Het effect van Hmim en GUA werd bijkomend getest in aanwezigheid van 1 M NaOH om het effect van coördinatiebindingen te onderzoeken. Onderstaande tabel geeft de details horende bij ieder uitloogmiddel.

Tabel 1. Gedetailleerde beschrijving uitloogexperimenten.

	Cholinehydroxide	Hmim	GUA
Afgevoegen massa staal [g]	0,5000	2,0000	2,0000
Reactietijd [uur]	0,5	24	24
Volume uitloogmiddel [ml]	5	20	20
Concentratie uitloogmiddel [M]	0;0,01;0,1;1	0;0,01;0,1;1	0;0,01;0,1;1
Vloeibaar/vast ratio [ml/g]	10	10	10
Test additie 1M NaOH	Neen	Ja	Ja

Analyses

Van de eluaten werd telkens de pH en de Oxidatie-Reductie Potentiaal (ORP) opgemeten. Daarnaast werden de metaalconcentraties bepaald d.m.v. ICP-OES analyses waarbij 2 ml staal werd aangelengd met 20 ml MilliQ water en 0,4 ml HNO₃. De elementaire samenstelling van de vaste residu's werd bepaald met de draagbare *XRF-Niton*. Tabel 2 geeft voor iedere afvalstroom specifiek weer welke elementen opgemeten werden. Onderling zijn er kleine verschillen zichtbaar doordat niet ieder element voorkwam in de afvalstromen.

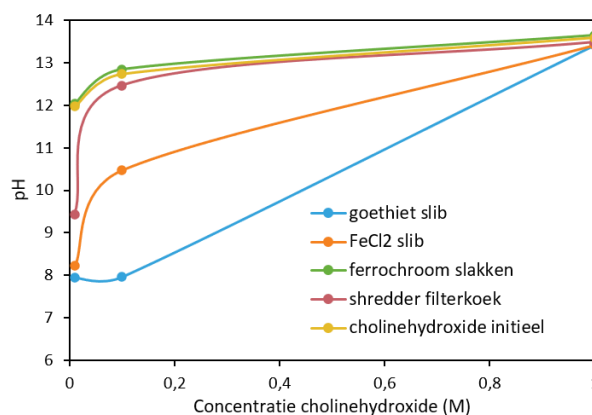
Tabel 2. Geanalyseerde elementen per afvalstroom.

Afvalstroom	Geanalyseerde elementen
Goethiet slib	In, Al, Fe, As, Ca, Cd, Cr, Mg, Mn, Pb, Sb, Sn, Ti, Zn, Cu
FeCl ₂ slib	Fe, (Si), Al, Mg, P, Ca, Ti, V, Cr, Mn, Ni, Zr, Nb
Ferrochroom slakken	Fe, Ca, Al, Mg, (Si), Cr, V, Mn

RESULTATEN EN DISCUSSIE

Effect uitloogmiddel op pH

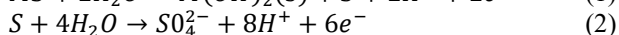
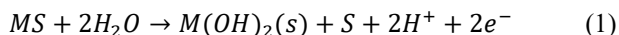
Voor het beschrijven van de uitloogexperimenten is de pH een belangrijke factor. De literatuur beschrijft de pH tijdens de uitloogexperimenten zelfs als de meest cruciale invloedfactor die het voorkomen van de meeste reacties in de oplossingen en de mineralen zal bepalen [25]. De pH bepaalt in welke vorm het uitloogmiddel zal voorkomen (al dan niet geprotoneerd) en zal dus ook de mogelijkheid om coördinatie bindingen te vormen bepalen. Ook kunnen de OH⁻ anionen zelf complexen vormen met kationen. Daarnaast beïnvloedt deze ook het voorkomen van onoplosbare metaalhydroxides of net oplosbare metaalkationen/ metaalcomplexen [26]. Om te achterhalen in welke vorm de metalen voorkomen bij de overeenkomende pH, kan gebruik gemaakt worden van Pourbaix diagrammen. Deze geven de potentiaal weer in functie van de pH. Daarnaast beïnvloedt de pH ook of er adsorptie plaatsvindt omdat de protonen en OH⁻ anionen ook geadsorbeerd kunnen worden aan het mineraal oppervlak en zo de adsorptie van andere ionen kunnen verhinderen. Bijkomend is de oppervlakte lading van de meeste mineralen pH afhankelijk [26]. Figuur 3 geeft de pH in functie van de concentratie cholinehydroxide weer van zowel de finale uitloogoplossingen als de initiële cholinehydroxide oplossing.



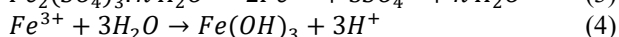
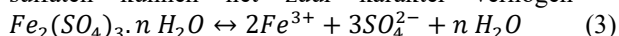
Figuur 3. pH in functie van de concentratie cholinehydroxide voor zowel de finale uitloogoplossingen als de initiële cholinehydroxide oplossing.

Figuur 3 illustreert dat bij lage cholinehydroxide concentraties de pH waarden van de onderlinge materialen verschilde. Merk op dat de curve van de ferrochroom slakken bijna exact samenvalt met de curve van de initiële cholinehydroxide oplossing. De curve van de ferrochroom slakken bereikt daarmee de hoogste pH waarde. Een verklaring hiervoor is de zeer hoge concentratie Ca in de ferrochroom slakken: (341200 mg/kg). De literatuur beschrijft dat deze afvalstroom voornamelijk Ca onder de vorm van CaO bevat die zodus grote hoeveelheden protonen kan vangen resulterend in een verhoogde pH van de oplossing [27]. Bij hogere pH regio's zal deze CaO neerslaan onder de vorm van

Ca(OH)₂. Daarnaast is ook zichtbaar dat de andere afvalstromen een zuur karakter vertonen doordat bij lage concentratie cholinehydroxide de finaal bereikte pH veel lager ligt dan de initiële pH. Dit zuur karakter van de afvalstromen indiceert mogelijks de aanwezigheid van zure sulfide verbindingen. Onderstaande reacties verklaren het ontstaan van protonen in aanwezigheid van water:

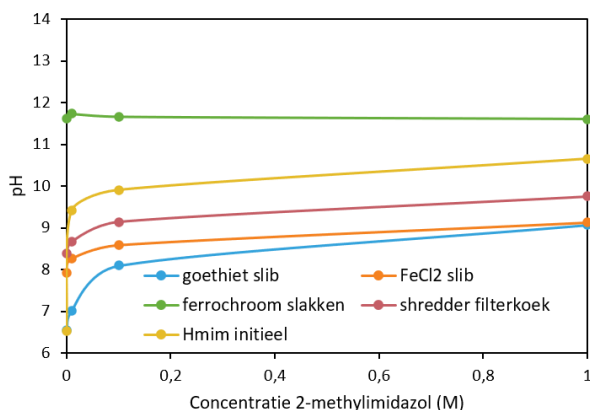


waarbij M = metaal [28]. Daarnaast bevatten de afvalstromen mogelijks pyriet (FeS₂) wat bijkomend in staat is OH⁻ anionen te adsorberen aan zijn oppervlak [29]. Ook Fe³⁺/Al³⁺ sulfaten kunnen het zuur karakter verhogen [30]:



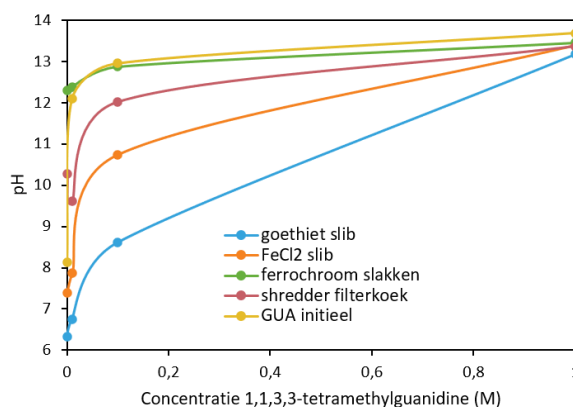
Verder kan in de andere verbindingen Ca mogelijks voorkomen onder de vorm van gips: CaSO₄·2H₂O wat vervolgens de pH verlaagt [31]. Volgende reactie treedt op: $2OH^- + CaSO_4 \cdot H_2O + 2CO_2 \leftrightarrow CaCO_3(s) + SO_4^{2-} + 2H_2O + H_2CO_3$ (5)

Figuur 4 geeft de pH in functie van de concentratie Hmim weer in afwezigheid van NaOH voor zowel de finale uitloogoplossingen als de initiële Hmim oplossing. Voor zowel Hmim als GUA zijn de experimenten herhaald in aanwezigheid van 1 M NaOH. Het toevoegen van deze sterke base heeft als doel de pH van de oplossing te verhogen waardoor de organische bases bijna uitsluitend in gedeprotoneerde vorm voorkomen (zie Figuur 7). De aanwezige protonen kunnen de bases protoneren waardoor deze geen coördinatiebindingen meer kunnen aangaan met de metalen. De pH verhoging zal de vorming van coördinatiebindingen tussen stikstof en metalen bevorderen. Cholinehydroxide is expliciet niet getest in aanwezigheid van 1 M NaOH doordat dit molecuul geen coördinatiebindingen kan vormen. Het is wel zo dat dit molecuul onstabiel is en kan uiteenvallen tot trimethylamine. Trimethylamine bevat een stikstof met een vrij elektronenpaar wat het theoretisch mogelijk maakt om coördinatiebindingen te vormen. De literatuur betwijfelt dit echter door de sterische hinder veroorzaakt door de drie methylgroepen. De pH in aanwezigheid van NaOH is enkel gemeten voor GUA.

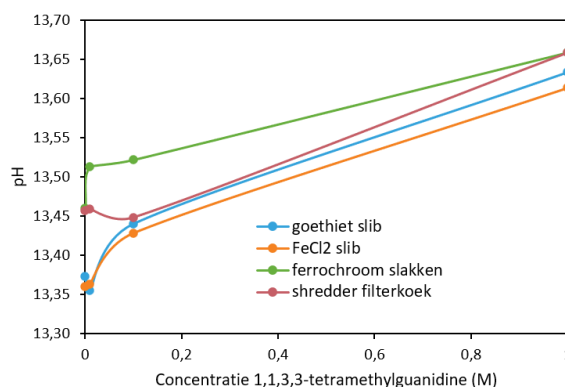


Figuur 4. pH in functie van de concentratie Hmim in afwezigheid van NaOH voor zowel de finale uitloogoplossingen als de initiële Hmim oplossing.

Figuur 4 toont ook verschillen qua pH voor de verschillende materialen onderling na toevoegen Hmim. Het verloop van de curves is wel identiek: eerst een matig tot sterke stijging gevolgd door een zeer zwakke toename in pH. Opvallend ook hier is dat de pH van de ferrochroom slakken significant hoger ligt waarvoor dezelfde verklaring geldt als eerder gegeven. Figuur 5 en 6 tonen het pH verloop van de uitloogexperimenten met GUA in respectievelijk aan- en afwezigheid van NaOH.

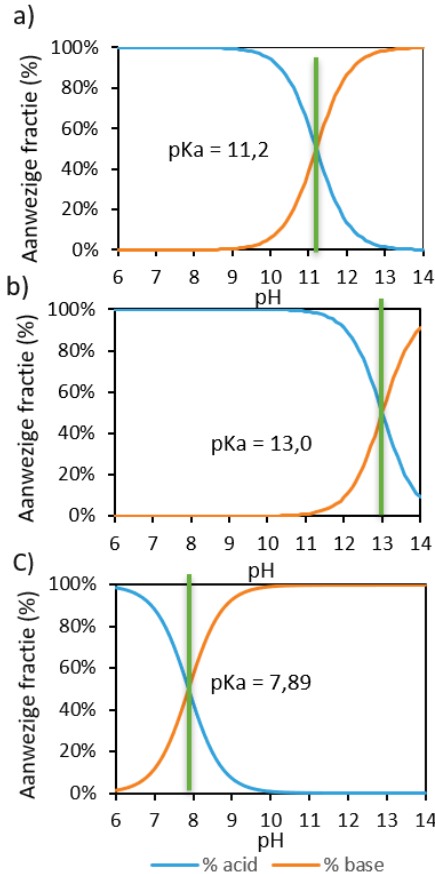


Figuur 5. pH verloop GUA in afwezigheid van NaOH.



Figuur 6. pH verloop GUA in aanwezigheid van NaOH.

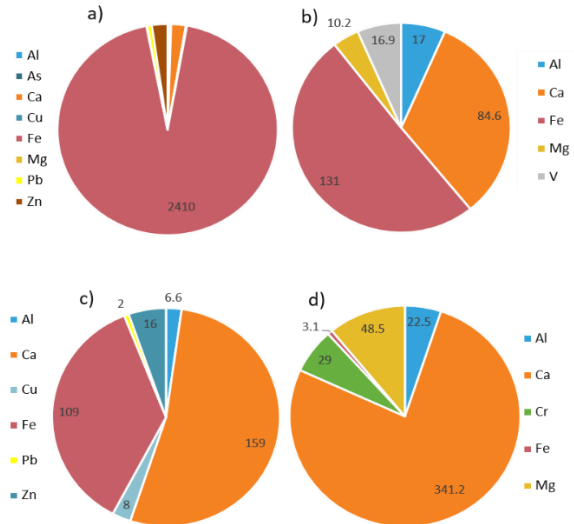
Figuur 5 en 6 tonen wederom dat de ferrochroom slakken de hoogste pH-waardes bereiken. De pH waardes liggen bij gebruik van deze organische base hoger in vergelijking met de andere uitloogmiddelen doordat GUA de sterkste base is ($pK_a = 13$). Figuur 7 geeft de speciatie diagrammen weer van de drie uitloogmiddelen. Deze figuren geven het percentage weer van uitloogmiddel voorkomend als base (gedeprotoneerd) en als geconjugeerd zuur (geprotoneerd) in functie van de pH van de waterige oplossing. De pH van het uitloogstelsel zal het vormen van coördinatiebindingen door de uitloogmiddelen met metalen sterk beïnvloeden zoals eerder vermeld.



Figuur 7. Speciatie diagrammen cholinehydroxide (a), GUA (b) en Hmim (c).

Elementaire samenstelling minerale residuen

De elementaire samenstelling van de afvalmaterialen is onontbeerlijk bij het bepalen van de uitlooefficiëntie. Figuur 8 geeft de elementaire samenstelling van de afvalmaterialen weer. Enkel de meest voorkomende elementen zijn opgenomen.



Figuur 8. Samenstelling materialen: goethiet slib (a), FeCl₂ slib (b), shredder filterkoek (c) en de ferrochroom slakken (d) uitgedrukt in g/kg.

Figuur 8 toont dat alle vier de afvalstromen grote hoeveelheden Fe en Ca bevatten. Enkel de ferrochroom slakken bevatten relatief weinig Fe. De gewenste waardevolle metalen (e.g. Cu, Zn, Pb,..) komen slechts in veel kleinere fracties voor en dit toont meteen het belang van een selectieve uitloging aan. Zo biedt dit onderzoek grote kansen. Daarnaast komen Zn en Pb in het goethiet slib in relatief grote hoeveelheden voor. Hetzelfde kan geconstateerd worden voor Cr in de ferrochroom slakken. In de shredder filterkoek biedt vooral Zn mogelijkheden en voor de FeCl₂ voornamelijk V.

Resultaten uitlogingsexperimenten goethiet slib

In deze sectie is per materiaal de uitlooefficiëntie weergegeven i.f.v. de concentratie organische base. De uitlooefficiëntie voor ieder specifiek metaal is berekend op basis van volgende formule:

$$\%E = \frac{C_u \cdot V_L \cdot 10^6}{m_{\%i} \cdot m_{staal}} \cdot 100\% \quad (6)$$

Waarbij volgende symbolen staan voor:

%E: de uitlooefficiëntie van het specifieke metaal

C_u : de concentratie metaal in de uitloogvloeistof [$\mu\text{g/L}$]

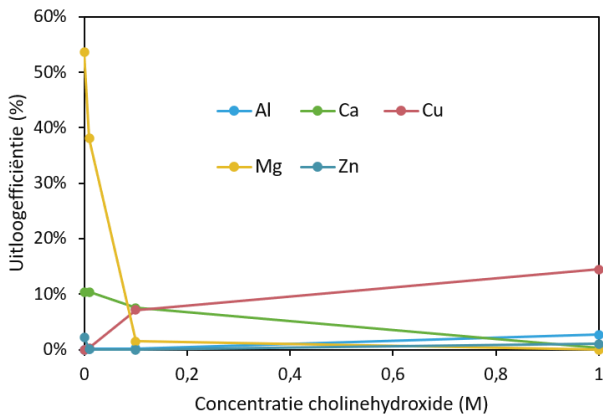
V_L : het volume uitloogvloeistof [L]

$m_{\%i}$: het gehalte van het specifieke metaal in de initiële afvalstroom [g/g]

m_{staal} : massa van het staal (g)

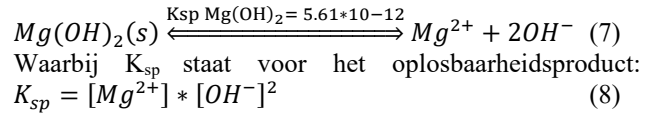
Enkel de elementen die wel degelijk onder invloed van de organische base uitlogden, zijn weergegeven. Verder zijn ook de belangrijkste matricelementen (Ca, Mg, Fe en Al) bestudeerd om de selectiviteit van deze methode te achterhalen. Om de oplosbaarheid van metalen te interpreteren, wordt vaak verwezen naar Pourbaix diagrammen. Deze diagrammen zijn opgemaakt voor een specifiek systeem in water, maar alsnog kunnen deze relevant voor deze studie zijn wanneer het voorkomen van coördinatiebindingen tussen uitloogmiddel en het metaal als verwaarloosbaar beschouwd kan worden. Figuur 9 geeft de resultaten weer

voor het goethiet slib met cholinehydroxide als uitloogmiddel.



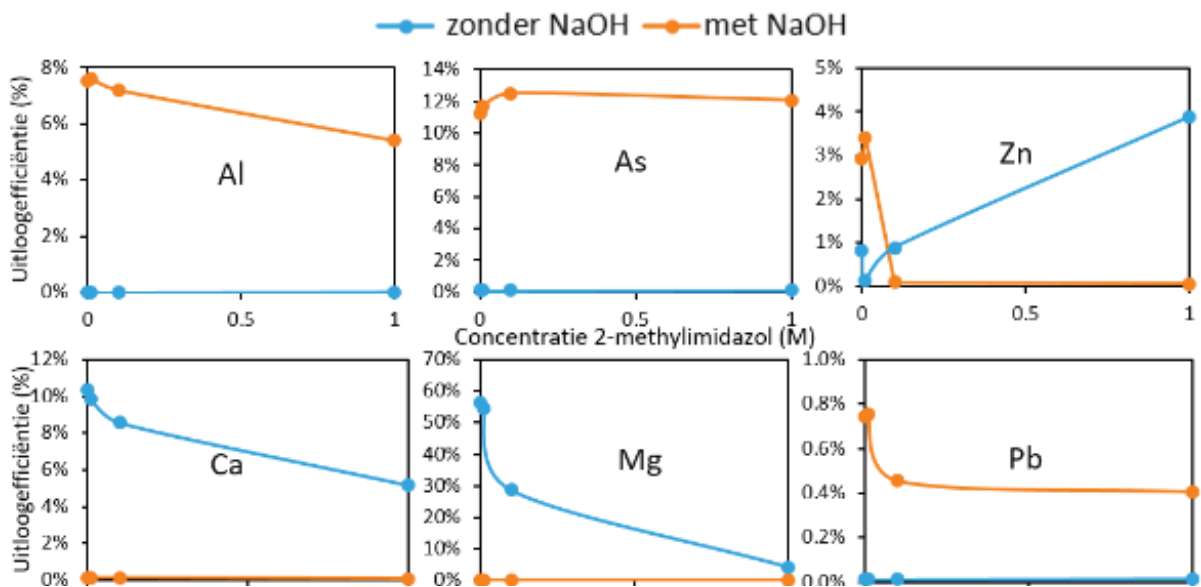
Figuur 9. Uitlooefficiëntie i.f.v. concentratie cholinehydroxide voor het goethiet slib.

In figuur 9 is zichtbaar dat de uitlooefficiëntie voor Cu stijgt in functie van de concentratie cholinehydroxide. Een zelfde verloop is zichtbaar voor Al, al is de stijging hier minder significant. Een verklaring voor deze verhoogde efficiëntie kan gekoppeld worden aan de pH. In de meer basische omgeving zullen Cu en Al beter oplossen resulterend in een verhoogde uitlooefficiëntie. Bij een concentratie van 1 M cholinehydroxide is een pH van ca. 13 gemeten. Pourbaix diagrammen tonen aan dat in dit pH gebied voor Al de oplosbare verbindingen: AlO_2^- en AlO_2^- voorkomen en voor Cu kunnen er oplosbare CuO_2^{2-} verbindingen ontstaan. Ook voor Zn is een stijgende trend zichtbaar die verklaard kan worden door het ontstaan van de oplosbare ZnO_2^{2-} verbindingen in sterker basisch milieu. Voor Mg daalt de uitlooefficiëntie drastisch tussen 0,01 en 0,1 M cholinehydroxide en treedt er geen uitloging meer op bij 1 M cholinehydroxide. De verhoogde aanwezigheid van OH^- ionen vormt een slecht oplosbare hydroxide neerslag. Volgende evenwichtsreactie treedt op:

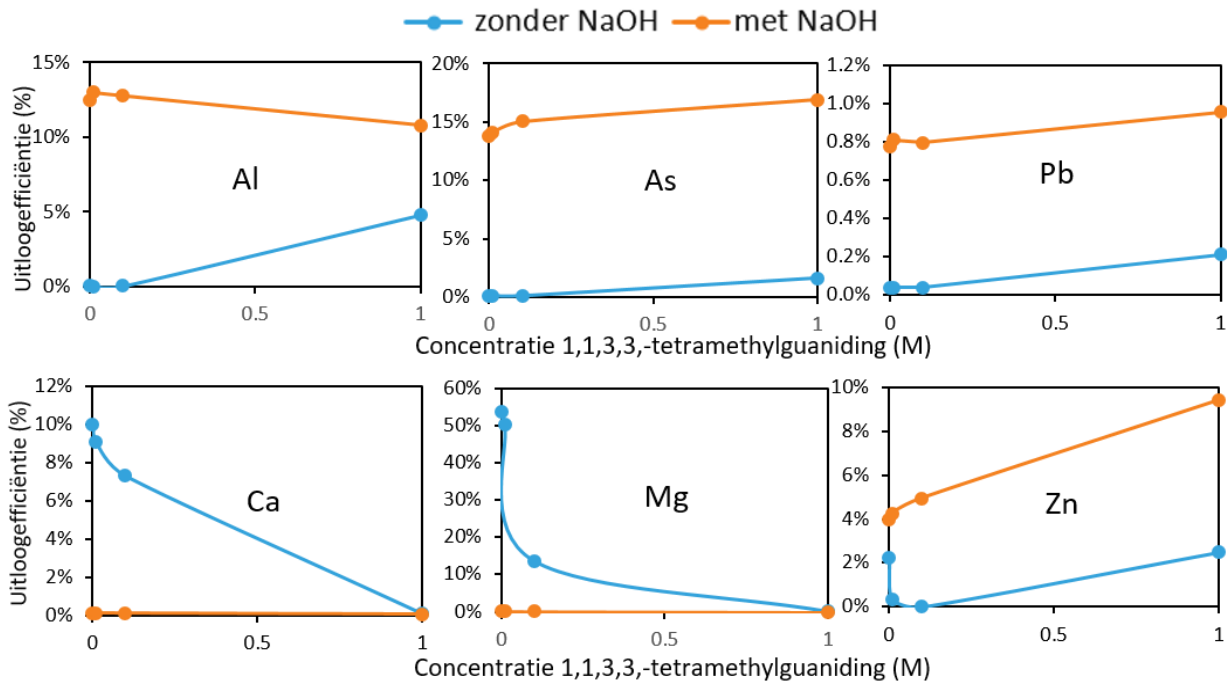


Waaruit volgt dat de oplosbaarheid van Mg daalt bij toenemende pH. Voor Ca is hetzelfde verloop zichtbaar en zal er ook een slecht oplosbare hydroxide neerslag ontstaan: $K_{s Ca(OH)_2} = 4,68 \cdot 10^{-6} = [Ca^{2+}] \cdot [OH^-]^2 \quad (9)$ Voor Ca is de afname in efficiëntie niet zo significant. Vermits het uitloggen van metalen zo min mogelijk Ca en Mg mag opbrengen, vormt de hoogste concentratie cholinehydroxide hier het beste resultaat.

Figuur 10 toont voor Ca en Mg gelijkaardige verlopen (in afwezigheid van NaOH) in vergelijking met cholinehydroxide als uitloogmiddel. Ook hier veroorzaakt een hogere concentratie Hmim een hogere pH (zie Figuur. 4). Het feit dat basisch milieu zorgt voor onoplosbare metaal hydroxide neerslagen is bevestigd door de experimenten te herhalen in aanwezigheid van 1 M NaOH waar de uitlooefficiëntie voor Ca en Mg 0% bleef. Voor Al is er geen uitloging bekomen in afwezigheid van NaOH wat verklaard kan worden doordat Hmim een zwakkere base is dan cholinehydroxide en zodus de pH minder sterk verhoogt (tot ca. pH =9). Pourbaix diagrammen tonen aan dat in dit pH gebied vooral onoplosbare verbindingen gevormd worden zoals: Al, Al_2O_3 en $Al(OH)_3$. Verder is het zichtbaar dat na toevoegen van NaOH de efficiëntie sterk is gestegen voor Al. Pourbaix diagrammen van Al tonen aan dat in de meer alkalische omstandigheden de oplosbare $AlO_2^-/Al(OH)_4^-$ verbindingen worden gevormd. Het ontstaan van coördinatiebindingen tussen Al en Hmim is onwaarschijnlijk omdat hogere concentraties Hmim geen verhoging in uitloging veroorzaken. Voor As is een gelijkaardige curve bekomen als voor Al. As kan in verschillende vormen voorkomen. Het kan onder andere Fe-As complexen (i.e. $Fe_2(OH)_2(H_2O)_nAsO_2(OH)_2^3$) vormen als-



Figuur 10. Uitlooefficiëntie i.f.v. de concentratie Hmim voor het goethiet slib.



Figuur 11. Uitlooefficiëntie i.f.v. de concentratie GUA voor het goethiet slib.

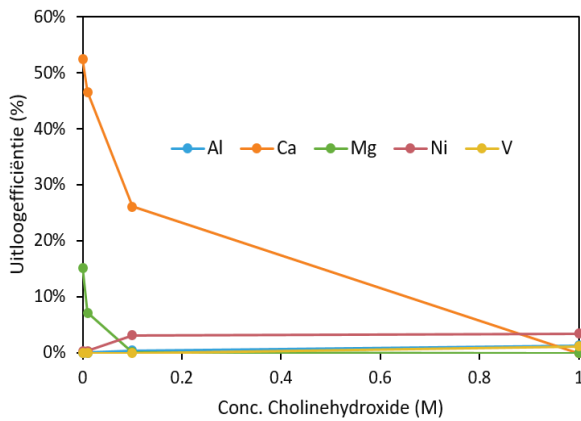
ook verschillende verbindingen vormen met oxides en sulfides [32]. Deze grote verscheidenheid resulteert in verschillende systemen die ieder een specifiek Pourbaix diagram vragen. In hoge pH gebieden komt As voor als oplosbaar oxyanion AsO_4^{3-} [33]. Verder is er hier voor de uitloging van Cu een opvallend resultaat gekomen. De uitlooefficiëntie bedroeg onder de verschillende omstandigheden 0%. Enkel 1 M Hmim in afwezigheid van NaOH leverde 16% uitloging op. De bijhorende pH bedraagt ca. 9 (Figuur. 4). Bij een pH van 9 komen enkel onoplosbare Cu verbindingen (Cu , Cu_2O , $\text{Cu}(\text{OH})_2$) voor. Dit wijst erop dat er oplosbare complexen gevormd worden tussen Hmim en Cu. De literatuur bevestigt het voorkomen van Cu-imidazol complexen bij een pH van 9 [34]. In afwezigheid van NaOH is er vanaf 0,1 M Hmim uitloging voor Zn gekomen. De pH bedraagt hier 8 waarbij er, volgens Pourbaix diagrammen oplosbare Zn^{2+} ionen kunnen ontstaan. Hmim komt bij deze pH al voor meer dan 50% voor in gedeprotoneerde vorm (Figuur 7). Toch is de verhoogde uitloging toe te wijden aan de pH doordat in aanwezigheid van NaOH is te zien dat Hmim een negatieve invloed uitoefent op de uitloging van Zn doordat het Hmim in sterk basisch milieu ($\text{pH} > 10$) uitsluitend gedeprotoneerd voorkomt (Figuur 7) en dus veel sneller coördinatiebindingen met Zn kan aangaan. Hierdoor zal er een neerslag ontstaan van het gevormd metaalcomplex ZIF-8 [35]. ZIF-8 is onoplosbaar in water doordat de gevormde coördinatiebinding tussen Zn en N zeer sterk resulterend in hoge stabiliteit [36]. Verder wordt hier een zeer stabiele kristallijne structuur gevormd waarbij Zn omringt wordt door vier Hmim moleculen [37].

Figuur 11 geeft de uitlooefficiëntie weer voor het goethiet slib met GUA als uitloogmiddel. Deze toont voor Ca en Mg gelijkaardige curves in vergelijking met Hmim als uitloogmiddel. Dit toont dus nogmaals het belang van de pH voor

de uitloging. Voor Al treedt in afwezigheid van NaOH uitloging op bij 1 M GUA. Hieruit volgt dat Al zal beginnen uitloggen vanaf pH gelijk aan ca. 12,5 sinds dit de overeenkomende pH waarde is. GUA is de sterkste base van de drie organische uitloogmiddelen ($\text{pK}_a=13$) en veroorzaakt zodus de sterkste pH stijging. Bij 0,1 M GUA bedraagt de pH 8.6. Pourbaix diagrammen tonen aan dat vanaf $\text{pH} = \text{ca. } 9$ er oplosbare $\text{AlO}_2^-/\text{Al}(\text{OH})_4^-$ verbindingen gevormd worden. In aanwezigheid van NaOH ligt de uitlooefficiëntie van Al zelfs nog hoger en daalt deze zwak tussen 0,01 en 1 M GUA. Voor As kan hetzelfde geconcludeerd worden als voor Al. In afwezigheid van NaOH is de stijging in uitlooefficiëntie wel veel zwakker. In hoge pH gebieden komt As voor als oplosbaar oxyanion AsO_4^{3-} zoals eerder vermeld [33] [38]. Verder is er een verschil terug te vinden in de curve voor As waarin NaOH aanwezig is. Hier stijgt de efficiëntie met toename van de concentratie GUA. As bezit valentie-elektronen op de d-orbitalen waar N gemakkelijk coördinatiebindingen mee kan aangaan [23] [24].

Cu is niet specifiek weergegeven doordat het zeer lage uitlooefficiëntie waardes opleverde (ca. 0%). Voor Zn en Pb is de beste uitloging bekomen in aanwezigheid van NaOH. GUA is in staat oplosbare metaalcomplexen te vormen met Zn in sterker alkalisch milieu doordat er een sterke toename zichtbaar is in uitloging met slechts een geringe pH stijging. Voor Pb volgt er een zwakke toename in uitloging die het gevolg is van de geringe pH stijging. De hoge pH, bereikt door NaOH toe te voegen, zorgt voor het ontstaan van oplosbare ZnO_2^{2-} en PbO_2^{2-} verbindingen volgens Pourbaix diagrammen bevestigd door de hogere uitloging.

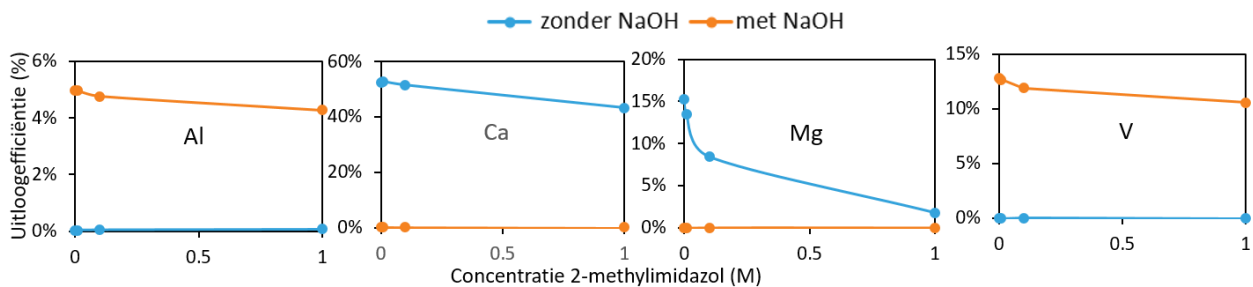
Resultaten uitlogingsexperimenten FeCl₂ slib



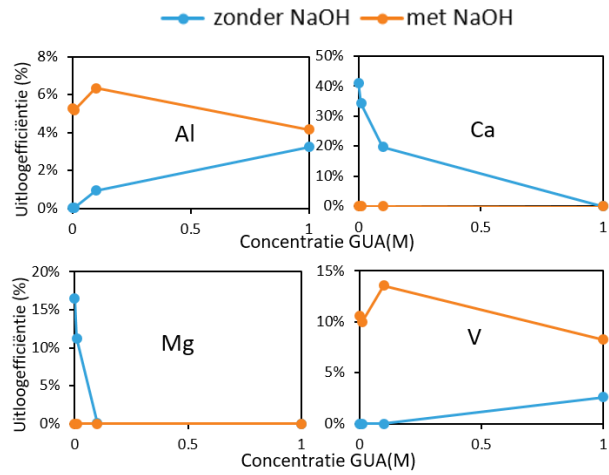
Figuur 12. FeCl₂ slib met cholinehydroxide als uitloogmiddel.

Figuur 12 toont de uitlooefficiëntie bekomen met cholinehydroxide als uitloogmiddel. Voor Ca en Mg is een gelijkaardige trend zichtbaar als bij het goethiet slib: een daling in de uitloog efficiëntie met een toename van de cholinehydroxide concentratie. De curve van Ni en V vallen samen. Hun uitloog efficiëntie stijgt zwak met een toename in concentratie cholinehydroxide door het ontstaan van een basischere omgeving waardoor er oplosbare verbindingen kunnen ontstaan zoals: NiO₃²⁻ en VO₄³⁻ [30].

Figuur 13 geeft de uitloog efficiëntie weer van de FeCl₂ slib met Hmim als uitloogmiddel. Deze toont voor Ca en Mg gelijkaardige curves als bij cholinehydroxide. De uitlooefficiëntie daalt in functie van de pH en dus bij stijgende concentratie Hmim. In vergelijking met cholinehydroxide is de daling zwakker doordat Hmim ook een zwakkere base is. Voor Al is geweten dat er slechts uitloging is bij voldoende alkalische milieu (pH ≥ 12). In afwezigheid van NaOH is er net zoals bij het goethiet slib geen uitloging bereikt. In aanwezigheid van NaOH stijgt de uitlooefficiëntie. Net zoals bij het goethiet slib is de hoogste uitloog efficiëntie bereikt in puur water bij 1 M NaOH. wat bevestigt dat Al beter oplost door de hogere pH. Verder toont dit aan dat er nauwelijks coördinatie bindingen gevormd worden tussen Al en Hmim. Voor V is een volledig gelijkaardig patroon zichtbaar als bij Al. Alhoewel de uitloog efficiëntie nog hoger ligt voor V. De literatuur beschrijft dat V in hoog alkalisch milieu (pH > 12) vooral voorkomt als oplosbaar anion (vanadaat) VO₄³⁻ [30] [39]. Figuur 14 toont de uitlooefficiëntie voor de FeCl₂ slib met GUA.



Figuur 13. Uitlooefficiëntie i.f.v. concentratie Hmim voor het FeCl₂ slib.

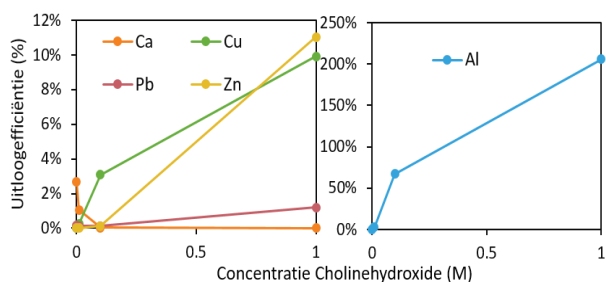


Figuur 14. Uitlooefficiëntie i.f.v. concentratie GUA voor het FeCl₂ slib.

Figuur 14 toont voor Ca en Mg gelijkaardige verlopen als met Hmim als uitloogmiddel. Merk op dat de daling in efficiëntie nog sterker hier is in vergelijking met Hmim als uitloogmiddel. Dit is te verklaren doordat GUA een sterkere base is dan Hmim waardoor de pH sneller stijgt en er sneller onoplosbare metaalhydroxides gevormd worden. Voor Al en V is zelfs in afwezigheid van NaOH uitloging bekomen ook doordat 1 M GUA een pH bereikt van ± 13. Voor V kan een optimale concentratie GUA uit figuur 14 afgeleid worden. In aanwezigheid van NaOH bedraagt deze 0,1 M GUA waarbij de pH ca. 13,42 bedraagt. Na dit optimum volgt een matige daling in efficiëntie.

Resultaten uitlogingsexperimenten shredder filterkoek

Figuur 15 beschrijft de uitlooefficiëntie voor de shredder filterkoek met cholinehydroxide als uitloogmiddel.



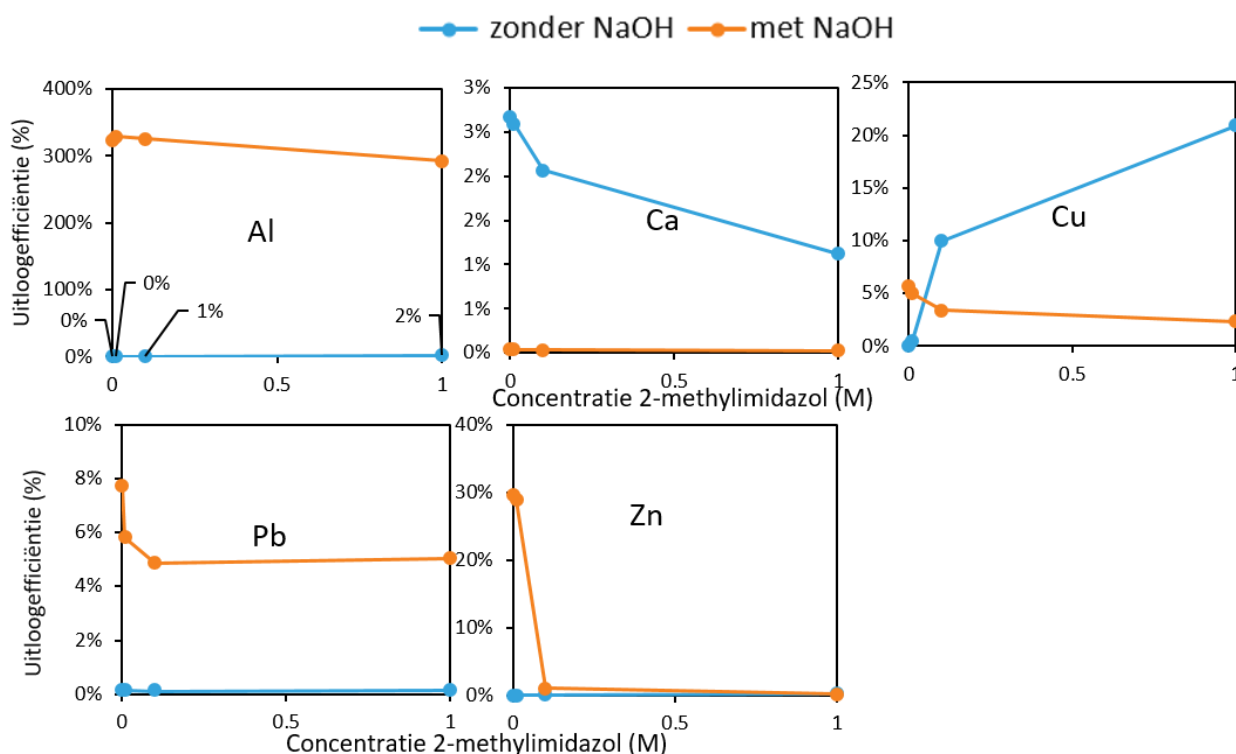
Figuur 15. Shredder filterkoek met cholinehydroxide als uitloogmiddel.

Een toename in concentratie cholinehydroxide leidt tot een toename in uitlooefficiëntie. Voor Cu, Zn en Al is deze stijging zeer sterk. Voor Al zijn zelfs waardes bekomen van ca. 200%. Dit resultaat is in theorie niet mogelijk, maar ontstaat louter doordat de initiële samenstelling van de afvalstromen bepaald werd d.m.v. XRF-analyses. Kleine afwijkingen tussen de twee verschillende analysetechnieken kunnen zorgen voor een dergelijke overschatting van de efficiëntie. Voor Ca is hetzelfde patroon zichtbaar als bij de vorige materialen: een daling in efficiëntie met een toename in concentratie cholinehydroxide door het ontstaan van $\text{Ca}(\text{OH})_2$ neerslag.

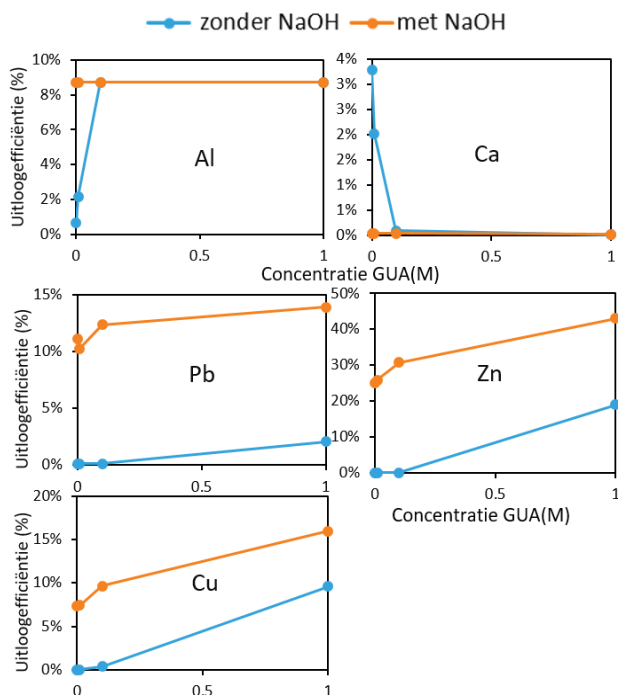
Figuur 16 geeft de resultaten weer voor de shredder filterkoek met Hmim als uitloogmiddel waarbij voor Ca en Al een volledig analoge curve bekomen is als voor de twee

voorgaand besproken materialen: een daling in uitloog in functie van de pH/concentratie Hmim. In afwezigheid van NaOH lost er amper Al op. Enkel in aanwezigheid van NaOH maakt de uitlooefficiëntie een sprong naar resultaten boven de 100%. In de hogere alkalische gebieden ontstaan de oplosbare $\text{AlO}_2^-/\text{Al}(\text{OH})_4^-$ verbindingen. Verder is te zien dat de efficiëntie daalt na 0,01 M Hmim toe te voegen waaruit volgt dat er nauwelijks oplosbare metaalcomplexen met Hmim gevormd worden. Voor Cu levert de afwezigheid van NaOH het beste resultaat op. Zoals eerder verklaard ontstaan in de hogere pH zones onoplosbare Cu-verbindingen ($\text{Cu}_2\text{O}/\text{Cu}(\text{OH})_2$) die de efficiëntie zodus negatief beïnvloeden. Verder bevestigt dit resultaat het ontstaan van oplosbare Cu-Hmim complexen die de uitloog bevorderen. Voor Zn en Pb zijn de beste resultaten bekomen in aanwezigheid van NaOH terwijl in afwezigheid van NaOH geen uitloog optreedt. In aanwezigheid van NaOH is de hoogste efficiëntie voor beide elementen bereikt in puur water. Een toevoeging van Hmim veroorzaakt hier een daling van de efficiëntie. Bij Zn daalt de efficiëntie zelfs naar 0% bij 1 M Hmim doordat er onoplosbare metaalcomplexen (ZIF-8) worden gevormd zoals eerder besproken. Verder is te zien dat ook hier de pH een cruciale rol speelt waarbij in alkalische milieus vooral het oplosbare ZnO_2^{2-} voorkomt.

Figuur 17 toont wederom voor Ca een gelijkaardig patroon als in de vorige curves duidelijk werd. Voor Al speelt de aan- of afwezigheid van NaOH niet meer zo'n grote rol doordat zelfs in afwezigheid van NaOH met 0,1 M GUA gelijkaardige resultaten bekomen werden als in aanwezigheid met NaOH. Bij 0,1 M GUA bedraagt de pH ca.12 wat bevestigt dat vanaf dan Al uitloogt. Verder toont Figuur 17 dat de curves van Cu, Pb en Zn een analoog verloop kennen.



Figuur 16. Uitlooefficiëntie i.f.v. concentratie Hmim voor de shredder filterkoek.



Figuur 17. Uitlooefficiëntie i.f.v. concentratie GUA voor de shredder filterkoek.

In afwezigheid van NaOH liggen de uitloopwaardes lager dan in aanwezigheid van NaOH. In beide situaties is er stijging waarneembaar met een toename in concentratie GUA. De aanwezigheid van oplosbare metaal-GUA complexen is bevestigd doordat in aanwezigheid van NaOH de pH slechts zwak toeneemt ($\pm 0,2$) tussen 0,01 en 0,1 M GUA en de uitlooefficiëntie van Cu en Zn sterk toeneemt [23] [24]. Voor Pb is er slechts een geringe toename waarneembaar in uitlooging waardoor het ontstaan van oplosbare coördinatiebindingen tussen GUA en Pb sterk betwijfeld wordt. De zwakke toename in uitlooefficiëntie zal het gevolg zijn van de zwakke toename in pH.

Resultaten Ferrochroom slakken

De resultaten van de Ferrochroom slakken zijn niet besproken doordat deze overal 0% uitlooging opleveren. Voor de matrixelementen ligt dit resultaat binnen de verwachtingen doordat deze afvalstroom een sterk alkalisch karakter heeft waardoor er onoplosbare metaalhydroxides ontstaan. Bovendien speelt vooral Cr hier een belangrijke rol doordat dit waardevol element nog aanzienlijk aanwezig is in de afvalstroom. Via deze methode raakt er nauwelijks Cr uitgeleogd doordat in het pH gebied (12,3-13,7) bij een ORP tussen 0 en -124 mV enkel de slecht oplosbare $\text{Cr}(\text{OH})_3$ verbindingen voorkomen [40]. Hieruit volgt de conclusie dat geen van deze drie organische uitloogmiddelen coördinatiebindingen met Cr in deze minerale stroom kunnen aangaan om de uitlooging te bevorderen.

Uitlogingsresultaten Fe

Voor de uitlooging van Fe is te zien dat de uitlooefficiëntie overal 0% bedraagt. Dit is een zeer gunstig resultaat wat bijdraagt aan een hoge selectiviteit van deze methode. In

deze basische omstandigheden worden $\text{Fe}(\text{OH})_2$ en $\text{Fe}(\text{OH})_3$ neerslagen gevormd. Daarnaast kan er ook volgens Pourbaix diagrammen Fe voorkomen in volgende vormen: Fe_3O_4 en Fe_2O_3 .

Conclusie

In deze studie is de invloed van organische, basische uitloogmiddelen op de herwinning van metalen onderzocht. Deze kunnen de selectiviteit van de methode positief beïnvloeden mede door het ontstaan van coördinatie bindingen.

De uitlooefficiëntie van matrixelementen Ca en Mg verlaagt drastisch met een toename van de concentratie organisch uitloogmiddel doordat de toename in pH onoplosbare metaal hydroxides veroorzaakt. Dit gebeurt al bij een pH = 8. Doordat cholinehydroxide en GUA erg sterke bases zijn, kunnen deze uitloogmiddelen de uitlooefficiëntie van Ca en Mg zelfs reduceren tot 0%. Dit is een groot voordeel t.o.v. zure uitloogmiddelen. Hoe lager de pH, hoe beter de voorgenoemde matrixelementen zullen uitlogen [41]. Verder is er door het creëren van basisch milieu een uitlooefficiëntie van 0% voor Fe bereikt door het ontstaan van $\text{Fe}(\text{OH})_2$ en $\text{Fe}(\text{OH})_3$ neerslagen. Dit is een veelbelovend resultaat doordat in zuur milieu loogt het matrixelement Fe zeer goed uit door het ontstaan van de oplosbare $\text{Fe}^{2+}/\text{Fe}^{3+}$ verbindingen [42]. De literatuur beschrijft met tartaarzuur en oxaalzuur voor Fe een uitloog efficiëntie van ca. 30% [41]. Dit is voor zure uitloogmiddelen een relatief lage waarde doordat oxaalzuur met Fe een oxalaatneerslag kan vormen [41]. Voor het matrixelement Al was er een uitlooging bij pH = 12. Deze uitlooging nam vanaf dan zeer sterk toe met een toename in pH door het ontstaan van oplosbare Al-verbindingen: $\text{AlO}_2^-/\text{Al}(\text{OH})_4^-$. Algemeen kan gesteld worden dat via deze methode een hoge selectiviteit is bereikt doordat het alkalisch milieu de uitlooging van matrixelementen verlaagt. Daarnaast levert cholinehydroxide veelbelovende resultaten voor de uitlooging van Cu, Zn en Ni. Hierbij is er een toename zichtbaar in uitlooging met een stijging in concentratie cholinehydroxide die te verklaren is door de toename in pH. 1 M cholinehydroxide levert een pH van 13,6 door het vrijzetten van hydroxyl anionen ($\text{pK}_a=11,2$). Volgens de Pourbaix diagrammen van de betreffende elementen zijn hier voornamelijk goed oplosbare verbindingen mogelijk zoals CuO_2^{2-} , ZnO_2^{2-} , HNiO_2^- . Hmim is de zwakste base ($\text{pK}_a=7,89$) van de drie organische uitloogmiddelen. Nochtans is voor Cu een opvallend resultaat gekomen waarbij 1 M Hmim zelfs de hoogste uitlooefficiëntie behaalt van 21%. Hiervoor dient er zelfs geen 1 M NaOH aanwezig te zijn doordat Hmim in staat is Cu op te lossen via coördinatiebindingen. Het optreden van deze complexvorming is een veelbelovend resultaat en kan de selectiviteit verhogen. Merk op dat dit resultaat relatief laag is in vergelijking met het organische zuur citroenzuur wat een uitlooefficiëntie van 99% voor Cu haalde [43]. Melkzuur daarentegen haalde ook slechts een uitloog efficiëntie van 23% voor Cu wat vergelijkbaar is met het verkregen resultaat [44]. Met Zn vormt Hmim mogelijks ook coördinatie-bindingen resulterend in een onoplosbaar complex ZIF-8 waardoor de uitlooefficiëntie gereduceerd wordt tot 0% vanaf 0,1 M Hmim. Daarnaast is deze base te zwak om voldoende sterk alkalisch milieu te creëren (pH > 12) waar de waardevolle

metalen zoals Pb, Ni en Cu verhoogde oplosbaarheid vertonen. Tot slot is GUA de sterkste base van de drie ($pK_a=13$). Hierdoor kan er zelfs uitloging van Zn, Cu en Pb bereikt worden in afwezigheid van NaOH bij 1 M GUA. Vooral voor Zn was er in deze omstandigheden een hoge uitlooefficiëntie bereikt (ca. 19%). In aanwezigheid van 1 M NaOH in puur water is de uitlooefficiëntie van de voornoemde metalen sterk verhoogd. Verder is er hier een sterke stijging zichtbaar i.f.v. de concentratie GUA. Door de aanwezigheid van de sterke base NaOH veroorzaakt GUA hier slechts een geringe pH stijging waaruit volgt dat GUA vooral voorkomt in basische vorm. Als gevolg kan GUA coördinatiebindingen vormen met Cu en Zn, wat leidt tot een verhoogde uitloging. Het ontstaan van metaalcomplexen in voldoende basische milieu biedt veel mogelijkheden voor de uitloging van de Cu, Zn en Pb.

Voor de uitloging van Cu is Hmim aangeraden doordat hier de hoogste uitlooefficiëntie werd bereikt ($\pm 20\%$) waarbij geen NaOH nodig was. Voor Zn en Pb is GUA sterk aangeraden doordat deze de sterkste pH verhoging veroorzaakt. In aanwezigheid van NaOH stijgt de pH tot boven 13 waarbij GUA in staat is metaalcomplexen te vormen met Cu en Zn.

Aanbeveling voor verder werk

Om de uitloging van waardevolle metalen te bevorderen kan een verhoging van de liquid/solid ratio perspectief bieden ^[45] ^[46]. Nu is deze verhouding constant 10. Door deze verhouding aan te passen verandert de reactiekinetiek en de massatransfer tussen uitloogmiddel en de vaste stof. Daarnaast biedt een verhoging van de temperatuur ook mogelijkheden om de uitlooefficiëntie te verhogen ^[47] ^[48]. De experimenten zijn nu uitgevoerd op kamertemperatuur. In totaliteit kan een model opgemaakt worden wat de reactiekinetiek weergeeft om zo de optimale omstandigheden te bepalen. Daarnaast kan ook een verdere verhoging in concentratie uitloogmiddel zorgen voor een verbetering van de uitlooefficiëntie van waardevolle metalen afgeleid uit de huidige correlaties. Vervolgens kan er tijdens de uitloogexperimenten ook gebruik gemaakt worden van een extra zuurstofstroom die de mobiliteit van de metalen kan bevorderen door oxidatiereacties ^[49].

Verder kan het gebruik van ultrasone drukgolven de uitloging optimaliseren. Het is een goedkope, snelle, eenvoudige en veilige methode die d.m.v. extra energie de reactietijd kan verlagen en daarbij de uitloging kan verhogen ^[50]. De aangelegde drukgolf veroorzaakt in oplossing de vorming van bellen gevolgd door implosies ^[51]. Hierdoor zullen er extreem hoge temperaturen en drukken ontstaan aan de interfase tussen de vaste stof en het uitloogmiddel resulterend in verhoogde chemische reactiviteit die de extractie van metalen zal bevorderen. Daarnaast dragen deze drukgolven bij tot het vergroten van het contactoppervlak tussen de vaste en vloeistoffase met een efficiëntere uitloging als gevolg. ^[52] ^[53]

Daarnaast kan de vorming van metaalcomplexen met de organische bases verder onderzocht worden met als doel de efficiëntie en selectiviteit van de uitloging te bevorderen.

Hierbij kan er gebruik gemaakt worden van FT-IR analyses ^[34].

Verder moet er gezocht worden naar verdere mogelijke behandelingen van de bekomen uitgeloopte vloeistoffen die een range van metalen bevatten. Om tot een succesvolle oplossing te komen is het nodig een nabehandeling te voorzien die de selectiviteit zal verhogen om zo een waardevol eindproduct te bekomen. Mogelijks bieden neerslagreacties hier een uitkomst ^[54]. Verder kan er onderzocht worden welke mogelijkheden er zijn voor het resterende residu. In veel gevallen kan dit gebruikt worden in bepaalde bouwmaterialen ^[55].

Eens de uitloogmethode geoptimaliseerd is, kan er gedacht worden aan opschaling van de experimenten om later in de praktijk grotere hoeveelheden afvalstroom te behandelen. Dit pilootproject omzetten naar de praktijk brengt grote uitdagingen met zich mee, en mogelijks kan dit geïntegreerd worden in bestaande uitlogingsinstallaties.

REFERENCES

- [1] M. Yellishetty, G. M. Mudd, P. G. Ranjith and A. Tharumarajah, "Environmental life-cycle comparisons of steel production and recycling: sustainability issues, problems and prospects," *Environmental science and policy*, vol. 14, no. 6, pp. 650-665, 2021.
- [2] L. Rahupathy and A. Chaturvedi, "Secondary resources and recycling in developing economies," *Sciences of the total environment*, no. 461-462, pp. 830-834, 2013.
- [3] A. K. Awasthi, F. Cucchiela, I. D'Adamo, J. Li, P. Rosa, S. Terzi, G. Wei and X. Zeng, "Modelling the correlations of e-waste quantity with economic increase," *Science of the total environment*, no. 613-614, pp. 46-53, 2018.
- [4] U. Nkwunonwo, P. Odika and N. Onyia, "A Review of the Health Implications of Heavy Metals in Food Chain in Nigeria," *The scientific world journal*, p. 11, 2020.
- [5] N. Rodriguez, L. Machiels, B. Onghena, J. Spooren and K. Binnemans, "Selective recovery of zinc from goethite residue in the zinc industry using deep-eutectic solvents," *Royal society of chemistry*, vol. 10, pp. 7328-7335, 2020.
- [6] T. Abio Atia and J. Spooren, "Microwave assisted alkaline roasting-water leaching for the valorisation of goethite sludge from zinc refining process," *Hydrometallurgy*, vol. 191, 2020.
- [7] F. R. M. Sprinzel, "Valorization of Ferrochrome Slag: Towards increasing the beneficial utilisation of

- Ferrochrome slag in South Africa," Stellenbosch University, 2016.
- [8] C. R. Borra, B. Blanpain, Y. Ponitkes, K. Binnemans and T. Van Gerven, "Recovery of Rare Earths and Other Valuable Metals From Bauxite Residue (Red Mud): A Review," *Journal of Sustainable Metallurgy*, no. 2, pp. 365-386, 2016.
- [9] R. A. Crane and D. J. Sapsford, "Towards Greener Lixiviants in Value Recovery from Mine Wastes: Efficacy of Organic Acids for the Dissolution of Copper and Arsenic from Legacy Mine Tailings," *Minerals*, vol. 383, no. 8, 2018.
- [10] B. Musariri, G. Akdogan, C. Dorfling and S. Bradshaw, "Evaluating organic acids as alternative leaching reagents for metal recovery from lithium ion batteries," *Minerals Engineering*, vol. 137, pp. 108-117, 2019.
- [11] R. Larba, I. Boucherche, N. Alane, N. Habbache, S. Djerad and L. Tifouti, "Citric acid as an alternative lixiviant for zinc oxide dissolution," *Hydrometallurgy*, Vols. 134-135, pp. 217-223, 2013.
- [12] P. Meshram, A. Mishra, Abilash and R. Sahu, "Environmental impact of spent lithium ion batteries and green recycling perspectives by organic acids – A review," *Chemosphere*, vol. 242, 2020.
- [13] Merck, "www.sigmaaldrich.com," Merck, [Online]. Available: <https://www.sigmaaldrich.com/catalog/product/aldrich/292257?lang=en®ion=US>. [Accessed 20 Mei 2020].
- [14] Merck, "www.sigmaaldrich.com," Merck, [Online]. Available: <https://www.sigmaaldrich.com/catalog/product/aldrich/m50850?lang=en®ion=US>. [Accessed 20 Mei 2020].
- [15] AA BLOCKS LLC, "www.aablocks.com," AA BLOCKS LLC, [Online]. Available: <https://www.aablocks.com/prod/80-70-6>. [Accessed 20 Mei 2020].
- [16] echa, "www.echa.europa.eu," echa, [Online]. Available: <https://echa.europa.eu/registration-dossier/-/registered-dossier/5289/4/22>. [Accessed 23 April 2020].
- [17] K. Haerens, E. Matthijs, K. Binnemans and B. Van Der Brugge, "Electrochemical decomposition of choline chloride based ionic liquid analogues," *Green Chemistry*, vol. 11, pp. 1357-1365, 2009.
- [18] K. Moonen and M. Gernon, "Stabilized choline solutions and methods for preparing the same". United States Patent PCT/EP2012/073337 , 22 November 2012.
- [19] Eastman, "www.productcatalog.eastman.com," Eastman, 2020. [Online]. Available: <https://productcatalog.eastman.com/tds/ProdDatash eet.aspx?product=71103663>. [Accessed 29 April 2020].
- [20] echa, "www.echa.europa.eu," ECHA, [Online]. Available: <https://echa.europa.eu/nl/brief-profile/-/briefprofile/100.010.697>. [Accessed 23 April 2020].
- [21] S. Chen, "The roles of imidazole ligands in coordination supramolecular systems," *CrystEngComm*, vol. 18, 2016.
- [22] I. Leito, T. Rodima, I. A. Koppel, R. Schwesinger and V. M. Vlasov, "Acid-Base Equilibria in Nonpolar Media. 1. A Spectrophotometric Method for Acidity Measurements in Heptane," *Journal of organic chemistry*, vol. 62, no. 24, pp. 8470-8483, 1997.
- [23] T. Ishikawa, "Guanidine Chemistry," *Chemical and pharmaceutical Bulletin*, vol. 58, no. 12, pp. 1555-1564, 2010.
- [24] E. K. Yetimoglu, M. Firlak, M. V. Kahraman and S. Deniz, "Removal of Pb²⁺ and Cd²⁺ ions from aqueous solutions using guanidine modified hydrogels," *Polymers for advanced technologies*, vol. 22, no. 2, pp. 612-619, 2011.
- [25] M. J. Quina, J. C. M. Bordado and R. M. Quinta-Ferreira, "The influence of pH on the leaching behaviour of inorganic components from municipal solid waste APC residues," *Waste Management*, vol. 29, no. 9, pp. 2483-2493, 2009.
- [26] T. Bakaric, B. Budic, B. Malic and D. Kuscer, "The influence of pH dependent ion leaching on the processing of lead-zirconate-titanate ceramics," *Journal of the European Ceramic society*, vol. 35, no. 8, pp. 2295-2302, 2015.
- [27] P. H. Kumar, A. Srivastava, V. Kumar, M. R. Majhi and V. K. Singh, "Implementation of industrial waste ferrochrome slag in conventional and low cement castables: Effect of microsilica addition," *Journal of Asian Ceramics Societies*, vol. 2, no. 2, pp. 169-175, 2014.
- [28] S. Aghazadeh, S. K. Mousavinezhad and G. Mahdi, "Chemical and colloidal aspects of collectorless flotation behavior of sulfide and non-sulfide minerals," *Advances in Colloid and Interface Science*, vol. 225, pp. 203-217, 2015.
- [29] Y. Li, J. Chen, D. Kang and J. Guo, "Depression of pyrite in alkaline medium and its subsequent activation by copper," *Minerals engineering*, vol. 26, pp. 64-69, 2012.

- [30] D. Langmuir, *Aqueous Environmental Geochemistry*, New Hersey: Prentice-Hall, Inc., 1997.
- [31] A. P. Lehoux, C. L. Lockwood, W. M. Mayes, D. I. Steward, R. J. G. Mortimer, K. Gruiz and I. T. Burke, "Gypsum addition to soils contaminated by red mud: implications for aluminium, arsenic, molybdenum and vanadium solubility," *Environmental chemistry and health*, vol. 35, pp. 643-656, 2013.
- [32] P. Lu and C. Zhu, "Arsenic Eh-pH diagrams at 25°C and 1 bar," *Environmental earth science*, vol. 62, pp. 1673-1683, 2011.
- [33] D. M. Sherman and S. R. Randall, "Surface complexation of arsenic(V) to iron(III) (hydr)oxides: structural mechanism from ab initio molecular geometries and EXAFS spectroscopy," *Geochimica et cosmochimica acta*, vol. 67, no. 22, pp. 4223-4230, 2003.
- [34] J. Khalid and K. D. Haithm, "Preparation And Spectral Characterization Of Some Transition Metal complexes with new Azo Imidazole ligand and study some industrial application," *Al-Qadisaya Journal for Science*, vol. 16, no. 4, 2011.
- [35] J. Lu, S. Zhou, S. Zhang, C. Zhang and Q. Wang, "Remarkable Enhancement of Proton Conductivity by Introducing Imidazole into MOFs and Forming Composite Membranes," *European Journal of inorganic chemistry*, no. 6, pp. 794-799, 2019.
- [36] H. Zhang, M. Zhao and Y. Lin, "Stability of ZIF-8 in water under ambient conditions," *Microporous and mesoporous materials*, vol. 279, pp. 201-210, 2019.
- [37] X. Feng, T. Wu and M. Carreon, "Synthesis of ZIF-67 and ZIF-8 crystals using DMSO (Dimethyl Sulfoxide) as solvent and kinetic transformation studies," *Journal of Crystal Growth*, vol. 455, no. 2, pp. 152-156, 2016.
- [38] C. Tabein, A. Hashimoto, T. Igarashi and T. Yoneda, "Leaching of boron, arsenic and selenium from sedimentary rocks: II. pH dependence, speciation and mechanisms of release," *Science of the total environment*, Vols. 473-474, pp. 244-253, 2014.
- [39] M. Takaya and K. Sawatari, "Speciation of Vanadium(IV) and Vanadium(V) using Ion-exchange Chromatography and ICP-AES," *Industrial health*, vol. 32, pp. 165-178, 1994.
- [40] J. Jerabkova, V. Tejnecky, L. Boruvka and O. Drabek, "Chromium in Anthropogenically Polluted and Naturally Enriched Soils: A Review," *Scientia Agriculturae Bohemica*, vol. 49, no. 4, pp. 297-312, 2018.
- [41] H. Geng, F. Wang, C. Yan, Z. Tian, H. Chen, B. Zhou, R. Yuan and Y. Yao, "Leaching behavior of metals from iron tailings under varying pH and low-molecular-weight organic acids," *Journal of hazardous materials*, vol. 383, 2020.
- [42] M. Lwambiyi, K. Maweja, K. Kongolo, N. M. Lwambiyi and M. Diyambi, "Investigation into the heap leaching of copper ore from the Disele deposit," *Hydrometallurgy*, vol. 98, no. 1-2, pp. 177-180, 2009.
- [43] P. Meshram, U. Prakash, L. Bhagat, Abhilash and H. Zhao, "Processing of Waste Copper Converter Slag Using Organic Acids for Extraction of Copper, Nickel, and Cobalt," *Minerals*, vol. 10, no. 3, 2020.
- [44] K. Fedje, C. Ekberg, G. Skarnemark and B. Steenari, "Removal of hazardous metals from MSW fly ash—An evaluation of ash leaching methods," *Journal of hazardous materials*, vol. 173, no. 1-3, pp. 310-317, 2010.
- [45] S. M. J. Mirazimi, F. Rashchi, E. Vahidi and N. Mostoufi, "Optimization and Dissolution Kinetics of Vanadium Recovery from LD converter slag in alkaline media," *Metallurgy of nonferrous metals*, vol. 57, no. 4, pp. 395-404, 2016.
- [46] S. R. Al-Abed, G. Jegadeesan, J. Purandara and D. Allen, "Leaching behavior of mineral processing waste: Comparison of batch and column investigations," *Journal of Hazardous Materials*, vol. 153, no. 3, pp. 1088-1092, 2008.
- [47] P. Raschman, L. Popovic, A. Fedorockova, M. Kyslytsyna and G. Sucik, "Non-porous shrinking particle model of leaching at low liquid-to-solid ratio," *Hydrometallurgy*, vol. 190, 2019.
- [48] B. Musariri, G. Akdogan, C. Dorfling and S. Bradshaw, "Evaluating organic acids as alternative leaching reagents for metal recovery from lithium ion batteries," *Minerals Engineering*, vol. 137, pp. 108-117, 2019.
- [49] F. Yin, P. Xing, Q. Li, C. Wang and Z. Wang, "Magnetic separation-sulphuric acid leaching of Cu–Co–Fe matte obtained from copper converter slag for recovering Cu and Co," *Hydrometallurgy*, vol. 149, pp. 189-194, 2014.
- [50] A. Elik, "Ultrasonic-assisted leaching of trace metals from sediments as a function of pH," *Talanta*, vol. 71, no. 2, pp. 790-794, 2007.
- [51] K. Ashley, "Ultrasonic extraction of heavy metals from environmental and industrial hygiene samples for their subsequent determination," *Trends in analytical chemistry*, vol. 17, no. 6, pp. 366-373, 1998.

- [52] J. L. Luque-Garcia, L. d. Castro and M. D, "Continuous ultrasound-assisted extraction of hexavalent chromium from soil with or without on-line preconcentration prior to photometric monitoring," *Analyst*, vol. 127, no. 8, pp. 1115-1120, 2002.
- [53] D. G. Shchukin, E. Skorb, V. Belova and H. Möhwald, "Ultrasonic Cavitation at Solid Surfaces," *Advanced materials*, vol. 23, no. 17, pp. 1922-1934, 2011.
- [54] J. Wang, X. Huang, L. Wang, Q. Wang, Y. Yan, N. Zhao, D. Cui and Z. Feng, "Kinetics study on the leaching of rare earth and aluminum from FCC catalyst waste slag using hydrochloric acid," *Hydrometallurgy*, vol. 171, pp. 312-319, 2017.
- [55] L. Horckmans and R. Swennen, "Herkennen van materialen gebruikt in wegenbouw en voor verharding in kader van verwijderingsstructuur voor nonferro residu's. Een opdracht in kader van BeNeKempen.," OVAM, Mechelen, 2008.
- [56] B. Sahu, A. Biswas and G. Kapure, "A Short Review on Utilization of Ferrochromium Slag.," *Mineral processing and extractive metallurgy review*, vol. 37, no. 4, pp. 211-219, 2016.
- [57] X. Zhang, D. Fang, S. Song, G. Cheng and X. Xue, "Selective leaching of vanadium over iron from vanadium slag," *Journal of hazardous materials*, vol. 368, pp. 300-307, 2019.

ANNEXES